Promotor	Prof. Dr. G.J. de Lange
Co-promotor	Dr. G.J. Reichart

Members of the dissertation comittee

Prof. Dr. J.B.M. Middelbrug, Utrecht University
Prof. Dr. L.J. Lourens, Utrecht University
Prof. Dr. R. Zahn, Autonomous University of Barcelona
Prof. Dr. F.J. Jorissen, University of Angers

Jos Wit
jos.wit@gmail.com

This research was funded by the Darwin Center for Biogeosciences

USES publication Nr. 26

LPP Contributions Series 38

ISBN: 978-90-6266-314-9

Printed by Wöhrman Print Service, Zutphen

Cover design and layout by J.C. Wit.
Cover Photo by curtisy of L.J. de Nooijer.

Calibration, validation and application of foraminiferal carbonate based proxies: reconstructing temperature, salinity and seawater Mg/Ca

Kalibratie, validatie en applicatie van op foraminiferen gebaseerde carbonaat proxies: het reconstrueren van temperatuur, saliniteit en zeewater Mg/Ca

(met een samenvatting in het Nederlands)

Proefschrift

ter verkrijging van de graad van doctor aan de Universiteit Utrecht op gezag van de rector magnificus, prof.dr. G.J. van der Zwaan, ingevolge het besluit van het college voor promoties in het openbaar te verdedigen op vrijdag 2 november 2012 des middags te 4.15 uur

door

Johannes Cornelis Wit

geboren op 15 maart 1982
te Haarlem

Promotor: Prof. Dr. G.J. de Lange

Co-promotor: Dr. G.J. Reichart

Dit proefschrift werd (mede) mogelijk gemaakt met financiële steun van het Darwin Centre for Biogesciences

Reis ver
Drink wijn
Denk na
Lach hard
Duik diep
Kom terug....

(Spinvis, 2011)

Contents

Chapter 1
General introduction

After 10,000 years of relative stability, atmospheric CO_2 concentrations are rapidly increasing since the beginning of the industrial revolution, mainly because of the burning of fossil fuels. Over the last 150 years atmospheric CO_2 concentrations increased by as much as 110 parts per million (ppm), from 280 to 390 at present (Figure 1.1). The rate of this anthropogenic CO_2 increase may well be faster than ever before in the Earth's geological past (IPCC, 2007). For example, during the last transition from glacial to inter-glacial conditions CO_2 concentrations increased by ~ 100 ppm in about 4000 years (Figure 1.1) (Petit et al., 1999). Atmospheric CO_2 is a potent greenhouse gas as it admits short waved solar radiation (energy), but omits long waved radiation, thereby trapping heat in the atmosphere. Atmospheric CO_2, therefore, functions as a warm blanket retaining heat in the Earth's atmosphere. The synchronous pacing of changes in temperature and atmospheric CO_2 concentration clearly demonstrates the link between CO_2, as a greenhouse gas, temperature and global climate (Petit et al.,

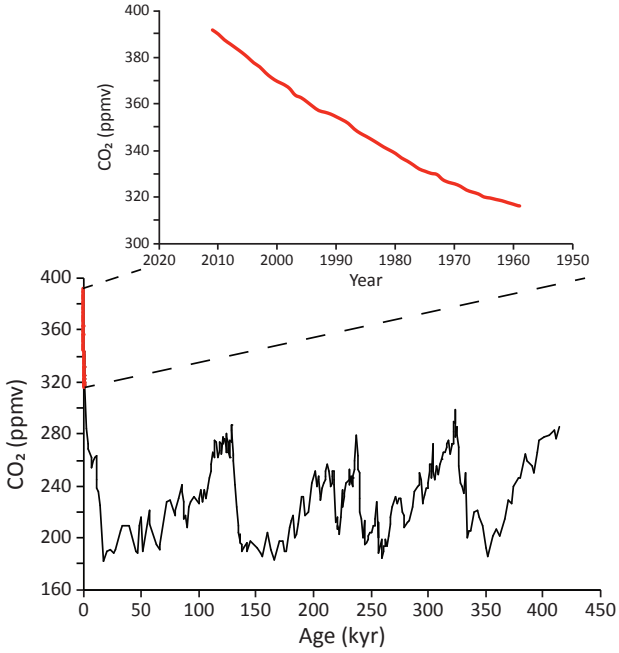

Figure 1.1 Atmospheric CO_2 levels over the last 400,000 years from the Antarctic Vostok ice core (Petit et al., 1999) and for the last 60 years from the Mauna Loa Observatory (Tans and Keeling, 2012).

1999). Understanding effects of rising CO_2 on climate change is of vital importance for reliable predictions on the future climate and its potential effect on the socio-economic environment. Increasing droughts or changes in precipitation patterns as a result of increasing temperature, for example, have a major impact on the agricultural potential of certain areas. Increasing temperatures and acidification of surface waters due to increased CO_2 may affect aquatic ecosystems, which in turn has implications for aquaculture and fishery. Rising temperatures, furthermore, lead to a decrease in large continental ice sheets, causing a rise in global sea level. This steady rise in sea level gradually increases the risk of flooding coastal areas, which are the most densely populated areas on our planet. The ability to accurately predict these changes is, therefore, of vital importance.

Changes in climate can be predicted by development and application of numerical climate models, which are capable of simulating climate change on both regional and global scale (IPCC, 2007). Verification of such models is achieved through comparison with present-day climate monitoring. This way climate models are validated under more or less steady state conditions, assuming that present-day climate feedbacks remain valid under changing climate conditions (Bradley, 1999). Since such an assumption cannot be made a-priori, these climate models should be tested under transient conditions as well. Similarly, behavior of these models under long-term very different environmental conditions, such as substantially higher atmospheric CO_2 concentrations has to be verified independently. The time-series and contrasting climate conditions needed for these validations are, however, not available from the instrumental record. Accurate reconstructions of past climates are thus necessary to obtain records of past climates to validate numerical models under long-term transient conditions and non-analogue climatic conditions. Geologists use existing knowledge of present day environments to interpret the paleo-record, which is also known as "the present is the key to the past". With the ongoing global warming and the need for reliable climate predictions, this is now modified to the statement that "the past is the key to the future" (Hay et al., 1997).

Reconstructing changes in past climate requires continuous sedimentary archives and measurable variables relating to environmental conditions during deposition. The relation between an environmental parameter and such a measurable variable is called a proxy-relationship, which means that environmental parameters can be reconstructed indirectly, i.e. "by proxy". Deep-sea sediments, containing micro-fossils of marine organisms, often provide such continuous sedimentary records. Changes

in relative abundance of these micro-fossils, especially foraminifera, and their chemical composition are, therefore, frequently used as proxies.

Foraminifera (Protista) are single celled amoeba-like organisms living in virtually all marine and fresh water habitats (Holzmann et al., 2003). Characteristic for foraminifera are their reticulate pseudopodia, originating from their cell, which form a dynamic net (Hemleben et al., 1989). The cell structure of a large group of foraminifera is supported by an external 'test', produced by the foraminifera themselves that can consist of calcium carbonate (collectively called the calcareous foraminifera, figure 1.2), sediment particles (agglutinated foraminifera) or organic compounds (allogromid foraminifera) (Pawlowski et al., 2003). Marine foraminifera are present all over the world in a wide variety of habitats, from the water column (planktonic foraminifera) down to the ocean floor (benthic foraminifera). The earliest benthic foraminifera have been found in deposits from Cambrian age (~520 Ma) while

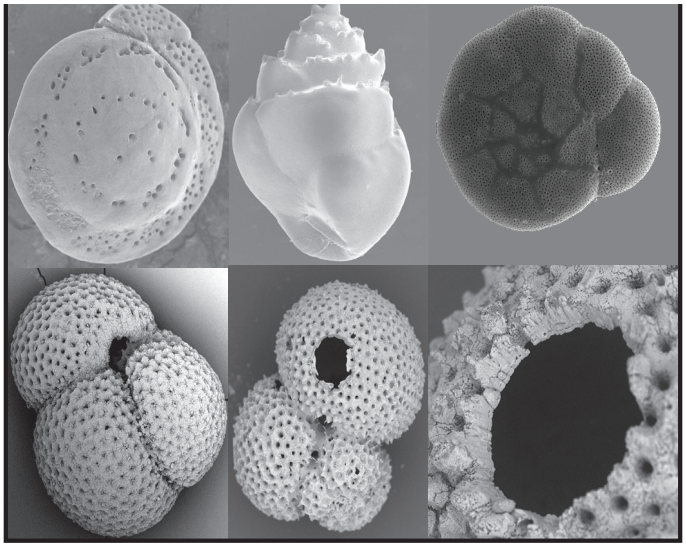

Figure 1.2 Examples of calcareous foraminifera used in this thesis. Upper panel (left to right) *Cibicides kullenbergi*, *Bulmina marginata* and *Ammonia tepida*. Lower pannel (left to right) *Globigerinoides ruber*, *G. ruber* with laser ablation crater and a close-up of an ablation crater. (photos: courtesy of K. Koho and L.J. de Nooijer)

planktonic foraminifera first appeared about 200 Ma ago (Pawlowski et al., 2003 and references therein). The fossil remains of foraminifera are well preserved in marine sediments over millions of years. Hence, foraminifera are ideal proxies signal carriers

to reconstruct past climates and changes therein.

In addition to the use of foraminiferal relative abundances to reconstruct past environments (Imbrie and Kipp, 1971), the chemical composition of foraminiferal carbonate test themselves can be used as a paleo-proxy. Calcareous foraminifera add chambers to their test during their life cycle following a tightly biological controlled calcification mechanism (Erez, 2003, De Nooijer et al., 2009a, 2009b) (Figure 1.3). This mechanism starts with vacuolization of seawater into the foraminiferal cell (Erez, 2003). From this seawater Ca^{2+} is being concentrated into a so-called Ca-pool (Erez, 2003), while dissolved inorganic carbon (DIC) is concentrated into a carbon pool (Ter Kuile et al., 1989, Erez, 2003, De Nooijer et al., 2009b). The concentration mechanism of calcium into the Ca-pool is regulated via either trans-membrane transport or ion-specific pumps (De Nooijer et al., 2009b). During this transport other divalent ions, such as Mg^{2+} and Sr^{2+}, are possibly accidently introduced to the Ca-pool, or actively discriminated against. Inorganic carbon is concentrated via internal regulation of the

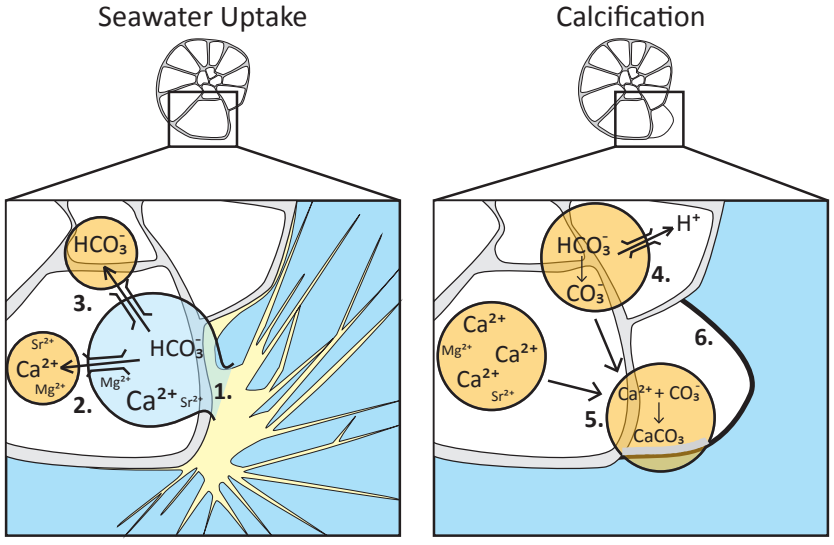

Figure 1.3 Simplified calcification pathway for hyaline foraminifera (Courtesy of L.J. de Nooijer). **1)** Seawater for calcification is introduced to the foraminiferal cell by endocytosis (Erez, 2003, De Nooijer et al., 2009a, b). **2,3)** Concentration of Ca^{2+} and Dissolved Inorganic Carbon (DIC) into two separate intracellular calcium- and inorganic carbon-pools (De Nooijer et al., 2009a). **4)** inorganic carbon is converted to CO_3^{2-} by elevating the pH prior to calcification (De Nooijer et al., 2009b). **5)** Simultaneous release of high pH-vesicles and Ca^{2+} from both pools result in the formation of a new chamber of calcium carbonate. **6)** The site of calcification is protected by an organic template.

foraminifer's pH, resulting in elevated pH values and therefore higher carbonate ion concentrations (CO_3^{2-}) (De Nooijer et al., 2009b). During calcification both pools are combined for the formation of calcium carbonate ($CaCO_3$) by the foraminifer (Figure 1.3). Within this process of calcification stable oxygen and carbon isotopes are incorporated into the foraminiferal shell as well as a number of minor or trace elements as a result of the Ca and carbonate ion concentration and transport mechanisms.

Relative abundance of incorporated trace and minor elements and the ratios of stable isotopes often depend on one or more environmental parameter. The stable oxygen isotope composition of foraminiferal test carbonate, for instance, is determined by a combination of seawater temperature and oxygen isotopic composition, which in turn is often related to global ice volume (Epstein et al., 1953, Shackleton, 1974, Bemis et al., 1998). The isotopic composition of foraminiferal calcite tests was introduced as a proxy for temperature by Emiliana (1955). Emiliana (1955) showed periodical alternations in seawater temperatures of up to 6 °C in Caribbean, Atlantic and Pacific deep-sea sediments. These periodical alternations represented the glacial inter-glacial cycles, characteristic of the Pleistocene, thereby demonstrating the potential of foraminiferal stable isotopes as a paleo-climate proxy. Although later studies showed that a large part of the variability, up to 4 °C, was derived from the waxing and waning of continental ice sheets, resulting in glacial inter-glacial variability in the oxygen isotopic composition of the seawater (Shackleton, 1974).

Incorporation of ions other than calcium and carbonate in calcium-carbonate is known to depend on one or more environmental parameters for almost a century (Clark and Wheeler, 1922). The use of foraminiferal trace/minor element incorporation as a proxy for the paleo-environment was, however, greatly hindered by the difficulty of analyzing these elements in small-sized samples. Incorporation of Li, Sr, Mg and Na was even shown not to depend on environmental parameters, such as temperature, because of these analytical difficulties (Delaney et al., 1985). The incorporation of cadmium in foraminiferal calcite as a proxy for deep ocean circulation and nutrient chemistry was one of the first successful uses of foraminiferal trace metal incorporation as an environmental proxy (Boyle, 1992). After this pioneering study, a whole set of calibrations for a number of trace/minor elements incorporated into foraminiferal calcite as a proxy for an environmental parameter was developed using culture experiments, plankton tows, sediment traps and core-top studies. Examples of the most important environmental parameters calibrated include temperature (magnesium), carbonate ion concentration (uranium), salinity (magne-

sium combined with $\delta^{18}O$) and the elemental composition of the ocean (magnesium, barium, manganese) (Nürnberg et al., 1996, Elderfield and Ganssen, 2000, Russell et al., 2004, Elderfield et al., 2006, Segev and Erez, 2006). The chemical composition of foraminiferal test carbonate can thus be used to reconstruction these environmental parameters and thereby, past climates. However, the incorporation of these elements into foraminiferal test carbonate is often not depending on a single parameter but a number of environmental parameters (Nürnberg et al., 1996, Elderfield et al., 2006, Segev and Erez, 2006). The calibration and validation of new proxies and improving the accuracy and precision of existing ones by quantifying and correcting for these secondary influences is, thus, one of the main challenges in paleoclimatology. This thesis covers a number of calibrations and validations of new and existing proxies based on the stable isotope and trace/minor element composition of the carbonate test of foraminifera. Subsequent application of these proxies to the fossil record resulted in a number of novel reconstructions that are presented and discussed.

Foraminiferal test carbonate based proxies: Calibration, Validation and Application

Accuracy and resolution of paleo-climate reconstructions can be limited by bioturbation and/or reworking of sediments. Bioturbation mixes sediments of different ages and short-term changes are, therefore, potentially smoothed in the sedimentary record. This impacts rate calculations and dampens high frequency variability. **Chapter 2** describes the development of a new method to estimate bioturbation by determining oxygen isotopes (calcitic $\delta^{18}O$) on individual planktonic foraminiferal tests of *Globorotalia inflata* from a series of boxcore samples in the Eastern North Atlantic. The frequency distribution of individual $\delta^{18}O$ measurements is interpreted by using simple spreadsheet end-member modeling. This allows unmixing of temperature records affected by bioturbation into multiple distributions, representing the original and the bioturbated component within each sample. The simple spreadsheet model, furthermore, allows quantification of the average of each distribution. The measured $\delta^{18}O$ signal is corrected for bioturbation, increasing the accuracy of foraminiferal $\delta^{18}O$ as a proxy in paleoclimatology.

In **chapter 3** we assess the potential of analyzing oxygen isotopes and Mg/Ca on the test of individual planktonic foraminifer *Globigerinoides ruber* as a proxy for the seasonal temperature contrast (seasonality). Temperature reconstructions are often based on the analysis of many (e.g. 40) fossil foraminiferal specimens. Those speci-

mens may have calcified in different seasons. Seasonal variability in sea surface temperatures is, however, often orders of magnitude larger than inter-annual variations of a single season and even changes in average temperature from glacial to interglacial conditions. Analyzing single specimens from one sample allows reconstructing a range of past temperatures. Results of single-specimen analyses show that (1) average $\delta^{18}O$ derived temperatures correlate with modern annual average temperatures for most sites, (2) the range in $\delta^{18}O$ and Mg/Ca derived temperature estimated from single specimen analysis resembles the range in seasonal temperature values at the sea surface (0–50 m) in the Mediterranean Sea and the Atlantic Ocean. This implies that it is potentially possible to reconstruct the seasonal range in temperatures using single-specimen analysis of (combined) Mg/Ca and $\delta^{18}O$.

In **chapter 4** a new Mg/Ca-temperature calibration is presented for the benthic foraminifer *Bulimina marginata*, based on series of culture experiments. During calcification by foraminifera, low amounts of other ions enter the microscopically small site where the foraminifer's calcite is precipitated. The presence of these ions (Mg^{2+}, Na^{+}, $B(OH)_4^-$, etc.) is responsible for the formation of calcite with detectable 'contaminations' of these elements, commonly expressed as element ratios relative to calcium (Mg/Ca, Na/Ca, B/Ca, etc.). The incorporation of magnesium into foraminiferal test carbonate mainly depends on the temperature of the environment and therefore, the Mg/Ca of fossil foraminiferal calcite is a popular temperature-proxy. Measured Mg/Ca values for *B. marginata* correlate with temperature. Variability between cultured individuals of the same temperature experiment is, however, considerably, affecting the precision of the temperature reconstructions based on Mg/Ca in this species. This inter-individual variability is caused by the combined effect of three components: 1) an analytical error, 2) an environmental error and 3) a vital effect. Quantification of the analytical error and the effect of an experimentally induced environmental variable (e.g. temperature, salinity, etc) allow estimating the remaining vital effect. This inter-individual variability furthermore affects the accuracy of Mg/Ca based temperature reconstructions. The magnitude of the uncertainty is mainly depending on the sensitivity of the used species-specific calibration and the amount of individuals measured.

Chapter 5 uses the large differences between the sensitivity of Mg/Ca-temperature calibrations of different species to disentangle the effects of two environmental parameters on foraminiferal Mg/Ca. Besides temperature, the proportion of Mg^{2+} to Ca^{2+} in seawater (Mg/Ca_{SW}) also determines the Mg/Ca of foraminiferal calcite. Al-

though magnesium concentrations are relatively constant over shorter time scales, it fluctuates appreciably over longer time scales largely due to variability in weathering rates and sea floor spreading. The use and accuracy of the Mg/Ca-thermometer on longer time scales, therefore, hinges upon an accurate reconstruction of Mg/Ca_{sw}. In **chapter 5** we present a novel approach to reconstruct paleo Mg/Ca_{sw}, using the temperature-dependent offset in magnesium incorporation (sensitivity) between porcelaneous (high Mg) and hyaline (low Mg) benthic foraminifera. A novel Mg/Ca-temperature calibration for porcelaneous benthic foraminifer *Pyrgo* spp. is presented. In combination with an existing calibration for the hyaline species *Cibicides* spp., changes in Mg/Ca_{sw} through time can be reconstructed. The Mg/Casw values for the last 10 Ma varied between 3.3 and 5.1, corresponding well to the magnitude of changes in seawater Mg/Ca as derived from geochemical models. Applying this reconstructed Mg/Ca_{sw} to existing time series shows that Mg/Ca-based temperature reconstructions for the middle Pleistocene and earlier significantly underestimate absolute temperature, demonstrating the importance of reconstructing Mg/Ca_{sw} through time.

Whereas several proxies have been developed to reconstruct past sea surface temperatures, a tool that allows a reliable reconstruction of salinity remains among the most important challenges in current-day paleoceanography. In **chapter 6** we describe a novel proxy to independently and accurately reconstruct seawater salinity using foraminiferal Na/Ca. Specimens of the benthic foraminifer *Ammonia tepida*, cultured under controlled conditions at a range of salinities (30.0-38.6), show that test Na/Ca values increase linearly with salinity. Application of this calibration over a sapropel (S5 ~125 ka) from the Eastern Mediterranean showed that salinity decreased by 5 units during this interval, providing for the first time independent evidence for a major freshening of surface waters during sapropel formation. Foraminiferal Na/Ca values thus provide an accurate and robust tool to reliably reconstruct past changes in salinity.

Chapter 7 provides an example of combining a number of foraminiferal proxies measured on the same specimens. It has been demonstrated that temperatures reconstructed with foraminiferal Mg/Ca are not independent of changes in salinity (Nürnberg et al., 1996). Increasing salinity causes an overall increase in the activity of free $[Mg^{2+}]$ with respect to $[Ca^{2+}]$, thereby promoting incorporation of Mg into foraminiferal calcite and thus potentially biasing Mg/Ca-derived temperature reconstructions with changing salinity. The effect of salinity on foraminiferal Mg/Ca

temperatures is quantified and subsequently corrected for by using Na/Ca as a proxy for salinity (**Chapter 6**). Corrected temperatures are then combined with records for salinity and foraminiferal $\delta^{18}O$ over a sapropel (S5). The combined proxies show that the Mediterranean basin changed from an evaporation dominated basin with eastward increasing salinities to a basin with less evaporation and a more Atlantic signal. This overall change in basin hydrology might be more important than the impact of the increased Nile outflow as a cause for sapropel formation.

Chapter 2

Unmixing of stable isotope signals using single specimen $\delta^{18}O$ analyses

J.C. Wit[1], G.J. Reichart[1,2] and G.M. Ganssen[3]

1 Department of Geochemistry, Utrecht University, Budapestlaan 4, 3584 CD Utrecht, the Netherlands
2 Marine Biogeosciences, Alfred Wegener Institute for Polar and Marine Research, Am Handelshafen 12, D-27570 Bremerhaven, Germany
3 Department of Paleo-climatology and Geomorphology, Vrije Univer siteit Amsterdam, 1081 HV, The Netherlands

Submitted to Geochemistry, Geophysics, Geosystems.

Abstract

The resolution at which foraminiferal stable isotopes are applied in paleo-environmental studies is ever increasing, resulting in continuous sampling of sediment cores. The resolution of such continuously sampled records depends on the rate of sedimentation of foraminiferal shells in its relation to the intensity of bioturbation. Bioturbation essentially mixes sediment layers of different age, altering the primary climate signal, thereby impacting the accuracy of both the timing and magnitude of reconstructed climate changes. A new approach to assess and correct the impact of bioturbation is investigated here, based on the $\delta^{18}O$ of individual specimens of planktonic foraminifera *Globorotalia inflata* from a series of boxcore samples in the Eastern North Atlantic. Average $\delta^{18}O$ values decrease southward from 1.62 to 1.07 ‰ with the exception of site T86-11 (1.35 ‰). The $\delta^{18}O$ distribution of each station can be fitted with a uni- to polymodal distribution. A non-unimodal distribution strongly suggests admixing of bioturbated individuals. Quantification of these distributions allows deconvolving the original and bioturbated signals and subsequently provides a correction for bioturbation.

2.1 Introduction

The oxygen isotopic composition of foraminiferal test carbonate is a proven and established tool for reconstructing past changes in sea water temperature and ice volume (Epstein et al., 1953, Shackleton, 1974, Bemis et al., 1998). The stable isotopic composition of the foraminiferal test is increasingly applied in high-resolution studies. The study of sub-Milankovitch and sometimes even (sub-)centennial time scale variability has become increasingly important to understand climatic changes on time scales relevant to mankind. This implies that cores are nowadays often studied at the highest possible resolution and thus sampled continuously. In such cases the resolution of the records depends on sedimentation rate of the foraminiferal shells in relation to the intensity of bioturbation. Bioturbation is the process by which burrowing animals mix sediments from "older" and "younger" layers. This alters a primary climate signal in two ways. First, the recorded climate signal is lengthened by the upward/downward transport of sediment, which leads to an overestimation of the duration of the climate event. Second, in the case of short events, more intense bioturbation leads to dampening of the amplitude of the original climate signal, as both underlying and overlying sediments are mixed with the sediments deposited during the event (Guinasso and Schink, 1975, Schink and Guinasso, 1977, Peng et al., 1979, Hutson, 1980, Peng and Broecker, 1984, Bard et al., 1987, Barker et al., 2007, Keigwin and Guilderson, 2009). Hence, magnitude of these short-lived events will be underestimated while the event duration will be overestimated in the reconstruction. Bioturbation thus affects our ability to accurately date climate events and to quantify their magnitude. Since $\delta^{18}O$ signals are generally based on averaging analyses of multiple specimens, understanding the impact of bioturbation is essential for assessing true timing and magnitude of the signals derived from stable oxygen analysis.

Because of technical improvements allowing to accurately measure $\delta^{18}O$ of individual planktonic foraminifera, paleoceanographers no longer have to rely on $\delta^{18}O$ values based on multiple specimens, but can also use the distribution of $\delta^{18}O$ values from individual specimens around this average to reconstruct past environments. This distribution of single specimen $\delta^{18}O$ values can for instance be used as a tool to reconstruct the seasonal cycle in sea surface temperatures (Wit et al., 2010, Ganssen et al., 2011). This interpretation, however, requires that the impact of bioturbation can be quantified. Here, we investigate the impact of bioturbation by measuring single specimen $\delta^{18}O$ of planktonic foraminifera *Globorotalia inflata* from a series of boxcore samples in the Eastern North Atlantic.

2.2 Methods

Samples from a North-South transect (57.9-35.6 °N) in the North East Atlantic Ocean were recovered during two cruises of the R/V Tyro in the North Atlantic (Figure 2.1, table 2.1) (Ganssen and Kroon, 2000). Pre-measurement sample treatment followed standard lab procedures for oxygen isotope measurements (Wit et al., 2010). Single specimens of planktonic species *G. inflata* from the 355 to 425 µm size range were measured for $\delta^{18}O$ on a Mat Finnigan 252 gas-source mass spectrometer with an automated Kiel type carbonate preparation line at the Vrije Universiteit Amsterdam. Results for $\delta^{18}O$ are reported relative to the Vienna Pee Dee Belemnite (V-PDB), using the NBS-19 standard, and have an internal reproducibility of 0.08 ‰. Sample averages are based on the unweighted average of the individual $\delta^{18}O$ measurements of each station.

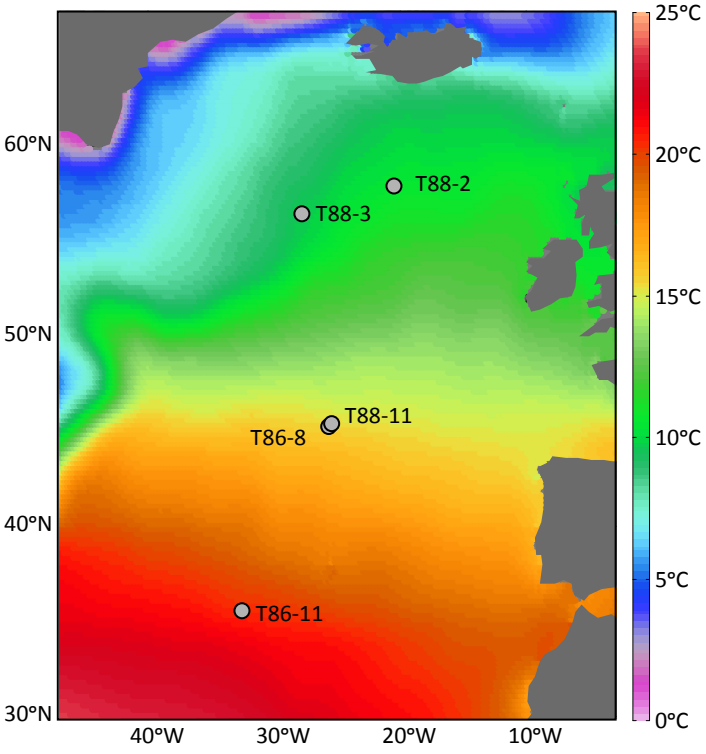

Figure 2.1 Annual average North Atlantic sea surface temperatures from the World Ocean Atlas 01 (WOA01), with the locations of the used core locations (Conkright et al., 2001)

Sample	Location			$\delta^{18}O$ (V-PDB)			
	Lat. (N)	Long. (W)	Depth (m)	Average	σ	DF	p-value
T88/2	57.9	20.5	2911	1.64	0.39	25	0.82
T88/3	56.4	27.8	2819	1.62	0.27	36	0.41
T88/11	45.4	25.4	2741	1.14	0.27	34	0.66
T86/8	45.3	25.7	3232	1.07	0.32	36	0.26
T86/11	35.6	32.6	2220	1.35	0.59	40	0.00

Table 2.1 Core location, depth, average $\delta^{18}O$, standard deviation, p-value and Degrees of Freedom (DF) from the Shapiro-Wilks test. A p-value < 0.05 is significant and indicates that the distribution is deviating from normality.

Single specimen $\delta^{18}O$ data was plotted as a histogram with a bin size of 0.2 ‰ in order to analyze the frequency distribution of each station. Frequency distributions were tested for normality and subsequently fitted with a Gaussian distribution, using a standard curve fit in an Excel spreadsheet (Appendix 2.1). The Gaussian curve was fitted to the data using the sum of squared error and the Excel solver function to minimize the error between the measured data and the modeled Gaussian distribution. Since bioturbation is the mixing of sediments of different age, $\delta^{18}O$ distributions affected by bioturbation should display a bi- or polymodal distribution.

2.3 Results

Average $\delta^{18}O$ values decrease southward from 1.62 to 1.07 ‰ with the exception of site T86-11 (1.35 ‰) (Figure 2.2). A Shapiro-Wilk test was performed for each station, using the individual $\delta^{18}O$ measurements to verify whether distributions significantly deviate from normality (Table 2.1, Appendix 2.2). Identified outliers (outlier > average ± 3 standard deviations) were excluded from the Shapiro-Wilk analyses, as they have a major impact on the test (Field, 2009). For most of the stations, the $\delta^{18}O$ values are normally distributed according to the Shapiro-Wilk test. The probability statistic (p-value) for site T86-11, however, was significant, indicating that the $\delta^{18}O$ values for this site are not normally distributed.

2.4 Discussion and Conclusions

North Atlantic surface water temperatures show a clear North-South gradient with temperatures increasing towards the South (Figures 2.2 and 2.3) (Conkright et al., 2001). *Globorotalia inflata* is a non-spinose planktonic foraminifera living around

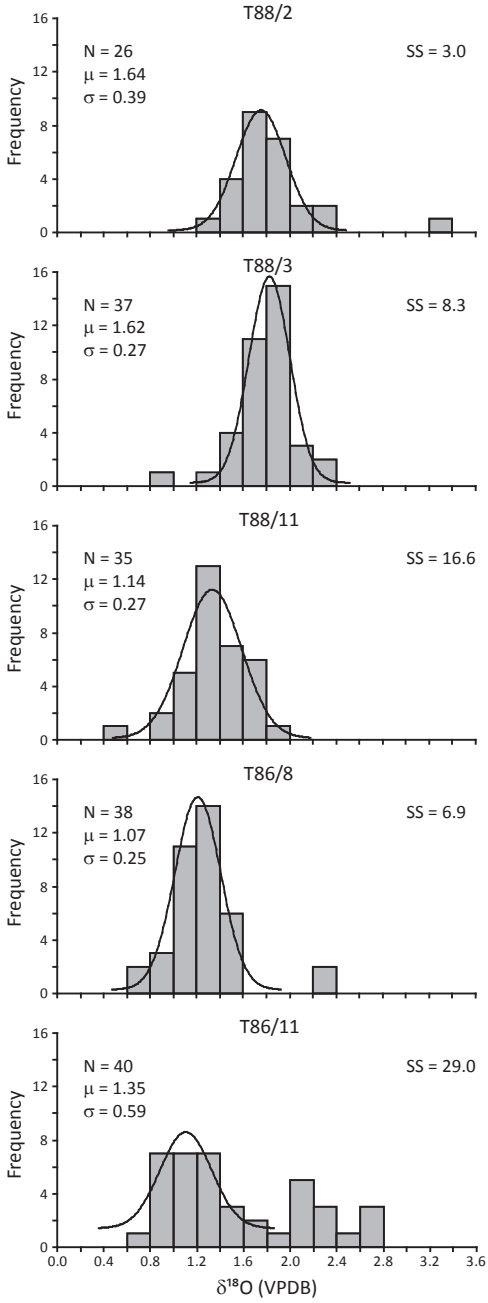

Figure 2.2 Frequency and modeled Gaussian distributions for measured $\delta^{18}O$ of *G. inflata*, with the number of measurements (N), the average $\delta^{18}O$ (μ) and standard deviation (σ). The sum of squares (SS) is used as a fit between the measured and modeled frequency distribution.

100-400 meters water depth, typically found in thermocline waters (Fairbanks et al., 1982, Hemleben et al., 1989, Ganssen and Kroon 2000). Average oxygen isotope values measured on planktonic foraminifer *G. inflata* along this North-South transect should, therefore, reflect this latitudinal temperature gradient. Measured average $\delta^{18}O$ values along this transect for *G. inflata* were converted to temperatures using the $\delta^{18}O$ temperature equation of O'Neil et al. (1969) as refitted by Shackleton (1974) (Equation 2.1).

$$T = 16.9 - 4.38(\delta^{18}O_c - \delta^{18}O_w) + 0.1(\delta^{18}O_c - \delta^{18}O_w)^2 \quad (2.1)$$

Values for $\delta^{18}O_w$ were calculated using WOA01 salinity values and their relation to $\delta^{18}O_w$ for the North Atlantic (Equation 2.2 from Ganssen and Kroon, 2000, Conkright et al., 2001)

$$\delta^{18}O_w = 0.55S - 19.45 \quad (2.2)$$

Values for $\delta^{18}O_w$ were converted from V-SMOW to V-PDB, using the 0.27 ‰ correction after Hut (1987). Temperatures based on the average oxygen isotope values, with

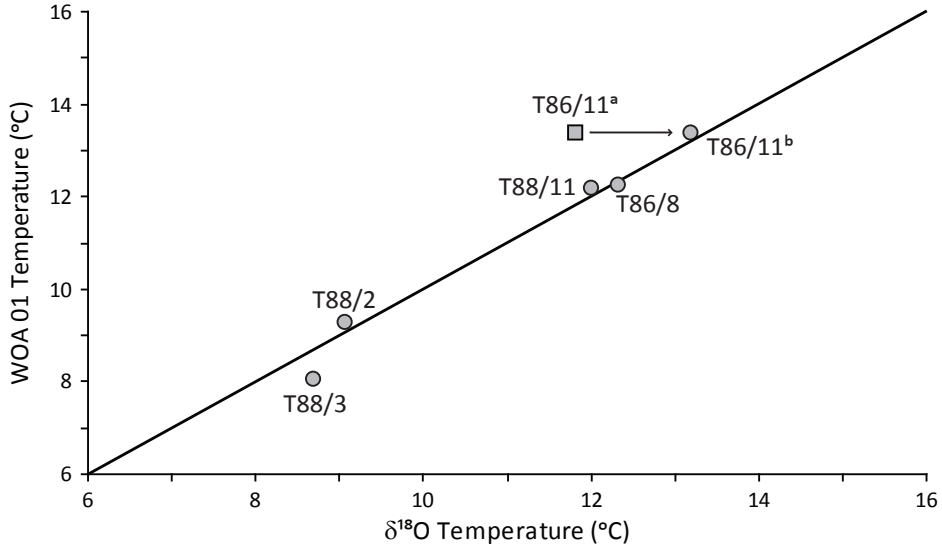

Figure 2.3 Average $\delta^{18}O$ derived temperature for *G. inflata* and the annual average seawater temperature between 100 and 400 meters water depth from the WOA01 (Conkright et al., 2001). T86/11[a] (square) is the $\delta^{18}O$ derived temperature as measured, while T86/11[b] is the temperature derived after correcting for bioturbation.

the exception of site T86/11, correlate well with annual mean temperatures between 100 and 400 meters water depth from the World Ocean Atlas 2001 (Conkright et al., 2001) (Figure 2.3). The standard deviations of the measured temperatures correlate well with the seasonal range in WOA01 temperatures, again with the exception of site T86/11S. The average $\delta^{18}O$ of T86/11S is 1.35 ‰ (11.8 °C), which is too cold compared to present day temperatures (Figure 2.3). The Shapiro-Wilks test on the single specimen $\delta^{18}O$ distribution failed and the frequency distribution for site T86/11 is deviating from normality (Table 2.1). The larger standard deviation indicates that multiple populations of foraminifera are present within the measured average. An end member model was used to dissect the distribution into multiple Gaussian distributions, all with their own average and standard deviation (Figure 2.4, Appendix A). The average of 1.35 ‰ consists of three different Gaussian distributions having an average of 1.02, 2.03 and 2.54 ‰ respectively. The relative contribution of each population to the measured average $\delta^{18}O$ is 68, 23 and 9 % respectively.

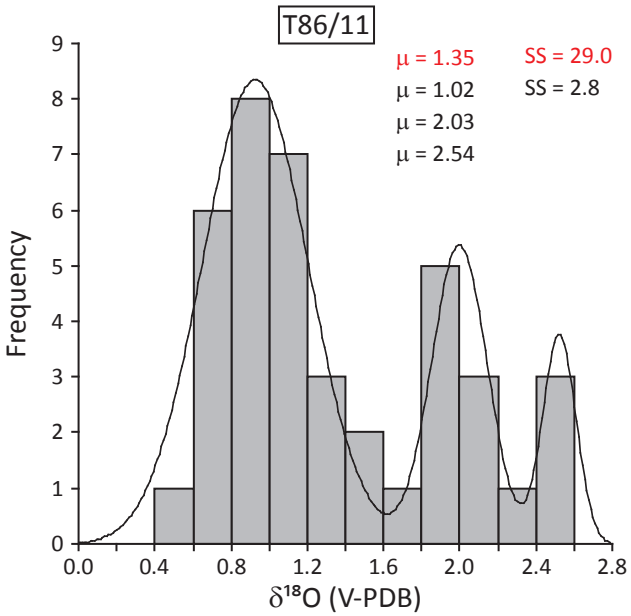

Figure 2.4 Frequency distribution and modeled Gaussian curve for site T86/11. The upper panel is the original modeled distribution. The lower panel displays the modeled Gaussian curves after recognizing multiple distributions present and entails the correction for bioturbation. The sum of squares (SS) is used to express the difference between the model and the measured frequency distribution.

The population with an average $\delta^{18}O$ of 1.02 ‰ seems to reflect the present day situation since this value correlates well with what is expected based on temperature and salinity (Figure 2.3) (WOA01, Conkright et al., 2001). Higher oxygen isotopic values reflect lower temperatures. The two most recent periods with appreciably lower temperatures in the North Atlantic compared to today are the Younger Dryas (YD) and the Last Glacial Maximum (LGM). Although temperatures during the Little Ice Age were probably somewhat lower than today, this would have an effect on stable oxygen isotopes of less than about 0.2 ‰ (Keigwin, 1996). The oxygen isotope values of 2.03 and 2.54 ‰ are thus most probably originating from older sediments, the YD or LGM respectively. This implies that specimen initially deposited during these two episodes have been bioturbated upward by at least 20 cm. (LGM is situated at around 20cm depth in the corresponding piston core, Ganssen unpublished data). Comparing the values of these two deconvolved signals with a *G. inflata* based $\delta^{18}O$ record for the last 20 ka at a nearby location (33°42'N, 57°35'W) (McManus et al., 2004) shows that the $\delta^{18}O$ value of 2.03 is typical for the Younger Dryas (12.5-14.2 ka), while 2.54 corresponds to the LGM (17.5-19.8 ka) (McManus et al., 2004).

Our data based on the analyses of single specimen planktonic foraminifer *G. inflata* shows that frequency distributions can be fitted with a uni- to polymodal distribution. A non-unimodal distribution strongly suggests admixing of specimen from a different source, such as through bioturbation. Quantification of these distributions allows deconvolving the original and bioturbated signals. In the core studied here one third of the $\delta^{18}O$ values measured were actually bioturbated upward from older sedimentary layers with a contrasting isotopic value. A similar contribution of younger specimen can be expected in the older layers. This shows that under low sedimentation rates an appreciable part of the signal can be derived from bioturbated sediments, significantly impacting climate reconstructions depending on averaged $\delta^{18}O$ values of foraminifera.

Acknowledgements

This research is funded by the Utrecht University and the Darwin Centre for Geobiology project "Biological validation of proxies for temperature, salinity, oxygenation and pCO_2 based on experimental evidence using benthic foraminiferal cultures".

Chapter 3

Approaches to unravel seasonality in sea surface temperatures using paired single specimen foraminiferal $\delta^{18}O$ and Mg/Ca analyses

J.C. Wit[1], G.-J. Reichart[1,2], S.J.A Jung[3], D. Kroon[3,4]

1 Department of Geochemistry, Utrecht University, Budapestlaan 4 3584 CD Utrecht, the Netherlands
2 Marine Biogeosciences, Alfred Wegener Institute for Polar and Marine Research, Am Handelshafen 12, D-27570 Bremerhaven, Germany
3 School of GeoSciences, Grant Institute, University of Edinburgh, United Kingdom
4 Department of Paleo-climatology and Geomorphology, Faculty of Earth and Life Sciences, Vrije Universiteit Amsterdam, The Nether lands

Published in *Paleoceanography* 25, PA4220, doi:10.1029/2009PA001857, 2010

Abstract

Seasonal changes in surface ocean temperature are increasingly recognised as an important parameter of the climate system. Here we assess the potential of analyzing single specimen planktonic foraminifera as proxy for the seasonal temperature contrast (seasonality). Oxygen isotopes and Mg/Ca ratios were measured on single specimens of *Globigerinoides ruber*, extracted from surface sediment samples of the Mediterranean Sea and the adjacent Atlantic Ocean. Variability in $\delta^{18}O$ and Mg/Ca was then compared to established modern seasonal changes in temperature and salinity for both regions. The results show that (1) average $\delta^{18}O$ derived temperatures correlate with modern annual average temperatures for most sites, (2) the range in $\delta^{18}O$ and Mg/Ca derived temperature estimates from single specimen analysis resemble the range in seasonal temperature values at the sea surface (0-50 m) in the Mediterranean Sea and the Atlantic Ocean, and (3) there is no strong correlation between Mg/Ca and $\delta^{18}O$ derived temperatures from the same specimens in the current dataset, indicating that other parameters (salinity, carbonate ion concentration, symbiont activity, ontogenesis and natural variability) potentially affect these proxies.

3.1 Introduction

A considerable amount of paleoclimate literature has focused on past changes in annual temperature. However, seasonal variations in temperature can be orders of magnitude larger than inter-annual variations, and both may be crucial to understanding past climate change. For example, Denton et al. (2005) showed that the onset of the Younger Dryas event involved an abrupt decrease in mainly winter temperatures, resulting in a major shift in seasonal temperature contrast. Somewhat analogue, the Mg/Ca from planktonic foraminifera, in cores from the Caribbean, covering the Last Glacial Maximum and Termination I, showed an increase in seasonal temperature contrast, due to deteriorating winter conditions (Ziegler et al., 2008). These interpretations of the seasonal temperature contrast are tentative, because calibrated and direct proxies for seasonality are lacking.

Stable oxygen isotope and Mg/Ca values in shells of planktonic foraminifera are standard tools to unravel the average temperature history of the surface ocean (Shackleton, 1974, Bemis et al., 1998, Lea et al., 1999, Elderfield and Ganssen, 2000). Previous studies, however, rarely assessed the seasonal aspect within these proxies. Seasonal variations in precipitation/evaporation control the $\delta^{18}O$(water) and salinity of seawater, whereas temperature controls fractionation of stable isotopes during carbonate formation. The $\delta^{18}O$ in foraminifera, therefore, represents $\delta^{18}O_{water}$ and temperature, while Mg/Ca values mainly reflect the temperature of the ambient seawater (e.g. Epstein et al., 1951, Shackleton, 1974, Elderfield and Ganssen 2000, Anand et al., 2003). Hence, seasonal variations in sea surface temperatures should be reflected in the $\delta^{18}O$ and Mg/Ca values of individual specimens, as they reflect environmental conditions during calcification through the year. Applied to deep-sea sediments, variability in $\delta^{18}O$ and Mg/Ca between individual specimens of one sample would be indicative for the seasonal temperature range depending on bioturbation and sedimentation rate.

Due to the geographic location and its enclosed nature, the Mediterranean experiences large seasonal changes reflecting the alternating influence of the African monsoon and more temperate parts of the northern hemisphere climate system (Rossignol-Strick, 1985 and references therein, Hurrell, 1995). Thus forming an ideal environment for testing this potential proxy for seasonality. In order to test the wider use of the method outside the Mediterranean Sea, a site from the North Atlantic was also examined. This site is contrasting to the Mediterranean and has smaller seasonal variations due to the open ocean environment. *Globigerinoides ruber* is a shallow dwelling (0-50 m) spinose species mainly living in oligotrophic waters (Hemleben

et al., 1989). Because of its shallow habitat this species has been used to reconstruct sea surface temperatures in numerous locations (e.g. Elderfield and Ganssen, 2000, Ganssen and Kroon, 2000, Anand et al., 2003) and occurs throughout the year in the Mediterranean Sea (Pujol and Vergnaud-Grazzini, 1995, Bárcena et al., 2004).

Here we used a new approach aiming at quantifying seasonal temperature changes in marine sediments by combining single specimen oxygen isotope and Mg/Ca-data from planktonic foraminifera, following earlier approaches by Spero and Williams (1989), Billups and Spero (1996), Ganssen et al. (2005) and Koutavas et al. (2006). In order to test the general applicability of our approach, we determined paired $\delta^{18}O$ and Mg/Ca derived temperature estimates of individual tests of *G. ruber* in a suite

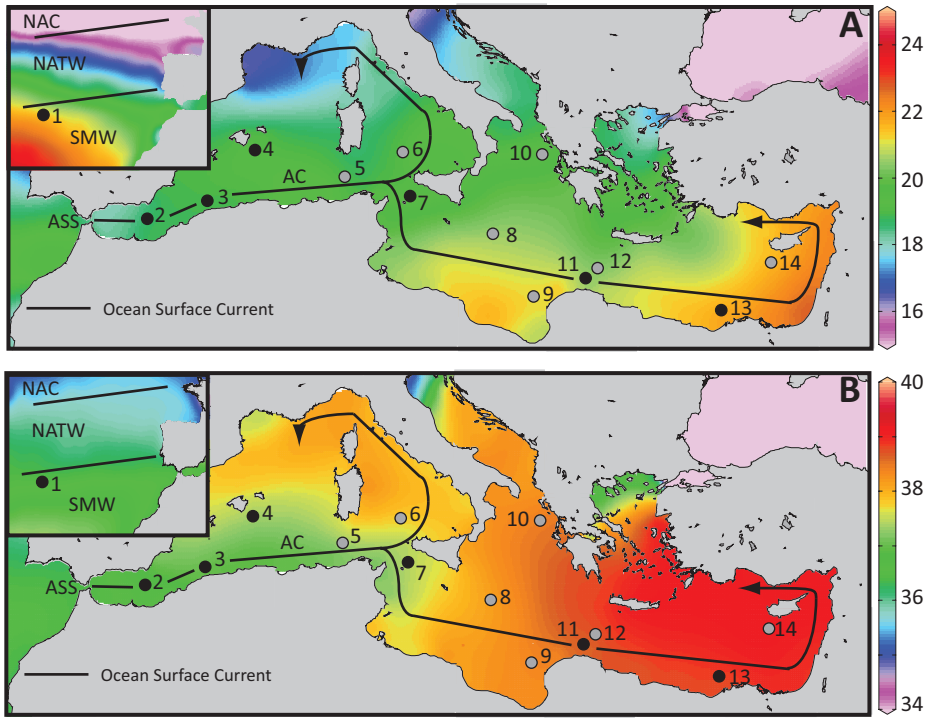

Figure 3.1 A) Annual average temperatures of the Mediterranean Sea and North Atlantic in °C. B) Annual average salinity of the Mediterranean Sea and North Atlantic. ASS = Atlantic Stream System, AC = Algerian Current, NAC = North Atlantic Current, NATW = North Atlantic Tropical Water, SMW = Subtropical Mode Water, Black dotes indicate sample locations where enough individual are measured to obtain a reliable measure of seasonality. Grey dots indicate sample locations where not enough samples were measured. The black arrows represent major surface currents. The number at each sample location corresponds to the number of each station in Table 3.1.

of surface sediment samples across the Mediterranean Sea, and then compared the results to the present day range in sea surface temperatures.

3.2 Surface Hydrography of the Mediterranean Sea

The Mediterranean Sea is a semi-enclosed basin, which can be divided into western and eastern basins (Figure 3.1). The general surface ocean circulation pattern is controlled by Atlantic surface water entering the Alboran Sea via the Strait of Gibraltar as the Atlantic Stream System (ASS) (Ovchinnikov, 1966, Millot, 1987). Further eastward the ASS continues as the Algerian Current (AC). The AC splits into two parts, one entering the Tyrrhenian Sea, the other entering the eastern Mediterranean through the Strait of Sicily (Ovchinnikov, 1966, Millot, 1987). The AC continues to flow through the Tyrrhenian Sea towards the Gulf of Lions. Further eastward the AC enters the Ionian Sea where it flows mainly eastward towards the Levantine Basin (Ovchinnikov, 1966).

Sample	Nr	Location	Longitude (E)	Latitude (N)	Depth (m)	WOA01 Temperature (°C)	Salinity
T86/11S	1	North Atlantic	-35.57	32.55	2220	20.84 (17.0-23.0)	36.62 (36.4-36.8)
T87/132	2	Alboran Sea	-2.91	35.78	936	17.34 (14.6-20.0)	36.79 (36.6-37.0)
T87/114	3	Algeria	2.59	36.94	1100	17.53 (14.5-20.8)	37.05 (36.9-37.2)
M40-4-88-1	4	Balearic Basin	4.60	38.94	1891	17.94 (14.1-22.6)	37.37 (37.3-37.5)
T87/83	5	Tunisia	8.76	37.70	1301	17.61 (14.3-21.3)	37.35 (37.1-37.7)
T87/61	6	Tyrrhenian Sea	11.34	38.25	1246	17.68 (14.1-21.8)	37.60 (37.5-37.8)
T87/49	7	Strait of Sicily	12.12	36.67	1205	18.20 (14.6-22.8)	37.42 (37.2-37.7)
T87/30	8	Ionian Sea	16.42	34.47	1400	19.60 (15.8-24.2)	38.07 (37.9-38.3)
M51-3-562	9	Libya	19.19	32.77	1391	19.90 (16.2-24.4)	38.33 (38.1-38.6)
T87/14	10	Greece	19.92	38.57	1999	17.98 (14.7-21.5)	38.49 (38.4-38.6)
T83/63	11	Libya	22.98	33.12	1093	19.36 (16.1-23.4)	38.63 (38.3-39.0)
M51-3-563	12	Libya	23.50	33.72	1851	19.26 (16.0-22.9)	38.76 (38.5-39.0)
T83/23	13	Nile Delta	29.41	31.88	1465	20.62 (16.5-24.8)	38.88 (38.2-39.1)
M51-3-569	14	Levantine Basin	32.58	33.43	1307	20.48 (16.6-24.6)	39.04 (38.9-39.3)

Table 3.1 Geographical position, depth temperature and salinity for all core top samples. Temperatures and salinity correspond to the 0-50 m depth average and come from the World Ocean Atlas 2001 (WOA01) database. Values are listed as averages, monthly minima and maxima (Conkright et al., 2002).

Seasonal temperature variation for surface waters (0-50 m) throughout the Mediterranean varies between 14.1 and 24.8 °C, with an annual average around 20 °C. Temperatures increase from west to east, as a result of the eastward surface water transport and the warm Mediterranean climate. The seasonal temperature contrasts are similar in the eastern and western Mediterranean being on average 7.3 ± 1 °C (Figure 3.1A, Table 3.1). Salinity (0-50 m) seasonally varies between 36.8 and 39.3, with an annual average of 38.2 over the entire Mediterranean Basin. The eastward flow of the surface waters, together with excess evaporation in the Mediterranean, causes a gradual increase in salinity from west to east (Figure 3.1B, Table 3.1). Seasonal changes in salinity do not vary from east to west, being 0.4 ± 0.2 (Table 3.1) on average.

Surface water transport in the central North Atlantic is mainly controlled by the north-eastward flowing Gulf Stream. Surface water (0-50 m) temperatures at central North Atlantic site T86/11S vary seasonally between 17.0 and 23.0 °C, with an annual average of 20.8 °C. Salinity seasonally varies between 36.4 and 36.8 with an annual average of 36.6. On an inter-annual time scale variability is probably controlled by branching of the Gulf Stream at 40°N-40°W into the North Atlantic Current (NAC) and the North Atlantic Tropical Water (NATW) (Hopkins, 1991). A second contributor to inter-annual variability is the shifting boundary between the NATW and the Subtropical Mode Water (SMW) (Hopkins, 1991) (Figure 3.1).

3.3 Methods

Core top sediment samples from areas covering a substantial part of the regional oceanographic differences in the Mediterranean Sea and the North Atlantic were used for picking planktonic foraminifera (Figure 3.1, Table 3.1). The T83, T86 and T87 box core samples were retrieved during 3 cruises of the R/V 'Tyro' covering all major basins of the Mediterranean Sea and North Atlantic (Ottens, 1991, De Rijk et al., 1999, Ganssen and Kroon, 2000). The M40/4, M51/3 and M52/2 core top samples were recovered during 3 cruises of the R/V 'Meteor' in the eastern Mediterranean (Hemleben, 2002, Hübscher, 2002).

A 1-2 cm core top slice from every sediment core was processed for foraminiferal analyses. In order to optimize sieving, samples were put in a sampling cup with distilled water and subsequently shaken for 90 minutes. Samples were wet-sieved into a >150 μm fraction and dried at 40 °C. The dried >150 μm fraction was subsequently sieved into 3 sub-fractions: 150-250, 250-400 and >600 μm. Specimens of the planktonic foraminiferal species Globigerinoides ruber were picked from the 250-400 μm

fraction.

The $\delta^{18}O$ values of single specimens of *G. ruber* were measured on a Mat Finnigan 252 gas-source mass spectrometer with an automated Kiel type carbonate preparation line and results were reported relative to the Vienna Pee Dee Belemnite standard (V-PDB). Calibration to the V-PDB was achieved through the NBS-19 standard. The internal reproducibility for $\delta^{18}O$ was ± 0.08 ‰. Estimates of the calcification temperatures based on stable oxygen isotopes were calculated using the temperature equation of O'Neil et al. (1969) as refitted by Shackleton (1974) (equation 3.1).

$$T = 16.9 - 4.38(\delta^{18}O_c - \delta^{18}O_w) + 0.1(\delta^{18}O_c - \delta^{18}O_w)^2 \quad (3.1)$$

The $\delta^{18}O_w$ values were calculated using the salinity - $\delta^{18}O_w$ relationship for the Mediterranean Sea based on the data from Pierre (1999) and Schmidt et al. (1999) (equation 3.2) and North Atlantic (Ganssen and Kroon, 2000).

$$\delta^{18}O_w = 0.285S - 9.47 \quad (3.2)$$

$\delta^{18}O_w$ values were converted from SMOW values to the V-PDB scale with the 0.27 ‰ correction of Hut (1987). We used annual average salinities for both areas, obtained from the World Ocean Atlas 01 (WOA01) database, since the seasonal timing of calcification is unknown (Conkright et al., 2002). Using annual average salinity introduced a potential error when calculating seasonal temperatures from individual foraminifera, even though seasonal variations in salinity were small for most sites (Table 3.4). Consequences of the use of annual average salinity for measured temperature variability will be dealt with in section 5.2.1.

We tested the measured $\delta^{18}O$ distributions for normality with a Shapiro-Wilk test (Table 3.2). None of the measured distributions significantly deviated from normality ($p < 0.05$) allowing a Gaussian filter to identify outliers. This approach enabled a quantitative comparison of the derived seasonal variation, expressed as 4 standard deviations (4 σ) with the maximum seasonal variation (range) as found in WOA01 database (Conkright et al., 2002). The whole range of WOA01 database temperatures was used, because temperature values already consisted of averaged monthly temperature data over multiple years and are, therefore, already filtered for outliers (Conkright et al., 2002).

Subsequently, we calculated 95% confidence limits of our standard deviations to

Sample	Standard deviation (°C)	Sample Size	Range 95% Confidence Intervals (°C)	Degrees of Freedom	p-value Shapiro-Wilk test
T86-11S	2.86	26	1.70	25	0.522
T87/132	1.94	16	1.57	15	0.421
T87/114	2.21	15	1.87	14	0.872
M40-4-88-1	2.39	17	1.86	16	0.629
T87/83	3.32	9	4.12	8	0.723
T87/61	2.47	15	2.09	14	0.372
T87/49	2.32	37	1.13	36	0.113
T87/30	2.95	15	2.49	14	0.387
M51-3-562	3.00	16	2.43	15	0.238
T87/14	3.28	8	4.51	7	0.147
T83/63	2.39	19	1.73	18	0.143
M51-3-563	3.42	15	2.89	14	0.960
T83/23	2.84	32	1.50	31	0.263
M51-3-569	3.08	10	3.50	11	0.580
Mediterranean	2.77	224	0.52	223	0.248
T86/11S (Mg/Ca)	3.76	15	3.18	14	0.067
T87/49 (Mg/Ca)	3.80	46	1.63	45	0.748

Table 3.2 Standard deviations with 95 % confidence intervals and p-values for the Shapiro-Wilk test per sample location. A $p > 0.05$ indicates that the sample distribution is not significantly deviating from normality.

evaluate their accuracy and to establish a clear criterion for a reliable estimate for seasonality, using the χ^2-distribution. Confidence limits may be calculated, since all measured distributions were not significantly deviating from normality. The standard deviation narrowed with increasing number of measurements. These constrains could be expressed as confidence intervals around the measured standard deviation and were calculated with equation 3.3.

$$\sigma\sqrt{(n-1)}/\ \chi^2\text{right} < \sigma > \sigma\sqrt{(n-1)}/\ \chi^2\text{left} \qquad (3.3, \text{Bluman, 2004})$$

In which σ was the measured standard deviation, n the number of measurements and χ^2right and χ^2left represented the values from the χ^2-distribution at the 95% confidence level. This implies a 95% probability of the standard deviation having a value within this confidence interval. Table 3.2 shows the 95% range around our calculated standard deviations based on single specimen analyses. We aimed to measure at least

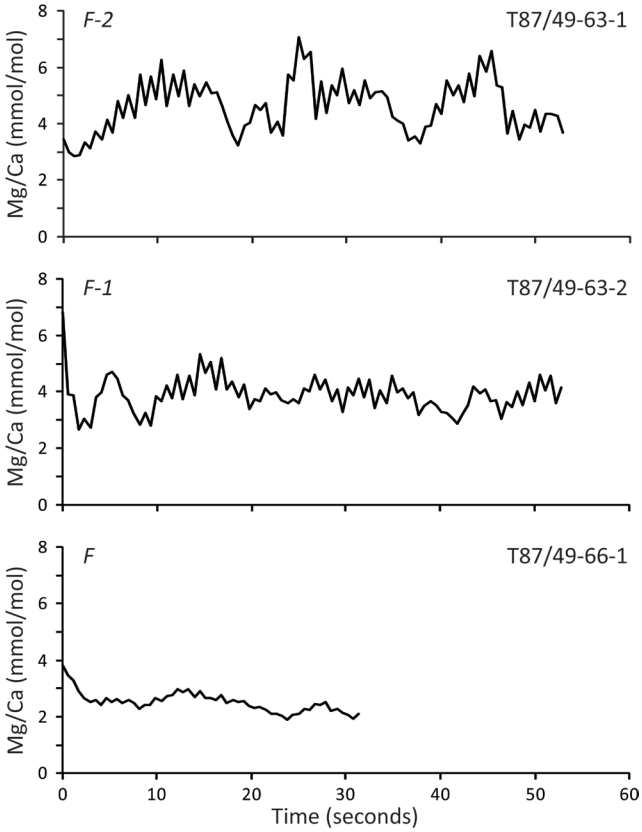

Figure 3.2 Measured Mg/Ca values for three different chambers of *G. ruber* during individual ablations. The Mg/Ca value of each test chamber is determined by averaging the Mg/Ca values acquired while ablating down-test. The last chamber (F) has less variability than F-1 and F-2, in line with previous results (Sadekov et al., 2008).

25 specimens per sample, in order to get a reliable seasonality estimate (4 σ). Standard deviations were only used for reconstructing seasonality if the range in confidence limits was smaller than 2 °C. This is a rather large range, due to the limited number of analyses available at each site. Although results appeared robust, large uncertainties are potentially associated with using limited sample sizes.

Samples for trace element analyses were six times sonically rinsed with MilliQ water and twice with MeOH for the removal of contaminated sediment following Barker et al (2003). Trace metal concentrations were measured on one or multiple chambers per individual with laser ablation ICP-MS. Multiple measurements per chamber were not possible, due to the limited test size and thickness of each individual chamber.

Foraminifera were ablated with a deep-ultraviolet-wavelength laser (193 nm) using a Lambda Physik excimer laser system with GeoLas 200Q optics. Test carbonate was ablated with a 80 μm beam diameter and a pulse repetition of 5 Hz for approximately 30-60 seconds with an energy density of 1 J/cm^2. Ablated material was transported on a He-gas flow and mixed with Argon. Element to calcium ratios were quantified using ^{24}Mg, ^{26}Mg, ^{27}Al, ^{42}Ca, ^{43}Ca, ^{44}Ca, ^{55}Mn, ^{88}Sr isotopes and their relative natural abundances on a quadrapole ICP-MS instrument (Micromass Platform). Raw counts were converted to elemental concentrations using computer software (Glitter). Elemental ratios were based on averaging the measured concentrations of the 100-300 pulses during each ablation (Figure 3.2). Calibration is performed against US National Institute of Standards and Technology SRM N610 glass (4 J/cm^2) and an in-house calcite standard GJR (1 J/cm^2) with ^{43}Ca as an internal standard (Reichart et al., 2003).

Changing the energy density from standard to sample could potentially influence trace metal concentrations measured. Laser ablation analyses, using different energy densities, was therefore compared to solution ICP-OES analyses of the same matrix matched calcite standard (GJR). Values showed no significant offset between results of both techniques and, therefore, changing energy density from standard to sample

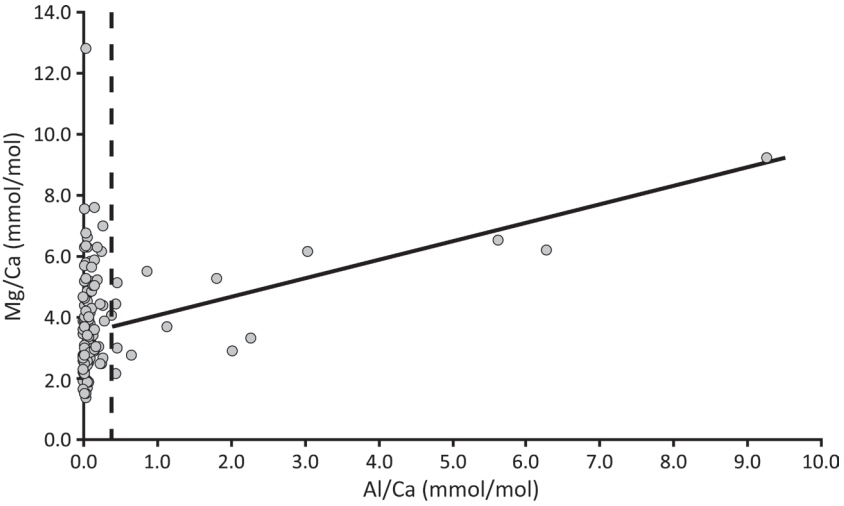

Figure 3.3 Mg/Ca plotted versus Al/Ca. The black line represents a relation between Al/Ca and Mg/Ca, suggesting a contaminant phase. Subsequently a cut-off point of 0.4 mmol/mol was used as the maximum acceptable Al/Ca value, below which no appreciable effect is noticed. Measurements to the right of the dotted line are therefore excluded from further consideration. Contamination is also recognised when evaluating the laser ablation profile of each individual measurement.

ICP-OES	Mg	Mn	Sr
Average	663	99	173
Standard deviation	35	0.40	4.3
Standard deviation (%)	5.2	0.41	2.5
N	3	3	3
LA-ICP-MS	Mg	Mn	Sr
Average	674	106	184
Standard deviation	61	7.2	15
Standard deviation (%)	9.1	6.9	8.0
N (4 year average)	643	643	643
Ratio	1.016	1.068	1.068

Table 3.3 Comparison between offline analyses of discrete samples dissolved and subsequently measured on ICP-OES and Laser Ablation ICP-MS analyses of the in-hause calcite standard (GJR). Values are listed in parts per million (ppm).

caused no appreciable offset (Table 3.3). Measurements were checked for contaminations by evaluating Al and Mn profiles acquired during ablation. Clay particles or post-depositional Mn-rich inorganic coatings, still attached to tests after cleaning, potentially offset the analyses. Both have a higher Mg concentration compared to the test, biasing the Mg measurements. Samples with high Al and Mn concentrations were, therefore, excluded from further evaluation (Figure 3.3). Measured Mg/Ca values were converted to temperature using the calibration of Anand et al. (2003) (equation 3.4).

$$Mg/Ca = 0.395e^{(0.09T)} \quad (3.4)$$

This calibration is based on a series of sediment trap samples spanning 6 years, covering multiple seasonal cycles (Anand et al., 2003). The calibration of Dekens et al. (2002), based on core top samples, closely resembled the calibration by Anand et al. (2003), whereas the calibration by Elderfield and Ganssen (2000) suggested a somewhat higher sensitivity of the foraminiferal Mg/Ca ratio to temperature.

Measured Mg/Ca distributions were also tested for a normal distribution pattern with a Shapiro-Wilk test. Both stations T87/49 and T86/11S were not deviating from normality and results could be fitted with a Gaussian curve. Standard deviations were

only used for reconstructing seasonality if the range in the 95% confidence limit was smaller than 2 °C, following the same approach as used for the oxygen isotopes.

3.4 Results

Here we present the combined results from the Mediterranean and Atlantic box-cores. For stations T87/83, T87/30, T87/14, M51-3-562, M51-3-563 and M51-3-569 not enough stable oxygen isotope data were available (i.e. confidence intervals larger than 2 °C) whereas for station T86/11S not enough Mg/Ca data was obtained. These stations are therefore not discussed individually (Figure 3.1, Table 3.2). The $\delta^{18}O$ data for individual samples display a normal (Gaussian) distribution pattern (Tables 3.2, 3.4, Appendix 3.1, Figure 3.4). The observed basin wide range in stable oxygen isotope variability in the Mediterranean Sea is 3.30 ‰, with a minimum of -0.90 ‰ (M40-4-88-1) and a maximum of 2.20 ‰ (M51-3-563). Figure 3.5 shows the distribution of the calculated $\delta^{18}O$ derived temperatures together with the observed temperatures from the World Ocean Atlas 2001 database (Conkright et al., 2002). Variation (4 σ) in $\delta^{18}O$ derived temperature for the Mediterranean sample locations is between 7.8 °C (T87/132) and 13.7 °C (M51-3-563) (Table 3.4).

Sample	4 σ $\delta^{18}O$ (°C)	Range Temperature (°C)	4 σ Salinity (°C)	4 σ $[CO_3^{2-}]$ (°C)
T86-11S	8.50	5.97	0.57	0.21
T87/132	7.76	5.41	0.48	0.16
T87/114	8.84	6.31	0.33	0.18
M40-4-88-1	9.56	8.49	0.30	0.19
T87/83	13.28	6.99	0.89	0.30
T87/61	9.88	7.64	0.47	0.28
T87/49	9.28	8.20	0.71	0.32
T87/30	11.80	8.39	0.61	0.34
M51-3-562	12.00	8.25	0.74	0.43
T87/14	13.12	6.83	0.28	0.22
T83/63	9.56	7.39	1.03	0.47
M51-3-563	13.68	6.88	0.78	0.51
T83/23	11.36	8.32	1.11	1.60
M51-3-569	12.32	7.66	0.55	1.63
Mediterranean	11.08	10.72	0.43	0.94

Table 3.4 Measured and observed $\delta^{18}O$ seasonality expressed as 4 σ. $\delta^{18}O$ variation (4 σ) for site T86/11S excludes two cold outliers. Salinity and temperature values are from the WOA01 database (Conkright et al., 2002). $[CO_3^{2-}]$ values are calculated using TCO_2 and alkalinity database values and the CO_2SYS program (Lewis and Wallace, 1998, Goyet et al., 2000).

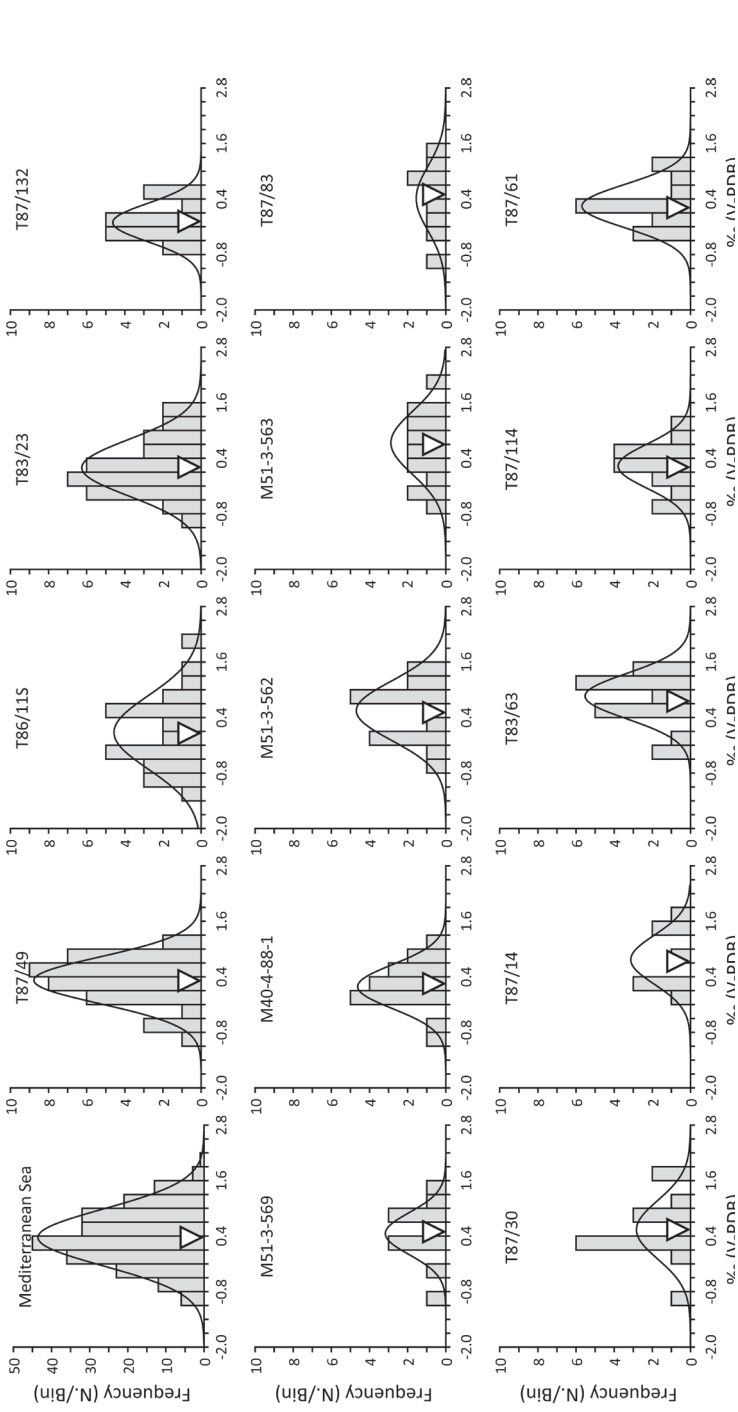

Figure 3.4 $\delta^{18}O$ distribution for all sites and the Mediterranean Sea. All distributions are fitted with a Gaussian curve (black line). The frequency axis displays the number of measurements within each bin of the histogram. The open triangle (point down) represents the average $\delta^{18}O$.

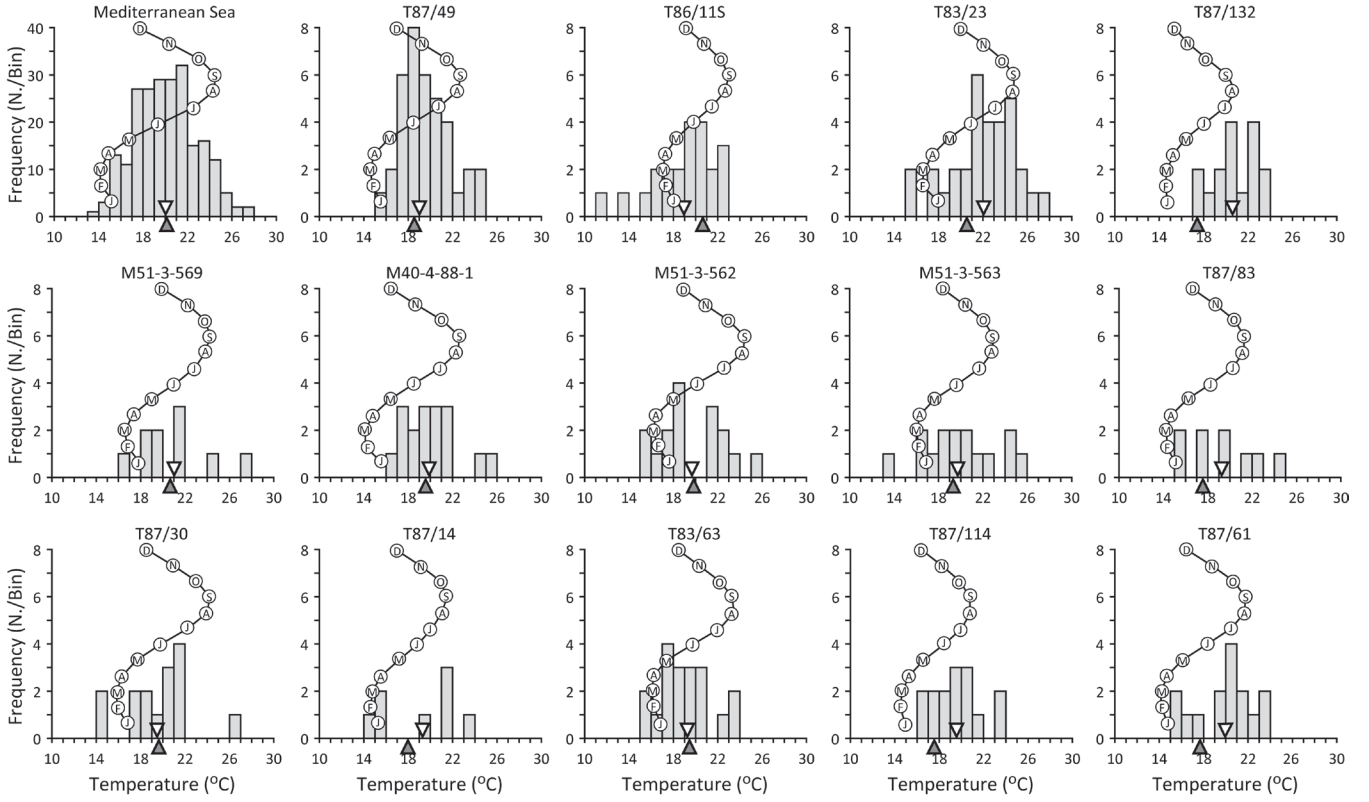

Figure 3.5 $\delta^{18}O$-temperature distribution for all sites and Mediterranean Sea water. Calculated temperatures are compared with observed sea surface temperatures (0-50 m) per month from the WOA01 Database (Conkright et al., 2002). The Frequency axis displays the number of measurements in each bin of the histogram. The open triangle (point down) represents the average $\delta^{18}O$ derived temperature, the closed triangle (point up) represents the average WOA01 derived temperature.

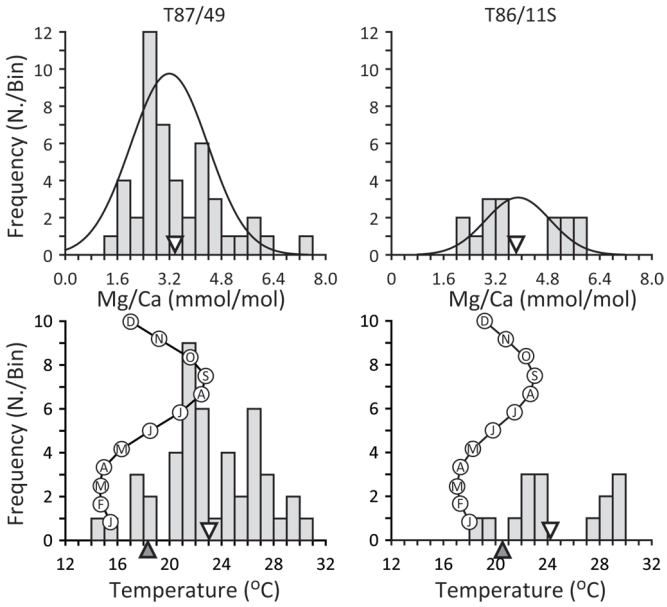

Figure 3.6 Mg/Ca and Mg/Ca derived temperature distributions for sites T87/49 and T86/11S. Mg/Ca distributions are fitted with a Gaussian curve (upper panels). The frequency axis displays the number of measurements in each bin of the histogram. Mg/Ca derived temperatures are compared with observed sea surface temperatures (0-50 m) per month from the WOA01 Database (Conkright et al., 2002). The open triangle (point down) represents the average Mg/Ca derived temperature, the closed triangle (point up) represents the average WOA01 derived temperature.

The measured distributions for Mg/Ca can be represented by a Gaussian curve (Table 3.2). A comparison between single specimen Mg/Ca measurements of Mediterranean site T87/49 and Atlantic site T86/11S, with fitted normal distribution, and the temperature distribution from the WOA01 is shown in figure 3.6. The variation (4 σ) in Mg/Ca data from individual specimen of cores T87/49 and T86/11S is 3.87 mmol/mol (11.3 °C) and 3.63 mmol/mol (10.0 °C) respectively (Appendix 3.2). The variability in Mg/Ca data (1 σ) between individual test chambers for site T86/11S alone ranges between 0.03 and 4.22 mmol/mol.

3.5 Discussion

3.5.1. Seasonal changes in temperature

3.5.1.1 Boundary conditions for reconstructing seasonality

Within a specific area of the ocean, the potential of a particular proxy to reconstruct seasonality will depend on how accurately it reflects the seasonal variability in water properties through time. For this study we have selected the planktonic foraminiferal species *G. ruber* because it reproduces at roughly constant levels throughout the year in the Mediterranean Sea and the Atlantic Ocean (Ottens, 1991, Pujol and Vergnaud-Grazzini, 1995, Bárcena et al., 2004). The variability in the chemical/physical properties at the sea surface throughout the year should, therefore, be recorded in specimens of *G. ruber* taken from the underlying sediment. The data generated in this study tests this assumption by separately evaluating the average $\delta^{18}O$ and Mg/Ca-derived temperature estimates for each site. When comparing observed annual average temperatures with estimates thereof based on $\delta^{18}O$ and Mg/Ca data, the respective data sets reasonably match each other, (Figures 3.4-3.6). Furthermore, observed differences between average $\delta^{18}O$ or Mg/Ca derived temperatures, and annual WOA01 temperatures are tested for significance using an independent t-test (Table 3.5). None of the $\delta^{18}O$ derived averages fail the null hypothesis, supporting that $\delta^{18}O$ values for *G. ruber* are recording annual average sea surface temperatures. Mg/Ca derived temperatures do, however, not accurately match the annual average temperature (Figure 3.6, Table 3.5). This might be mainly related to two causes. First, Mg/Ca-temperature calibrations are species-specific and vary with regional oceanographic settings. Second, Mg/Ca values in the current study are derived from point measurements using laser ablation ICP-MS, while published Mg/Ca-temperature calibrations are based on Mg/Ca-data from whole foraminiferal test (Elderfield and Ganssen, 2000, Dekens et al., 2002, Anand et al., 2003). This potentially causes an offset between Mg/Ca derived and annual temperatures, because of the more rigorous cleaning techniques used in whole foraminiferal test analyses, which preferentially removes Mg-rich carbonate phases, lowering the overall concentration (Barker et al., 2003).

Another factor impinging on seasonality reconstructions relates to migration of foraminifera through the water column during their life cycle. The effects of changes in depth habitat can be assessed by documenting the $\delta^{13}C$ and $\delta^{18}O$ values of individual foraminifera (Spero and Williams, 1988, 1989). The $\delta^{13}C$ values of Mediterranean Sea surface waters (0-50 m) are rather constant over short time scales (Pierre,

Sample	t-statistic	DF	Significance
T86/11S	-0.813	32	0.42
T87/132	1.879	17	0.077
T87/114	0.490	25	0.63
M40-88-1	1.890	27	0.070
T87/83	1.159	19	0.26
T87/61	1.625	25	0.12
T87/49	1.659	47	0.10
T87/30	-0.105	25	0.92
M51-3-562	-0.021	25	0.98
T87/14	0.937	18	0.36
T87/63	-0.219	29	0.83
M51-3-563	0.506	25	0.62
T83/23	0.464	42	0.65
M51-3-569	0.418	20	0.68
Mediterranean	-0.492	234	0.62
T86/11S (Mg/Ca)	1.990	18	0.072
T87/49 (Mg/Ca)	4.114	56	0.009

Table 3.5 Independently calculated t-statistic and its significance when comparing average $\delta^{18}O$ and Mg/Ca derived temperatures to annual temperatures reported in the WOA01 database. None of the $\delta^{18}O$ derived t-statistics are significant ($p < 0.05$), indicating that *G. ruber* captures the annual temperature at each sample location. Calculated t-statistics for Mg/Ca derived temperatures are (almost) significant, indicating that the Mg/Ca of *G. ruber* is not representing annual temperatures at both sample locations.

1999). Variability in $\delta^{13}C$ from foraminifera living within the upper euphotic zone is, therefore, mainly caused by changes in symbiont activity (Spero and Williams, 1988, 1989, Spero, 1992, Spero and Lea, 1993). Symbiont activity, in turn, is controlled by light intensity in the water column, which is a function of water depth. High light levels correspond to shallow water conditions with enriched $\delta^{13}C$ values, while low light conditions correspond to deeper depth habitats and subsequent depleted $\delta^{13}C$ values (Spero and Williams, 1988, 1989). Variations in settling depth also affect $\delta^{18}O$ values recorded in foraminifera with increasing values generally reflecting deeper habits. If variability in $\delta^{18}O$ caused by depth migrations would play a significant role in our calibration, we expect a negative correlation between decreasing $\delta^{13}C$ values and rising $\delta^{18}O$ values for individual foraminifera as shown by Spero and Williams (1988, 1989). For all but one station (station T87/114), the r values for the $\delta^{18}O$-$\delta^{13}C$ correlations and the respective significance levels (Appendix 3.3 and Table 3.6) show

no such correlation. Hence, this finding suggests that our seasonality reconstruction should be largely unaffected by variations in settling depth of *G. ruber* in this study. Data from station T87/114 have not been used for our seasonality reconstruction.

Additional parameters potentially interfering with our seasonality calibration are variations in sedimentation rates and bioturbation. A low sedimentation rate implies that a larger time interval is sampled, potentially enhancing variability within the sample. Subsequently, bioturbation increases the time interval captured in an individual sample, which also enhances the variability present in the sample. If we use the sedimentation rates at nearby locations of 10-30 cm/kyr (Rupke et al., 1974 and references therein, Tadjiki and Erten, 1994, Rutten et al., 2000) as a guideline, the core top samples used in this study encompass 70-200 years. Lower sedimentation rates would result in a longer time period covered in individual samples. Climate variability within the Mediterranean region for the past 200 years encompasses the Little Ice Age (DeMenocal et al., 2000, Schilman et al., 2001), potentially increasing the interannual variability in our data set. The good fit between $\delta^{18}O$ derived annual average

Sample	r	Significance
T86/11S	0.078	0.70
T87/132	-0.368	0.22
T87/114	-0.617	0.043
M40-4-88-1	-0.477	0.072
T87/83	-0.425	0.29
T87/61	-0.312	0.32
T87/49	-0.228	0.19
T87/30	0.240	0.43
M51-3-562	0.603	0.049
T87/14	0.018	0.97
T87/63	0.058	0.83
M51-3-563	0.470	0.24
T83/23	0.525	0.002
M51-3-569	0.312	0.38
Mediterranean	0.115	0.12

Table 3.6 Calculated correlation coefficients (r) and their significance level when comparing measured $\delta^{13}C$ and $\delta^{18}O$ values of individual foraminifera for each station. Pearson's r values are calculated, since $\delta^{13}C$ and $\delta^{18}O$ distributions are not deviating from normality.

and database observed annual average temperatures (Figure 3.5), however, suggests that inter-annual variability as a result of low sedimentation rates and bioturbation only plays a minor to moderate role in the current calibration.

3.5.1.2 Reconstructing seasonality

The previous lines of argument support the notion that not only annual average temperatures can be reconstructed using foraminiferal $\delta^{18}O$ and Mg/Ca data. The variability as seen in our $\delta^{18}O$ and Mg/Ca data set, measured on single specimen foraminifera, should predominantly reflect seasonal variations in sea surface temperature. We, therefore, made a direct comparison between the temperature variation (4 σ) deduced from the $\delta^{18}O$ data and the observed temperature range of the WOA01 (Max-Min), using only samples with a range in confidence limits of the standard deviation smaller than 2 °C (Table 3.2, Figure 3.7). The linear correlation between $\delta^{18}O$ derived temperature variation and WOA01 temperature range is remarkably good ($R^2 = 0.70$) with a slope of 1.14. We note that the regression line does not go through the origin, which is indicative of other factors influencing this relation as well. This suggests that $\delta^{18}O$ measurements on individual foraminifera can be used to reconstruct the seasonal temperature contrast, although other causes for $\delta^{18}O$ variability must be kept in mind.

3.5.2 Additional causes for $\delta^{18}O$ and Mg/Ca variability

In addition to seasonal changes in sea surface temperature other factors may influence shell chemistry and stable isotopic composition such as 1) salinity, 2) carbonate chemistry ($[CO_3^{2-}]$), 3) symbiont activity, 4) ontogenetic effects and 5) natural variability caused by unknown factors (Spero et al., 1997, Schiebel and Hemleben, 2005). We evaluate these parameters, calculating their potential impact on the $\delta^{18}O$-Mg/Ca variability and, therefore, the recording of seasonality.

3.5.2.1 Salinity

Local fluctuations in the precipitation/evaporation balance can alter the S-$\delta^{18}Ow$ relation (Rohling, 1999). In the Mediterranean Sea, however, the S-$\delta^{18}0w$ relation is relatively constant on a monthly to seasonal time scale limiting the bias in our data due to variations in the evaporation/precipitation balance (Rohling and Bigg 1998). Also, the use of average annual salinity values instead of actual salinity values during calcification adds uncertainty to the $\delta^{18}O_c$ derived temperature. A seasonal offset of

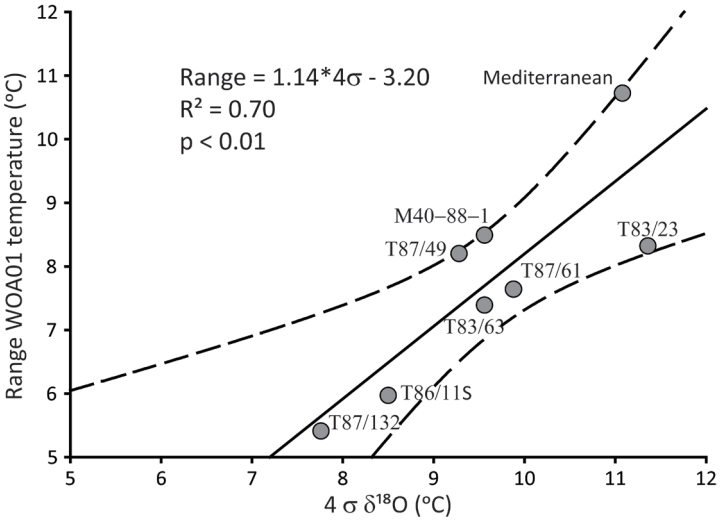

Figure 3.7 Four standard deviations of $\delta^{18}O$ derived temperatures versus the range (max-min) in WOA01 temperature for each sample location with 95 % confidence limit of the standard deviation being less than 2 °C. The Mediterranean data point is obtained by combining all measured $\delta^{18}O$ data from the Mediterranean boxcores, including stations with too large confidence limits for the standard deviations, and comparing them to the combined database temperatures of those same boxcores. This results in all other data plotted in this figure also being included in the Mediterranean data point, potentially biasing the independency of this point. The correlation coefficient is significant at the 99% level ($p < 0.01$). The dotted lines represent the 95% confidence limits of the regression line, but do not include the 95% confidence interval as calculated for each site in table 3.2.

0.1 in salinity would lead to an uncertainty of 0.12 °C in $\delta^{18}O$ derived temperatures,

when using equation 3.1 and 3.2 (Table 3.4), based on the WOA1 data. The effect of salinity is directly opposing the temperature effect on $\delta^{18}O_c$. Warm dry summers are concurring with high salinities in the Mediterranean, while low salinities are occurring during the relatively cold and wet winter. Warm summer temperatures result in lower $\delta^{18}O_c$ values, while the co-varying high summer salinities cause higher $\delta^{18}O_c$ values and vice versa in the winter. The combined effect due to inter-annual variations in summer and winter salinities through time, adds up to standard deviations in salinity between 0.06 and 0.24, implying a 2-11% uncertainty in $\delta^{18}O$ derived temperature.

Seasonal variations in salinity can also interfere with Mg/Ca as a temperature proxy. A change of 0.1 in salinity translates into an increase of 0.06 °C in Mg/Ca based tem-

peratures (Kisakürek et al., 2008), independent of changes in carbonate chemistry (Dueñas-Bohórquez et al., 2009). Fluctuations in salinity could thus explain 1.8% (T86/11S) and 2.2 % (T87/49) of the measured Mg/Ca derived temperature standard deviations.

3.5.2.2 Carbonate chemistry

Changes in the carbonate chemistry of the ambient seawater ($[CO_3^{2-}]$) potentially influence foraminiferal $\delta^{18}O$ and Mg/Ca values (Spero et al., 1997, Russell et al., 2004). The concentration of CO_3^{2-} in seawater influences the oxygen isotope signal of *G. ruber* with -0.0022 ‰ per µmol/kg change (Russell and Spero, 2000). An increase of 10 µmol/kg in carbonate ion concentration leads to an increase of 0.09 °C for $\delta^{18}O$. Calculated standard deviations in $[CO_3^{2-}]$ and its influence on $\delta^{18}O$ derived temperatures for all sites are in table 3.4. Changes in carbonate ion concentration could explain 2-14 % of the measured standard deviation in $\delta^{18}O$ derived temperatures.

The same calculations were made to evaluate the carbonate ion effect on the Mg/Ca derived temperatures. The Mg/Ca concentration in symbiont bearing planktonic species *Orbulina universa* changes with -0.021 µmol/kg per unit change in $[CO_3^{2-}]$ (Russell et al., 2004). Assuming this slope to be the same order of magnitude for *G. ruber*, since both species are symbiont bearing and live in a similar habitat, an increase of 10 µmol/kg in carbonate ion concentration leads to a decrease of 0.27 °C for Mg/Ca based temperatures. Hence, 4.2 % (T86/11S) and 6.5 % (T87/49) of the standard deviation of Mg/Ca derived temperatures could be attributed to a carbonate ion effect.

3.5.2.3 Symbiont Activity

A major impact of symbiont activity on foraminiferal $\delta^{13}C$ values has been demonstrated (Spero and Williams, 1988, Spero and Williams 1989, Spero, 1992, Spero and Lea, 1993). Impact of symbiont activity on foraminiferal $\delta^{18}O$ is, however, much smaller (Spero et al., 1997). Hence a linear relationship between the temperatures during the main period of reproduction of *G. ruber* and the overall $\delta^{18}O$ temperature at each site is still expected. Except for sites T87/132 (Alboran Sea) and T83/23 (Nile Delta) such a relationship indeed exists. With regard to the Alboran Sea, this area of the Mediterranean Sea is largely influenced by the Atlantic Ocean, leading to a more seasonal reproduction pattern of *G. ruber*. Fluctuations in Nile runoff reflect seasonal changes in precipitation, which has a large influence on the $\delta^{18}O$-salinity relation, explaining the aberrant data at station T83/23. Overall, the correlation between the

general $\delta^{18}O$ derived temperature and the temperature during peak reproduction periods of *G. ruber* supports the view that the effect of symbiont activity on oxygen isotopes is minor.

With regard to additional effects of symbiont activity on the Mg/Ca ratios in planktonic foraminifera, recent studies have reported large variations between individual foraminiferal tests (Lea et al.,1999) as well as within individual tests (Sadekov et al., 2008). Alternating layers of high and low Mg concentrations within the foraminiferal chambers of *G. ruber* found off West Australia for example suggested that the inter- and intra-individual variabiliyt in Mg/Ca could be connected to symbiont activity (Sadekov et al., 2008). Observations of the laser ablation Mg/Ca signal over single test chambers used in the present study revealed a similar layering of high and low Mg calcite (Figure 3.2). However, similar large variations in Mg/Ca are also found in symbiont barren species *Globigerina bulloides*, *Globorotalia inflata* and *Globorotalia truncatulinoides* (Anand and Elderfield, 2005, Hathorne et al., 2009), suggesting symbiont activity is only playing a minor role in Mg/Ca variability.

3.5.2.4 Ontogenetic Effects

Changes in growth rate related to different life stages of a foraminifer, hence size, have an important effect on the stable isotope composition of their shell (Kroon and Darling, 1995, Spero and Lea, 1996, Bijma et al., 1998). Changes in growth rate related to different life stages of a foraminifer, hence size, have an important effect on the stable isotope composition of their shell (Kroon and Darling, 1995, Spero and Lea, 1996, Bijma et al., 1998) The used size range for this study (250-400 μm) can explain a range in oxygen isotopes of 0.3 ‰ (Kroon and Darling, 1995). An ontogenetic effect on the oxygen isotopes could, therefore, explain 2.2 to 3.9 % of the measured 4 σ variability in this study. A possible ontogenetic overprint on the seasonality reconstruction should, therefore, be kept in mind when interpreting single specimen $\delta^{18}O$ variability. The impact of ontogenetic effects on $\delta^{18}O$ in foraminifera on paleo-climate reconstructions has been stipulated by Spero and Lea (1996). These ontogenetic effects may also influence the Mg/Ca distribution in foraminifera and can be divided in two components, namely the formation of a final layer of thick calcite enveloping the whole test (GAM-calcite) at the end of the foraminifers live cycle and a decreasing trend in trace metals and stable isotopes with test size (Nürnberg et al., 1996, Bijma et al., 1998). Measurements of GAM calcite in *G. sacculifer* indicate a decrease in Mg/Ca values after calcification of gametogenic calcite, in line with the decreasing trend with

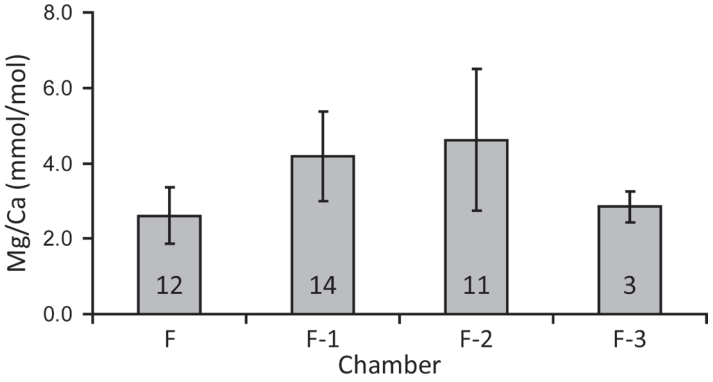

Figure 3.8 Mg/Ca intra-test variation for site T86/11S. Chambers are numbered from the final (F) chamber downward in the spiral. The number in each column represents the amount of individual foraminifera measured for the chamber average. Error bars are based on the variability, expressed as a standard deviation, between the measurements of single chambers.

test size (Bijma et al., 1998, Dueñas-Bohórquez et al., 2009). Observed intra-test variability shows a decrease in Mg/Ca values with chamber position in the test (Figure 3.8). An analysis of variance (ANOVA) was conducted to assess whether this trend was significant. Results show that the mean values for the last 3 chambers are significantly different ($F=7.028$ (20), $p < 0.05$). Furthermore, it is shown that the difference between the final chamber (F) and the F-1 and F-2 chambers is significant ($t = 4.59$ (26), $p < 0.05$), while the difference between the F-1 and F-2 chamber is not ($t = -0.647$ (16), $p > 0.05$). The significant decrease in Mg/Ca values would imply colder temperatures with increasing test size. This trend of decreasing temperatures is also seen in oxygen isotopes from symbiont bearing planktonic species *G. siphonifera* (Bijma et al., 1998), suggesting that ontogenetic effects are linked to the intra-test variability in Mg/Ca from *G. ruber*. The magnitude (9.8 °C) of the intra-test variability is, however, larger than any variation in temperature or seawater chemistry encountered during the foraminifers life cycle. The intra-test variability is, therefore, probably caused by differences in Mg/Ca incorporation with each ontogenetic stage of *G. ruber*. This is, however, not affecting the reconstruction of seasonality, since we picked from a size fraction which is sufficiently small (250-400 µm) to exclude any major ontogenetic effect on the average single specimen Mg/Ca derived temperatures.

3.5.2.5 Natural variability

Natural variability is here used to describe variation in $\delta^{18}O$ caused by unknown (biologically-controlled) mechanisms within the calcification process, and may have an

additional effect on the measured $\delta^{18}O$ variability. If natural variability is for instance 0.3 ‰, then every measured $\delta^{18}O$ value actually falls within a 0.3 ‰ range from the measured value and, therefore, introduces an additional uncertainty. Knowledge on the amplitude of natural variability within one population of foraminifera is, therefore, of vital importance for interpreting the measured standard deviations. Independent information on natural variability from the current dataset cannot be obtained, since this data is generated from a series of core top samples. We, therefore, used the data of Russell and Spero (2000) instead. They measured single specimen $\delta^{18}O$ on *G. ruber* tests from a series of sediment traps in the eastern equatorial Pacific and assume that natural variability is primarily species specific. This is realistic since natural variability is probably largely biologically controlled. The standard deviation over a 1.5-3 day period in the Pacific sediment trap is 0.87 °C (based on $\delta^{18}O$) and could potentially explain 25-45 % of the measured standard deviations in our samples.

Natural variability in Mg/Ca could have similar effects as it does for $\delta^{18}O$, and therefore may have an important impact on the measured Mg/Ca variability. To make an assessment on the natural variability within a population of *G. ruber* we used the Mg/Ca measurements of a plankton-pump dataset from Sadekov et al. (2008). This dataset has a standard deviation of 1.9 °C. Hence, natural variability could potentially explain 52 % (T87/49) and 63 % (T86/11S) of the measured standard deviation, again assuming that the values for natural variability are species specific.

3.5.4 $\delta^{18}O$-Mg/Ca derived temperature comparison

Despite uncertainties, single specimen $\delta^{18}O$ and Mg/Ca variability can be used for reconstructing sea surface temperature seasonality, as indicated by the good correlation between measured variability and WOA01 temperature data. The fact that our data are derived from the same individual foraminiferal test also allows calculating the linear correlation coefficient between $\delta^{18}O$ and Mg/Ca derived temperatures. Theoretically, if both proxies would record temperature of the ambient water perfectly, the R^2 of such a relation should be close to 1. No clear linear correlation is, however, observed when comparing $\delta^{18}O$ and Mg/Ca derived temperatures of core T86/11S and T87/49, implying an offset in one or both of the temperature proxies (Figure 3.9). One of the causes of this offset could be the position of T86/11S at the boundary of two major water masses in the North Atlantic, causing an error in the used $\delta^{18}O_w$ for calculating the oxygen isotope derived temperatures (Figure 3.1).

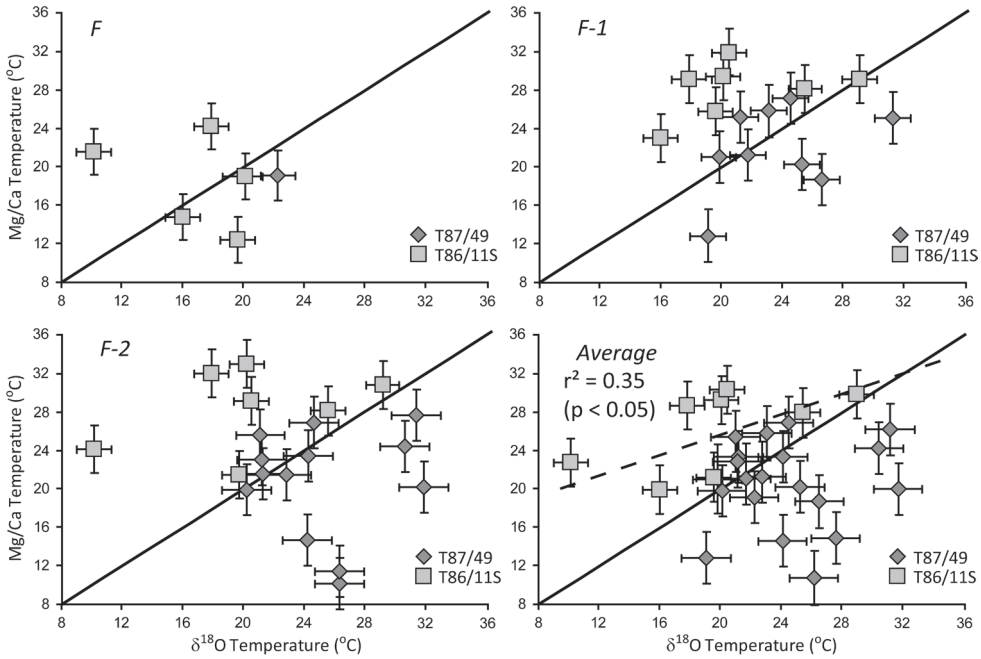

Figure 3.9 $\delta^{18}O$ versus Mg/Ca derived temperatures for sites T87/49 and T86/11S. Error bars include temperature uncertainties caused by salinity, carbonate ion concentrations and natural variability. Final chamber (F), second last chamber (F-1) and third last chamber (F-2) Mg/Ca derived temperatures are based on one chamber of a single foraminifer only. Mg/Ca derived temperatures for the average are based on measurements on multiple chambers of a single foraminifer. The dotted line in the average panel represents the regression line for the T86/11S samples. The correlation coefficient is significant at the 95% level ($p < 0.05$).

Values for T86/11S, however, appear to show a slight significant positive trend (dotted line Figure 3.9). Reconstructed $\delta^{18}O$ derived temperatures for site T87/49 did, however, record annual conditions as well as the seasonal temperature contrast (Figures 3.5 and 3.7). The question of what is causing this apparent offset between individual $\delta^{18}O$ and Mg/Ca derived temperatures, therefore, still remains. Here, we propose two possible causes. First, the Mg/Ca measurements are derived from laser ablation ICP-MS analyses on foraminiferal chambers and therefore represent point measurements. While the $\delta^{18}O$ composition of the foraminiferal shell is measured by dissolving the entire shell and represents an integrated values for the whole foraminifer. A direct comparison between these values could thus introduce an offset and/or variability between both temperature proxies. Second, single specimen $\delta^{18}O$ and

Mg/Ca variability is influenced by other parameters than temperature alone, as we already argued. Two of the discussed parameters, salinity and $[CO_3^{2-}]$, cause a systematic offset. These offsets are, however, not the same for $\delta^{18}O$ and Mg/Ca. As already shown, an 0.1 increase in salinity will cause an uncertainty of 0.12 and 0.28 °C in $\delta^{18}O$ and Mg/Ca derived temperatures respectively, causing a slight offset between both temperatures. An increase of 10 µmol/kg in $[CO_3^{2-}]$ will cause a 0.09 °C increase and a 0.27 °C decrease in $\delta^{18}O$ and Mg/Ca derived temperatures respectively, causing a 0.36 °C per 10 µmol/kg change. The mechanism behind natural variability remains unknown, causing the offset produced by natural variability to be unpredictable. In a worst case scenario natural variability could cause an offset of 2.8 °C (0.87 °C for $\delta^{18}O$ and 1.9 °C for Mg/Ca). All these factors combined could explain the large offset seen in figure 3.9.

3.6 Conclusions

The results show that averaged $\delta^{18}O$ derived temperatures measured on single specimen *G. ruber* test correspond to average annual temperatures, with the perquisite there is no seasonal bias at the sample location. Measured inter-test variations in both $\delta^{18}O$ and Mg/Ca of single specimen *G. ruber* tests largely concur with observed annual temperature variability (seasonality) if enough specimens are measured (i.e. confidence limits of the standard deviations < 2 °C). This suggests that both proxies of single specimen *G. ruber* tests independently record seasonality. But it remains largely unclear why the two temperature proxies from the same individual specimen differ. A possible explanation could be that seasonal changes in salinity, carbonate ion concentration and especially natural variability are causing a major part of the measured offset. Accurate reconstruction of seasonality, therefore, hinges on our ability to quantify these effects in the past. The biological mechanisms behind natural variability are still unknown and could be related to changes in the foraminifer's microenvironment. An assessment of these mechanisms is, therefore, of vital importance for reconstructing natural variability and, therefore, an accurate reconstruction of seasonality.

Acknowledgements

We would like to thank Simon Troelstra, Lia Auliaherliaty and Karl Emeis for providing samples. We appreciate the assistance of Paul Mason and Gijs Nobbe with laser ablation analyses. Hans de Moel is thanked for his help with the statistical data

treatment. Further, we want to thank Martin Ziegler and 3 anonymous reviewers for providing constructive comments on this manuscript and an earlier draft. This research is funded by the Utrecht University, the Vrije Universiteit Amsterdam and the Darwin Centre for Geobiology projects "Assessing the seasonality evolution in the Mediterranean Sea: calibration of carbonate-based proxies and application in selected time slices" and "Biological validation of proxies for temperature, salinity, oxygenation and pCO_2 based on experimental evidence using benthic foraminiferal cultures".

Chapter 4

A reappraisal of the vital effect in cultured benthic foraminifer *Bulimina marginata* on Mg/Ca values: assessing temperature uncertainty relationships

J.C. Wit[1], L.J. de Nooijer[1], C. Barras[2], F.J. Jorissen[2], G.J. Reichart[1,3]

1 Department of Geochemistry, Utrecht University, Budapestlaan 4 3584 CD Utrecht, the Netherlands
2 Laboratory of Recent and Fossil Bio-Indicators, Angers University, 2 Boulevard Lavoisier, F-49045, Angers, France
3 Marine Biogeosciences, Alfred Wegener Institute for Polar and Marine Research, Am Handelshafen 12, D-27570 Bremerhaven, Germany

Published in Biogeosciences 9, 1-12, 2012, doi: 10.5194/bg-9-1-2012

Abstract

The reconstruction of past temperatures is often achieved through measuring the Mg/Ca value of foraminiferal test carbonate. The diversity in foraminiferal Mg/Ca-temperature calibrations suggests that there is also a biological control on this proxy. This study presents a new Mg/Ca-temperature calibration for the benthic foraminifer *Bulimina marginata*, based on cultures under a range of temperatures (4-14 °C). Measured Mg/Ca values for *B. marginata* correlate with temperature ($Mg/Ca = (1.10 \pm 0.10)\ e^{(0.045\pm0.009)T}$, $R^2=0.28$ $p<0.01$). The inter-individual variability is, however, also significant (standard deviation is 10-35% of the average). Before applying this or any calibration, the effect of the inter-individual variability on the accuracy of the Mg/Ca-temperature calibration has to be evaluated. The inter-individual variability is quantified and split in three components, namely 1) an analytical error 2) an environmental effect and 3) a vital effect. The effect of inter-individual variability on the accuracy of Mg/Ca-temperature calibrations is depending on the sensitivity of the used calibration and the number of individuals measured (Temperature Uncertainty $= (0.33N^{-0.50})$/sensitivity). The less sensitive a calibration, the greater is the impact of inter-individual variability, which can partly be circumvented by measuring more individuals. This study shows the link between inter-individual variability and sensitivity and quantifies their influence on the accuracy of Mg/Ca-temperature calibrations.

Differences in the sensitivity of the Mg/Ca-temperature calibration of foraminifera may depend on the environmental conditions in which foraminifera live and their concurring ecological strategies.

4.1 Introduction

The ratio of magnesium to calcum in the calcite of benthic foraminifera (i.e. test Mg/Ca) is an important tool to reconstruct past bottom water temperatures. From basic thermodynamic principles it follows that the rate of substitution of Mg-ions for Ca in the $CaCO_3$ lattice increases with temperature. The incorporation of Mg into foraminiferal calcite is thus expected to primarily depend on changes in environmental temperature. However, incorporation of Mg is also affected by other environmental parameters, including salinity, carbonate ion concentration (CO_3^{2-}) and seawater Mg/Ca (Mg/Ca_{SW}) (Nürnberg et al., 1996, Elderfield et al., 2006, Wit et al., under review). Moreover, most foraminiferal species produce calcite with a Mg/Ca value approximately an order of magnitude lower than those from inorganic precipitation experiments (Bentov and Erez, 2006, Morse et al., 2007). This shows that, besides an environmental control, there is also a strong biological control on Mg incorporation. The difference in element (and isotope) composition between biologically and inorganically precipitated calcium carbonate is often abbreviated as the vital effect (Urey et al., 1951, Weiner and Dove, 2003) and is caused by biological impacts on the calcification process (Erez, 2003, Bentov and Erez, 2006, De Nooijer et al., 2009a). These include modifications of the internal pH, thereby affecting the carbonate ion concentration of the calcification environment, potentially altering the Mg/Ca of the calcite precipitated (Elderfield et al., 2006, Bentov and Erez, 2006, De Nooijer et al., 2009b). Active discrimination against magnesium during production of a privileged space in which high concentrations of Ca^{2+} are actively maintained is another example of how these vital effects impact foraminiferal Mg/Ca values (Erez, 2003, Bentov Erez, 2006, De Nooijer et al., 2009a). The vital effect is responsible for the difference in Mg/Ca values between species, indicated by large inter-species differences in Mg incorporation at the same temperature (Lear et al., 2002, Anand et al., 2003, Rathmann et al., 2004, Elderfield et al., 2006, Rosenthal et al., 2011, Toyofuku et al., 2011, Wit et al., under review). Variability in Mg/Ca between individual tests of the same species, furthermore, suggests that the biologically-induced offset might not be constant within one species. Part of such variability may be caused by changes in the (micro)-environment in which foraminifera calcify. Infaunal benthic species,

for example, experience rapidly changing chemical gradients in the sediment that can affect Mg incorporation and introduce intra- and inter-individual variability in Mg/Ca. The inter-individual variability as a result of vital effects is significantly affecting temperature reconstructions based on foraminiferal Mg/Ca values (Sadekov et al., 2008, Hathorne et al., 2009). The ability to quantify and recognize the amplitude, and changes therein, of the vital effect is thus of vital importance in improving the accuracy of the Mg/Ca-thermometer.

Despite differences between species-specific Mg/Ca-temperature calibrations, most calibrations found are described by an exponential function linking Mg/Ca and temperature (Equation 4.1)

$$Mg/Ca = \mathbf{a}\, e^{(\mathbf{b}T)} \qquad (4.1)$$

where T is the temperature in degrees Celsius and **a** and **b** are empirically derived species-specific constants. The pre-exponential constant **a**, equals the (theoretical) Mg/Ca at 0 °C and the exponential constant **b** describes the steepness of the slope with increasing temperature and is often referred to as the sensitivity of the Mg/Ca-temperature calibration.

Here a new Mg/Ca-temperature calibration based on cultured specimens of the benthic foraminifer *Bulimina marginata* is presented. Within the culture setup, maintained at a range of set temperatures, all other parameters influencing foraminiferal Mg/Ca values (salinity, carbonate ion concentration, seawater Mg/Ca) were kept constant in a controlled environment. Such a culturing approach in which environmental parameters are rigorously constant for all individuals is vital for the assessment of intra-individual variability in foraminiferal Mg/Ca due to biologically factors as benthic foraminifera, especially infaunal living species such as *B. marginata*, calcify in a wide range of biogeochemically different micro-environment. This study thus allows accurate quantification of inter- and intra-individual variability as a result of biologically controlled changes in the foraminiferal calcification process, as all other parameters are kept constant within the experiment. This calibration study thus provides insight into the environmental and biological factors potentially offsetting Mg/Ca-temperature calibrations and the effect on the accuracy of this paleothermometer.

Experiment	Temperature (°C)	Salinity	Alkalinity (µmol/l)	pH	DIC (µmol/l)	CO_3^{2-} (µmol/l)
1 [2]	4.1 ± 1.1	35.8 ± 0.1	2528 ± 13	7.80 ± 0.07	2492 ± 23	60 ± 8
2 [2]	6.0 ± 0.5	35.8 ± 0.1	2524 ± 12	7.80 ± 0.08	2480 ± 25	64 ± 10
3 [3]	7.9 ± 0.1	35.8 ± 0.1	2452 ± 30	7.93 ± 0.05	2357 ± 24	87 ± 7
4 [2]	9.3 + 0.7	35.8 ± 0.1	2524 ± 13	7.78 ± 0.09	2473 ± 29	69 ± 12
5 [2]	10.2 ± 0.1	35.8 ± 0.1	2454 ± 32	7.94 ± 0.05	2344 ± 41	96 ± 10
6 [1]	11.3 ± 0.3	34.7 ± 0.2	2470 ± 73	8.14 ± 0.22	2215 ± 18	187 ± 54
7 [2]	12.7 ± 0.1	35.9 ± 0.1	2473 ± 34	7.98 ± 0.04	2334 ± 32	114 ± 8
8 [1]	14.0 ± 0.2	35.0 ± 0.2	2500 ± 77	8.16 ± 0.03	2206 ± 6	214 ± 48
Average	9.7	35.6	2494	7.9	2373	107
σ	3.2	0.4	32.4	0.1	110.7	55.7

Table 4.1 Average and standard deviation of the main seawater parameters for all temperature experiments. Experiments contain samples from cultures at 1) Utrecht University, 2) University of Angers or 3) combined samples.

4.2 Methods

Living specimens of the benthic, symbiont-barren foraminifer *Bulimina marginata* were collected from two stations in the Bay of Biscay (450 m and 600 m deep). Isolated specimens were placed in culture set-ups between 4 and 14 °C (natural range for *B. marginata* in the Bay of Biscay) at Utrecht University and the University of Angers (8 experiments, table 4.1). Growth was monitored through incorporation of the fluorescent marker Calcein after which the foraminifera were introduced to the experimental set-up. This compound is a suitable marker for recognizing newly formed calcite (Bernhard et al., 2004), and does not affect the incorporation of Mg and Sr in foraminiferal calcite (Dissard et al., 2009).

Two different culture setups were used for this Mg/Ca-T calibration: 1) an open system using 250 ml water, of which the seawater was replaced weekly to bi-weekly and 2) a closed system with seawater circulation from a large reservoir (25 l) towards the different experiments (Barras et al., 2010). Temperature was controlled in climatic controlled incubators, which were set at the preferred temperatures. Seawater from both setups was sampled weekly to monitor salinity, total alkalinity and pH or dissolved inorganic carbon (DIC) of the media. Total alkalinity and DIC or pH were used to calculate the carbonate ion concentration ($[CO_3^{2-}]$), using the CO2SYS software (Lewis and Wallace, 1998) (Table 4.1).

Experiments ran for 2-3 months to maximize the chance of sufficient calcite addition. Specimens were harvested by sieving over a 63 µm mesh with de-ionized water. After

terminating each experiment, specimens were cleaned for 20 minutes in 5% NaClO to dissolve organic matter attached to the surfaces of the foraminiferal shells. Afterwards individual foraminifera were rinsed 3-6 times with MilliQ and 2 times with methanol (Utrecht samples) to prepare the samples for trace metal analysis (Barker et al., 2003, Wit et al., 2010, Rosenthal et al., 2011).

Elements were measured, on newly calcified chambers of adult foraminifera, as a ratio to calcium with laser ablation inductively coupled mass spectrometry (LA-ICP-MS), using a deep ultraviolet wave length laser (193 nm) with a Lambda Physik excimer laser system with Geolas 200Q optics and a quadrapole ICP-MS instrument (Micromass Platform) (Reichart et al., 2003). Laser ablation spot size was 80 μm and foraminiferal chambers were ablated through the whole outer test wall. Measured el-

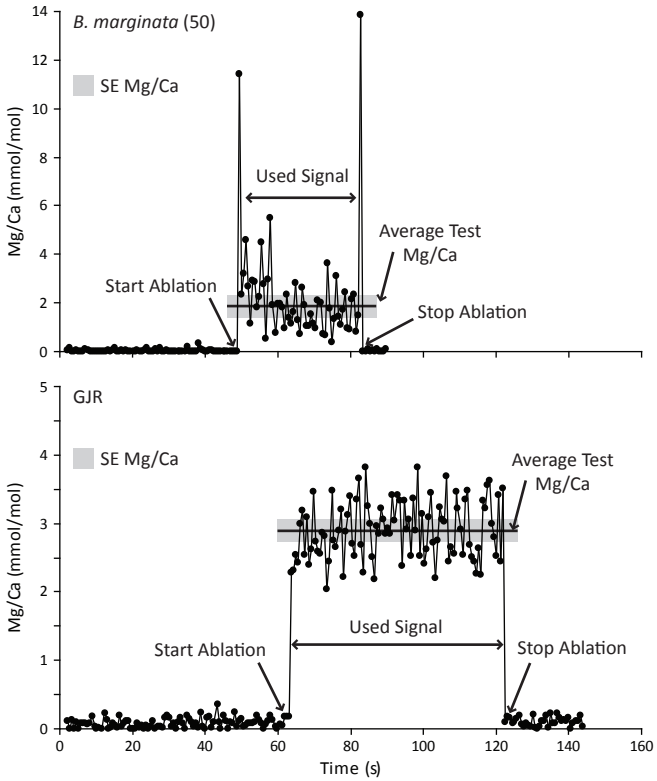

Figure 4.1 Laser ablation profiles for Mg/Ca measured on benthic foraminifer *B. marginata* (upper panel) and the inhouse GJR standard (lower panel). Parts of the profiles with elevated magnesium at the surface of the chamber walls are removed before calculating the average Mg/Ca. The absence of peak values for Mg/Ca in the GJR standard at the start and end of the ablation rule out any instrumental cause for the spikes observed in *B. marginata*.

ements included ^{24}Mg, ^{26}Mg, ^{27}Al, ^{42}Ca, ^{43}Ca, ^{44}Ca, ^{55}Mn, ^{88}Sr and their relative natural abundances. Mg/Ca ratios were determined using obtained ^{24}Mg concentration and assuming 40 wt% ^{44}Ca in $CaCO_3$. Counts for ^{26}Mg were used to check for consistency of the ^{24}Mg concentrations. Element/Ca ratios were calibrated against the NIST 610 and an in-house calcite standard, verifying that differences in ablation energy do not affect measured elemental concentrations (Hathorne et al., 2008, Wit et al., 2010). Of all measured data, about 22 % was discarded because ablation profiles were too short (less than 20-30 pulses at 6 Hz), contamination values for Al were to high (> 20 ppm) or the standard deviation of the measurement was too high (> 70 ppm for Mg). High standard deviations in individual measurements are indicative for a heterogeneous distribution of Mg through the foraminiferal chamber wall. Elemental ratios with respect to Ca were based on the average of each ablation profile (Figure 4.1). Individual foraminiferal Mg/Ca values were based on the average of 1-4 measured test-chambers. Foraminifera were measured for size, in order to assess any ontogenetic effect within the Mg/Ca-temperature calibration, using an ocular with a build in scale bar, which was scaled on a 1 mm slide. Size was determined by measuring the height of each individual *B. marginata*. The very small size of the first chambers makes it impossible to count the chamber number in this species, hampering comparison with previously reported ontogenetic trends (or absence thereof) in element/Ca ratios based on chamber number (Dueñas-Bohórquez et al., 2011a, De Nooijer et al., under review).

4.3 Results

All culture experiments were monitored for stability of temperature, salinity, alkalinity and pH (University of Angers) or DIC (Utrecht University) (Table 4.1). Individuals of *Bulimina marginata* calcified 1-4 new chambers in every experiment (Barras et al., 2010). The Mg/Ca of the newly formed calcite was measured by laser ablation ICP-MS. Recognition of enriched trace element concentrations at the inner and outer surface of the test wall enables removal of contaminations before calculation of the average foraminiferal Mg/Ca (Figure 4.1). Values for Mg/Ca of individual specimens range from 0.75 to 2.9 mmol/mol (Appendix 4.1). Inter-individual variability is calculated as a standard deviation expressed as a percentage of the average and varies between 5 and 25 %. Combining the results from individuals cultured at the same conditions (Figure 4.2) shows that Mg/Ca in *Bulimina marginata* increases exponentially with temperature (R^2 of the regression is 0.28, $p < 0.01$) and is described by

Equation 4.2.

$$Mg/Ca = (1.10 \pm 0.10)\, e^{(0.045 \pm 0.009)T} \quad (4.2)$$

The obtained Mg/Ca are not correlated with test size ($R^2 = 0.03$ $p > 0.10$, 300-600 μm, Figure 4.3), excluding the possibility that differences in maximum test diameter between conditions resulted caused differences in Mg/Ca between specimens grown at different temperatures.

4.4 Discussion

4.4.1 Mg/Ca-temperature calibration for *Bulimina marginata*

The Mg/Ca-temperature calibration indicates a relatively low sensitivity of Mg/Ca in the calcite of *B. marginata* to changes in temperature, as expressed by the low exponential constant (0.045 ± 0.009) (Equation 4.2). Values for Mg/Ca are relatively low (~1-3 mmol/mol) and similar to values for other calcitic hyaline foraminifera (Lear et al., 2002, Anand et al., 2003, Rathmann et al., 2004, Elderfield et al., 2006, Rosenthal et al., 2011). Analyses by Filipsson et al. (2010) suggested higher Mg/Ca values for *B. marginata*. Their results, however, were based on laser ablation rastering of the test surface. Since the outermost layer of calcite is commonly enriched in Mg (Figure 4.1 and Hathorne et al., 2009), their results may not be representative for the average chamber wall Mg/Ca. Despite the different analytical procedures and much higher absolute Mg/Ca values, the obtained Mg/Ca-temperature calibration of Filipsson et al. (2010) does have a similar sensitivity as the one presented here.

4.4.2 Ontogeny

Since the response of Mg/Ca to temperature is relatively low, additional impacts (e.g. size effects), may have a relatively large impact on the Mg/Ca-temperature calibration presented here. An effect of ontogeny on planktonic foraminiferal Mg/Ca has been stipulated (Nürnberg et al., 1996, Wit et al., 2010, Dueñas-Bohórquez et al., 2011a). Ontogenetic effects for benthic foraminiferal Mg/Ca values are generally less well known, although Hintz et al. (2006) reported elevated Mg/Ca values for the mid-life stage of *Bulimina aculeata* by measuring Mg/Ca on both the whole foraminifer and on micro-dissected chambers. However, the Mg/Ca values reported by Hintz et al. (2006) were exceptionally high (up to 84 mmol/mol), suggesting that a phase with elevated Mg concentrations biased their results. An ontogenetic trend observed in

the results of the micro-dissection method should be directly comparable to laser ablation Mg/Ca measurements of individual chambers. The mid-life stage from Hintz et al. (2006) corresponds to the chambers two position from the final chamber (F-2) from this study. Intra-test variability for the experiment at 14 °C was, therefore, tested by using an analysis of variance (ANOVA), because the experiment contained enough data for this analysis. The ANOVA was designed to test whether Mg/Ca values for F-2 were significantly elevated compared to the F, F-1 and F-3 chamber.

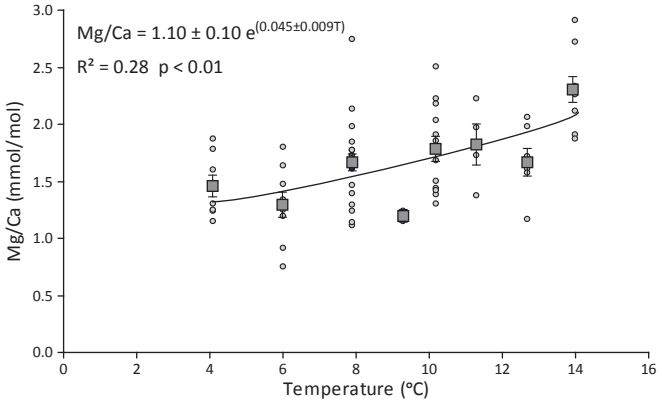

Figure 4.2 Mg/Ca versus temperatures for all experiments with *B. marginata*. The error bars are based on the standard error of the mean ($\sigma/\sqrt{n}$).

In our dataset, Mg/Ca for F-2 is not significantly different ($F(3, 13) = 0.071$, $p > 0.10$), nor is there a systematic difference in Mg/Ca with size (200-580 µm, $R^2 = 0.03$, $p > 0.10$), indicating that there is no significant size-related impact on the Mg/Ca of *B. marginata* (Figure 4.3). A positive and significant correlation between oxygen isotope values and size for *B. marginata*, possibly related to changes in growth rates, has been reported (Barras et al., 2010, Filipsson et al., 2010). The absence of an ontogenetic effect in Mg/Ca, while a significant effect on oxygen isotopes is recognized (Barras et al., 2010) fits the hypothesis that divalent cations (Ca and Mg) are transported to the site of calcification by a different mechanism as the DIC (Erez, 2003, De Nooijer et al., 2009a, Dueñas-Bohórquez et al., 2011b).

4.4.3 Inter-individual Mg/Ca variability, low sensitivity and temperature uncertainty relations

Measured inter-individual variability in foraminiferal test carbonate Mg/Ca of cultured foraminifera is larger than for other elements (Dissard et al., 2010a, Dueñas-

Bohórquez et al., 2011a,b). The standard deviation in Mg/Ca between individuals is an order of magnitude larger than what can be explained on the basis of the analytical uncertainty (on average 11 % of the mean, figure 4.1). Besides the relatively small analytical errors, variability in Mg/Ca is caused by a combination of 1) variability in culture conditions (e.g. temperature, salinity, seawater Mg/Ca (Mg/Ca_{SW}) and carbonate ion concentration) and 2) inherent biological effects (i.e. the vital effect).

For our results, the first cause of variability in foraminiferal Mg/Ca can be quantified using the measured variability in seawater temperature, carbonate ion concentration, Mg/Ca and salinity (Table 4.1). For instance, the temperature for the experiment at 6 °C varied with a standard deviation of 0.5 °C over the course of the experiment (Table 4.1). Using equation 4.2, this temperature variability can be translated to a range in foraminiferal Mg/Ca and expressed as a percentage of the Mg/Ca based on the average of the recorded temperature. For the experiment conducted at 6 °C, an

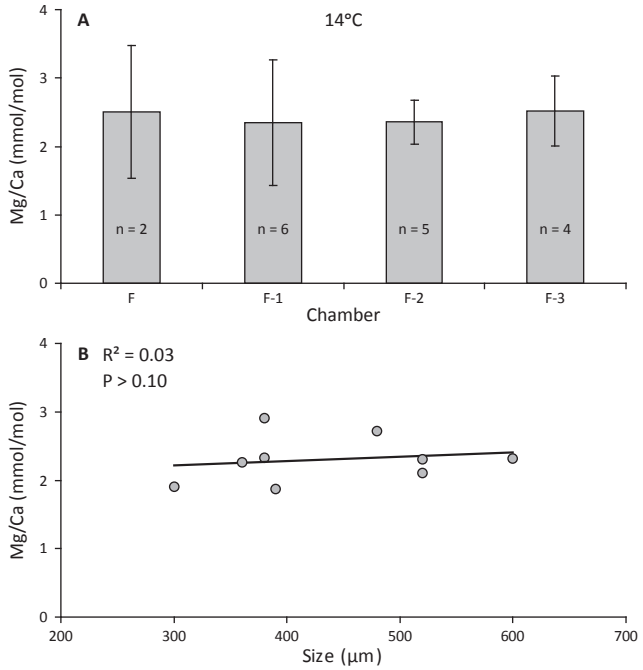

Figure 4.3 Mg/Ca versus size for experiment 8 (14 °C). The upper panel depicts the average Mg/Ca value per measured chamber and the number of individual chambers analyzed (n). The final chamber is indicated by F and counted down in the whorl afterwards (F-1, F-2, etc.) Measured Mg/Ca values are statistically not differing from on another. The lower panel displays the average Mg/Ca value of individual *B. marginata* born in the experiment versus their size. No trend can be observed between size and Mg/Ca.

uncertainty of 0.5 °C in temperature thus introduces an uncertainty in the average Mg/Ca value of 2.5 % (Table 4.2). This uncertainty is the maximum offset caused by variability in temperature for this experiment. A similar procedure can be applied to all other experiments and for the uncertainties in salinity, Mg/Ca_{SW} and carbonate ion concentration using the data from Table 4.1 and the sensitivities from the concurring Mg/Ca-parameter calibrations (Dueñas-Bohórquez et al., 2009, 2011b, Wit et al., under review) (Table 4.2). From this table it can be concluded that in our culture experiment variability in Mg/Ca_{SW} and temperature explain most of the variability in Mg/Ca, whereas variability in the culture medium's salinity and $[CO_3^{2-}]$ play only a minor role.

Variability in environmental parameters other than temperature, affecting Mg/Ca, causes an uncertainty in Mg/Ca-based temperature reconstructions. This uncertainty depends on the sensitivity of the Mg/Ca-T calibration and therefore varies between species. The impact of changes in salinity, Mg/Ca_{SW} and carbonate ion concentration on the uncertainty in reconstructed temperatures was calculated, using different Mg/Ca-parameter calibrations (Dueñas-Bohórquez et al., 2009, 2011b, Wit et al., under review). Using the calibration for *B. marginata* (equation 4.2) with varying sensitivities (exponential constant), the impact on temperature uncertainties of changes in salinity (1) Mg/Ca_{SW} (0.6 mol/mol) and carbonate ion concentration (50 µmol/kg) at any given temperature can be calculated as a function of the sensitivity of the calibration (Figure 4.4). It follows that at a low sensitivity this uncertainty in Mg/Ca translates in to a larger temperature uncertainty, while at higher sensitivities the uncertainty is much smaller (Figure 4.4).

The second source for the large inter-individual variability is the vital effect, caused by variability in the efficiency and rate of various cell-physiological processes that constitute the calcification pathway (Erez, 2003, Bentov and Erez, 2006, De Nooijer et al., 2009a). The impact of these processes can be estimated by correcting the observed Mg/Ca values for the maximum analytical error and the environmentally induced offsets calculated above. If the vital effect and the error of calibration equation would be zero, every measured foraminiferal Mg/Ca value would fit the calibrated regression line (Figure 4.5). Although impact of the vital effect cannot be determined directly, we can estimate its magnitude. The two examples in figure 4.5 show how the three types of variability in foraminiferal test Mg/Ca are related to the measured Mg/Ca values. The total range in test carbonate Mg/Ca caused by uncertainties in the four culture parameters over this experiment explains part of the observed inter-

individual variability (Figure 4.2, Table 4.2). The remaining component, expressed as the distance of the corrected Mg/Ca to the calibration curve, reflects the offset caused by the vital effect (Figure 4.5, Table 4.2). The estimated vital effect may be larger than plotted, since we assume that analytical and environment-induced offsets are all lower than the measured variability in foraminiferal Mg/Ca: i.e. they all work in the same 'direction' (Figure 4.5).

The impact of inter-individual variability on the accuracy of paleo-temperature reconstructions can be calculated by assuming the standard deviation in the Mg/Ca values (measure of variability) from this culture study to be applicable to other foraminiferal species as well. The average variability (standard deviation) within one temperature experiment for a population of *B. marginata* is 16.3 % (Appendix 4.1), which is similar to percentages found in other foraminiferal species (Sadekov et al., 2008, Dissard et al., 2010a, Wit et al., 2010, Dueñas-Bohórquez et al., 2011a). This percentage can be used to calculate a standard error ($\sigma/\sqrt{n}$) of the average Mg/Ca value at any temperature for a number of foraminiferal Mg/Ca-temperature calibrations. This results in a temperature uncertainty (range of (Mg/Ca + $\sigma/\sqrt{n}$) – (Mg/Ca – $\sigma/\sqrt{n}$)

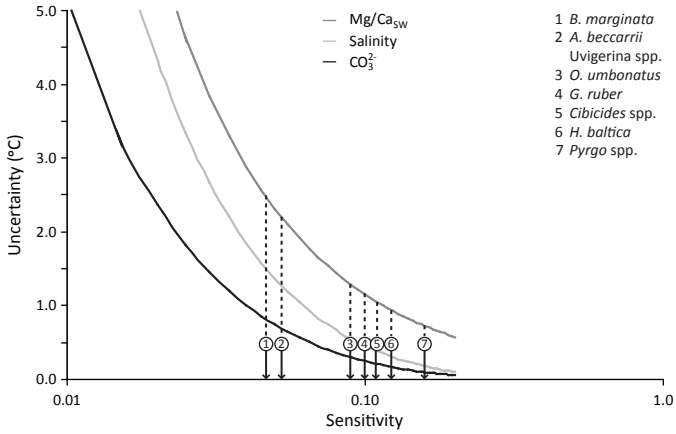

Figure 4.4 Temperature Uncertainty caused by variability in salinity (1), Mg/Ca_{SW} (0.6 mol/mol) and carbonate ion concentration (50 µmol/kg). Temperature uncertainties are calculated at 8 °C using the Mg/Ca-temperature calibration for *B. marginata* with a changing temperature sensitivity (exponential constant). Temperature sensitivities used for the different species are from table 4.4. Mg/Ca-parameter relations from a number of studies were used to calculate the uncertainty in temperature. Mg/Ca_{SW}: Wit et al. (under review), Salinity: Dueñas-Bohórquez et al. (2009), Carbonate ion concentration: Dueñas-Bohórquez et al. (2011b).

and thus expressed as a % of measured Mg/Ca), which is independent of the absolute temperature due to the exponential relation between Mg/Ca and temperature, but is depending on the number of foraminiferal specimens analyzed (Table 4.3). This can be done for a number of foraminiferal species for which the Mg/Ca-temperature calibration is known. The relation between the uncertainty and sensitivity can be calculated for each number of specimens analyzed(N) based on table 4.3 (equation 4.3).

$$\text{Temperature Uncertainty} = \mathbf{c}/\text{sensitivity} \quad (4.3)$$

The constant **c**, subsequently, varies with the number of individuals analyzed (N) for each temperature uncertainty and can be numerically expressed (Equation 4.4).

$$c = 0.33\ N^{-0.50} \quad (4.4)$$

Combining equations 4.3 and 4.4 results in:

$$\text{Temperature Uncertainty} = (0.33\ N^{-0.50})/\text{sensitivity}) \quad (4.5)$$

Experiment	σ % Temperature	Salinity [a]	Mg/Ca_{SW} [b]	Carbonate ion [c]	Measured
1	5.4	0.7	2.9	1.4	18.4
2	2.5	0.6	2.9	1.3	25.4
3	0.5	0.6	2.9	1.2	24.3
4	3.4	0.5	2.9	1.5	5.2
5	0.5	0.5	2.9	2.7	21.8
6	1.2	0.9	2.3	3.7	20.0
7	0.5	0.4	2.9	1.3	15.2
8	0.8	0.8	4.3	2.8	14.7

Table 4.2 Mg/Ca standard deviation (σ, as percentage of the average) based on the measured standard deviation of each parameter during the experiments. Standard deviations from Table 4.1 are used and converted to Mg/Ca values using the same Mg/Ca-parameter relations of a) Dueñas-Bohórquez et al. (2009) (0.11·Salinity + 1.00) b) Wit et al. (under review) (Mg/Ca = a·R·e(b·T)) c) Dueñas-Bohórquez et al. (2011b) (0.0012·$[CO_3^{2-}]$+1.50). Not all experiments had Mg/Ca_{SW} data, experiments without Mg/Ca_{SW} measurements were assumed to have variability according to the average variability of the measured experiments.

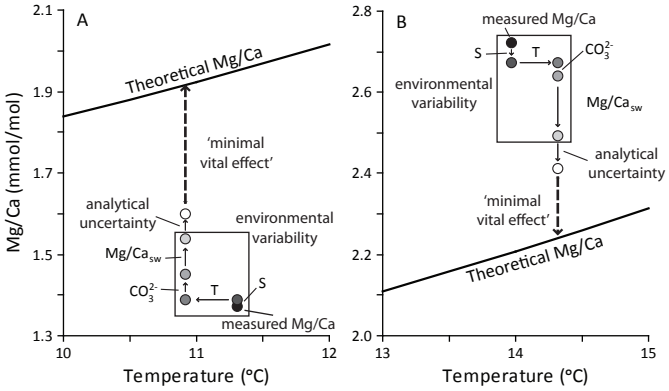

Figure 4.5 Maximum correction for variability in culture parameters for measured Mg/Ca values of *B. marginata* n°52 (A) and n°67 (B) (numbers corresponding to table 4.2). Corrections are based on the maximum variability of each experiment (Table 4.3). Variability was expressed as a correction in foraminiferal Mg/Ca using the same relations as for table 4.4.

With this equation, the number of specimens that need to be measured for a certain temperature uncertainty as a function of the sensitivity (exponential constant) of the used Mg/Ca-temperature calibration (Figure 4.6) can be determined. The value of 0.33 is in fact a doubling of the determined relative standard deviation used to calculate the temperature uncertainties. For species with a relatively low temperature sensitivity, more specimens need to be analyzed to obtain the same temperature uncertainty (Table 4.4). For example, 93 individuals of *B. marginata* need to be analyzed to obtain an uncertainty in temperature of 0.75 °C (Table 4.4), which is often impractical due to foraminiferal scarcity in geological samples and time needed for elemental analyses. Alternatively, the minimum sensitivity needed to for a certain accuracy in reconstructed temperature can also be expressed as a function of the number of individuals available for analyses of using equation 4.5 (Table 4.5). If, for instance, an accuracy of 1 °C is desirable and there are 20 individuals available for analyses, the sensitivity of the calibration should not be below 0.0738 (equation 4.5, table 4.5). This means that a reconstruction based on species such as *B. marginata*, *A. beccarri* and *Uvigerina* spp. will not provide the required precision when 20 or less specimens are analyzed.

Species	Sensitivity	N			
		10	20	30	40
B. marginata [1]	0.045	2.29	1.62	1.32	1.14
A. beccarrii [2]	0.053	1.95	1.38	1.12	0.97
Uvigerina spp. [3]	0.053	1.95	1.38	1.12	0.97
O. umbonatus [4]	0.090	1.15	0.81	0.66	0.57
G. ruber [5]	0.100	1.03	0.73	0.60	0.52
Cibicidoides spp. [6]	0.109	0.95	0.67	0.55	0.47
H. baltica [7]	0.123	0.84	0.59	0.48	0.42
Pyrgo spp. [8]	0.160	0.64	0.46	0.37	0.32

Table 4.3 The uncertainty in temperature (°C) as a temperature range (T_{max} – T_{min}) based on the averaged standard deviation (16.3%) of the culture experiments. $T_{max/min}$ is based on the Mg/Ca value at a temperature plus or minor the uncertainty ($\sigma/\sqrt{n}$). Temperature values are calculated using the species specific calibrations available for each species of foraminifera 1) This Study 2) Toyofuku et al. (2011) 3) Elderfield et al. (2006) 4) Rathmann et al. (2004) 5) Anand et al. (2003) 6) Lear et al. (2002) 7) Rosenthal et al. (2011) 8) Wit et al. (under review).

4.4.4 Controls on sensitivity

The sensitivity of a calibrated Mg/Ca-temperature relationship is crucial for the accuracy of reconstructed paleo-temperatures. Increasing the number of specimens can compensate for the large uncertainty when using low sensitivity species, although practicality limits this approach (Equation 4.5, Figure 4.6). The accuracy will ultimately depend on the combination of analytical errors, the vital effect and absolute calcitic Mg concentration, as an offset in Mg/Ca will have a relatively large impact on foraminifera with low Mg concentrations. Species that have a similar sensitivity, have calibration curves with a comparable steepness (Figure 4.7), but not necessarily the same Y-axis intercept. There appear to be three distinct sensitivities in the Mg/Ca response to temperature (Figure 4.7). The first group includes only the calibration for the miliolid benthic foraminifer *Pyrgo* spp. with a sensitivity of 0.16. The sensitivity of the second group varies between 0.09-0.13 and contains the foraminifera *Oridorsalis umbonatus*, *Cibicidoides* spp., *Globigerinoides ruber* (and most other planktonic species) and *Hyalinea balthica*. The third group entails *B. marginata*, *Uvigerina* spp. and *Ammonia beccarii*, which all have Mg/Ca-T sensitivities ranging from 0.04-0.06.

The miliolid benthic foraminifer *Pyrgo* spp. is the only species studied so far that belongs to the group with high sensitivity in Mg incorporation with respect to increasing temperature. Miliolid foraminifera calcify using a different calcification mecha-

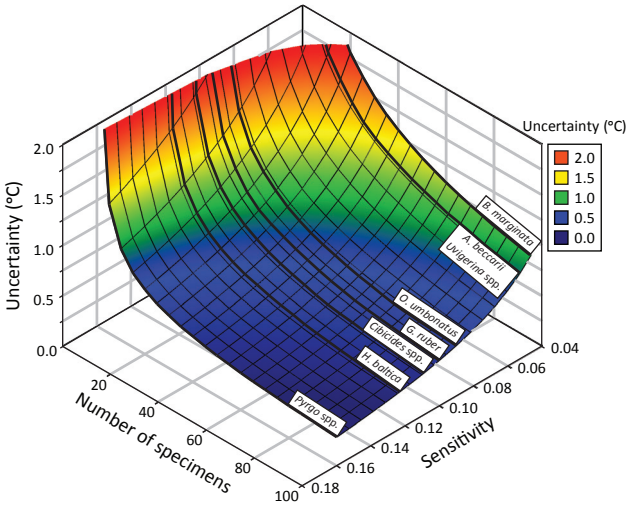

Figure 4.6 Relation between sensitivity of a temperature calibration, the number of specimens analyzed and uncertainty in temperature based on an average standard deviation in a population of foraminifera of 16.3 % of the average.

nism than that adopted by hyaline species (low and intermediate group) (Erez 2003, de Nooijer et al., 2009a). Although the exact influence of this difference in calcification mechanisms on the sensitivity is unknown, it is likely that their different calcification pathways cause the difference in sensitivity between hyaline and porcelaneous

Species	Sensitivity	Uncertainty (°C)					
		2.0	1.5	1.0	0.75	0.50	0.25
B. marginata [1]	0.045	13	23	52	93	210	837
A. beccarii [2]	0.053	9	17	38	67	151	604
Uvigerina spp. [3]	0.053	9	17	38	67	151	604
O. umbonatus [4]	0.090	3	6	13	23	52	210
G. ruber [5]	0.100	3	5	11	19	42	170
Cibicidoides spp. [6]	0.109	2	4	9	16	36	143
H. balthica [7]	0.123	2	3	7	12	28	112
Pyrgo spp. [8]	0.160	1	2	4	7	17	66

Table 4.4 Number of individuals needed to obtain a given uncertainty in temperature, based on the sensitivity of a Mg/Ca-temperature calibration and the averaged standard deviation of 16.3%. Uncertainty is expressed as a range (Max-Min) around the average reconstructed temperature. 1) This Study 2) Toyofuku et al. (2011) 3) Elderfield et al. (2006) 4) Rathmann et al. (2004) 5) Anand et al. (2003) 6) Lear et al. (2002) 7) Rosenthal et al. (2011) 8) Wit et al. (under review).

foraminifera.

The mechanisms responsible for the distinction between low and intermediate groups are unknown, but may be related to their evolutionary history or ecological strategies. Discrimination against Mg during calcification seems taxonomically related at least at a high level, since all known miliolid species produce calcite with high Mg/Ca (>50 mmol/mol), while only some hyaline species are producing high Mg calcite (Toyofuku et al., 2000). For hyaline species, three different clades were recognized based on 26 SSU sequence analyses (Schweizer et al., 2008). Foraminifers with the

N	Uncertainty (°C)					
	2.0	1.5	1.0	0.75	0.50	0.25
10	0.0522	0.0696	0.1040	0.1390	0.2090	0.4170
20	0.0369	0.0492	0.0738	0.0984	0.1480	0.2950
30	0.0301	0.0402	0.0602	0.0803	0.1210	0.2410
40	0.0261	0.0348	0.0522	0.0696	0.1040	0.2090

Table 4.5 Sensitivity (b: equation 1) as a function of a given uncertainty in reconstructed temperature and number of specimens (N) used for Mg/Ca analyses. Uncertainty is expressed as a range (Max-Min) around the average reconstructed temperature.

lowest temperature sensitivity have representatives from all three clades, indicating that the Mg/Ca-T sensitivity may not be (fully) related to taxonomic relationships within foraminifera.

Alternatively, differences in ecological strategies might provide an explanation on the species specific Mg sensitivity to temperature. Foraminifera inhabit environments with contrasting food regimes. The shallow to deep infaunal species *B. marginata* is mainly found at locations relatively rich in organic matter (Jorissen, 1987, Jorissen et al., 1992). The benthic cosmopolitan *Ammonia beccarii* / *A. tepida* (Hayward et al., 2004) inhabits shallow marine to brackish environments, often very rich in organic matter (Murray, 1968). The third species with a low Mg-T sensitivity, *Uvigerina* spp., is commonly found in mesotrophic environments, often characterized by fine-grained sediments with elevated organic content (Van der Zwaan et al., 1986), and lives in shallow infaunal depth habitats (Van der Zwaan et al., 1986, Fontanier et al., 2002, Schweizer et al., 2005).

The group of species with intermediate sensitivity of Mg incorporation to temperature change contains the benthic species *Cibicidoides* spp., *O. umbonatus* and *H.*

balthica and the planktonic species *G. ruber*. Most species within the genus *Cibicidoides* are epifaunal to shallow infaunal living close to or at the sediment-water interface, commonly in mesotrophic to oligotrophic, well oxygenated environments with relatively stable physio-chemical parameters (Jorissen et al., 1998, Gooday et al., 2003). The benthic foraminifer *O. umbonatus* has an epifaunal to shallow infaunal depth habitat and is mainly found in oligotrophic deep-sea environments (Jorissen et al., 1998, Rathmann et al., 2004). *Hyalinea balthica* is a shallow infaunal living benthic foraminifer, typical for upper bathyal environments with mesotrophic conditions, although in some studies an opportunistic behavior has been described (Hess and Jorissen, 2009, Rosenthal et al., 2011). The planktonic foraminifer *G. ruber* is a shallow dwelling (living in the upper 50 m of the water column), symbiont-bearing species, living preferentially in oligotrophic surface waters (Hemleben et al., 1989). Summarizing, all species of this group are typical for oligotrophic to mesotrophic environments.

All species of the low sensitivity group show some characteristics typical of an opportunistic lifestyle. *B. marginata* may reach very high densities in eutrophic settings (e.g. Jorissen, 1987, Jorissen et al., 1992), and is one of the few deep-sea species which reproduce in laboratory conditions (Barras et al., 2010). *Ammonia* spp. contains dominant taxa in a wide range of coastal ecosystems, where they tolerate large salinity and temperature variations. *U. peregrina* and *U. mediterranea* show a reproductive and growth response to phytoplankton bloom events in the Bay of Biscay (Fontanier et al., 2003, 2006). In the literature, all these taxa are generally considered as opportunists.

However, also for some species of the intermediate sensitivity group an opportunistic behavior is suspected. This is clearly the case for *Hyalinea balthica*, which has been described with very high densities in eutrophic submarine canyon environments (Hess and Jorissen, 2009). But also *Cibicidoides* species are sometimes occurring in high densities, and dominate the foraminiferal fauna (e.g., Koho et al., 2008). Conversely, both *G. ruber* and *O. umbanatus* are always considered as oligotrophic taxa, without any opportunistic tendency. Summarizing, there is indeed a tendency for the low sensitivity taxa to be more opportunistic than the intermediate sensitive taxa, but the separation between the two groups is not as clear as we would hope. A better knowledge about the ecological strategies of these species is necessary to confirm that the lower temperature sensitivity is indeed the result of a more opportunistic lifestyle.

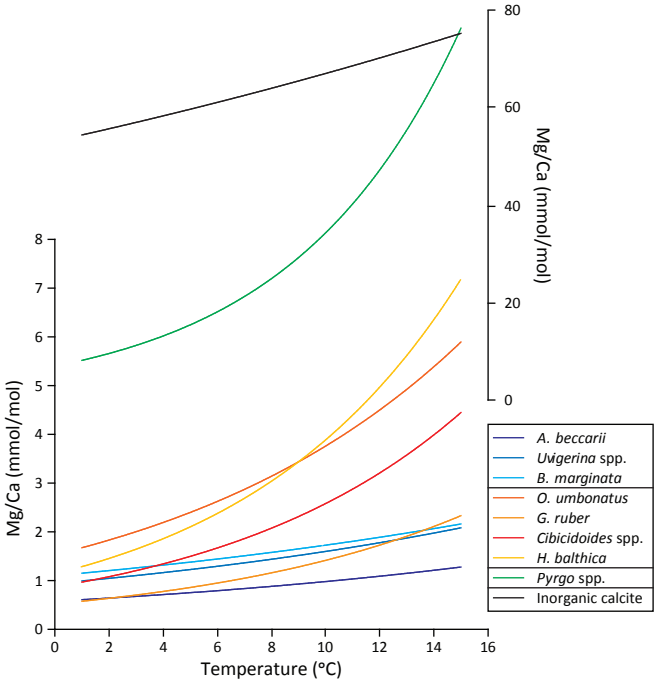

Figure 4.7 Different Mg/Ca-temperature calibrations for a number of foraminiferal species (Table 4.5) and inorganic calcite (black line). Calibrations with a similar Mg sensitivity to temperature have a comparable steepness of the calibration slope. Note that the calibration for *Pyrgo* spp. and inorganic calcite are plotted on a secondary y-axes. Mg/Ca values for these two calibrations are a magnitude of order larger compared to the other calibrations.

4.5 Conclusions

LA-ICP-MS-measured Mg/Ca in cultured *B. marginata* correlates with temperature, although the sensitivity of Mg incorporation to temperature is low. The calibration is not hindered by any ontogenetic effects. The inter-individual variability within this calibration is too large to be caused by variations in culture parameters over the course of the experiment, but is tied to an intrinsic 'vital effect' within the calcification process.

This inter-individual variability influences the practicality of the Mg/Ca-thermometer, especially impacting calibrations with a low sensitivity. Foraminifera with this low sensitivity are, therefore, not ideal for reconstructing paleo-temperatures, due to associating large uncertainties or large sample sizes needed for an accurate recon-

struction of temperature.

Although the biochemical mechanism responsible for the low sensitivity is yet unknown, it appears that foraminiferal species with this low sensitivity (*B. marginata*, *A. beccarii* and *Uvigerina* spp.) are living in more eutrophic environments. Foraminifera mainly living in oligotrophic to mesotrophic environments should, therefore, be used when reconstructing temperatures with the help of the Mg/Ca temperature proxy. Examples of such taxa are *Cibicidoides* spp., *O. umbonatus*, *G. ruber* but especially *H. balthica* and *Pyrgo* spp.

Chapter 5

Reconstructing ancient seawater Mg/Ca by combining porcelaneous and hyaline foraminiferal Mg/Ca-temperature calibrations

J.C. Wit[1], J. Haig[1, 2], F.J. Jorissen[3], E. Thomas[4, 5], G.-J. Reichart[1, 6]

1 Department of Geochemistry, Utrecht University, Utrecht, 3508 TA, the Netherlands
2 School of Earth and Environmental Sciences, James Cook University, Cairns, QLD 4870, Australia
3 Laboratory of Recent and Fossil Bio-Indicators, UPRES 2644 BIAF, Angers University, Angers cedex, 49045, France.
4 Department of Geology and Geophysics, Yale University, New Ha ven, CT 06520-8109, USA.
5 Department of Earth and Environmental Sciences, Wesleyan Univer sity, Middletown CT, 06459, USA
6 Marine Biogeosciences, Alfred Wegener Institute for Polar and Marine Research, Am Handelshafen 12, D-27570 Bremerhaven, Germany

Under reviwe in Geochemimica et Cosmochimica Acta

Abstract

The temperature of the deep ocean plays a vital role in the Earth's climate system. Paleo-reconstructions of deep-sea temperatures traditionally have been based on the oxygen isotope composition of deep-sea benthic foraminiferal calcite tests, although this parameter depends upon polar ice volume as well as temperature. More recent reconstructions used Mg/Ca values of these tests, with temperature calibrations based on empirical relations developed in the present-day oceans. The incorporation of Mg (D_{Mg}) into foraminiferal calcite is, however, not solely dependent on temperature, but also depends on the Mg/Ca value of seawater. Due to its long oceanic residence time, Mg concentrations remained relatively constant over time scales of a few hundred thousand years, but they varied significantly over longer geological time scales. Accurate reconstruction of past temperatures using foraminiferal Mg/Ca values, therefore, hinges on our understanding of Mg/Ca seawater changes over geological

time. We present a novel, independent approach to reconstruct paleo-seawater Mg/Ca using the temperature dependent offset in D_{Mg} between porcelaneous (high Mg) and hyaline (low Mg) benthic foraminifera. We calibrated the Mg/Ca-temperature dependence for *Pyrgo* spp. (one of the few common and large-sized porcelaneous taxa present in the deep-sea), and combined this with an existing calibration of hyaline *Cibicidoides* spp. to mathematically solve for changes in Mg/Ca seawater through time. The reconstructed Mg/Ca_{sw} values varied between 3.3 and 5.1, corresponding well to the pattern of changes in seawater Mg/Ca as derived from geochemical models, albeit with an offset.

5.1 Introduction

Benthic foraminiferal Mg/Ca is a well-established proxy for reconstructing the temperature of the deep ocean, although it is also influenced by the carbonate saturation state of deep waters (Rosenthal et al., 1997; Lear et al., 2000; Lear et al., 2002; Martin et al., 2002; Rathmann et al., 2004; Elderfield et al., 2006; Yu and Elderfield, 2008). The application of Mg/Ca of foraminiferal calcite as a temperature proxy is based on temperature-dependent changes in the empirical partition coefficient D, in which D is the ratio between Mg/Ca in the test and that of ions in seawater. Magnesium incorporation into test calcite (D_{Mg}) is, therefore, not only a function of temperature, but also depends on seawater Mg/Ca values. The elemental composition of the ocean is in turn controlled by a balance between the input of elements via rivers, the output due to carbonate and evaporite precipitation and through exchange in hydrothermal flow during seafloor spreading (Dickson, 2002; 2004; Holland, 2005). Magnesium input into the oceans is primarily controlled by carbonate and silicate weathering, whereas output depends on the mole for mole exchange of Mg for Ca in hydrothermal flows, or via dolomite formation (Hardie, 1996; Holland and Zimmerman, 2000; Holland, 2005). Removal of Mg from seawater through biomineralization is rather limited, whereas for Ca this is the most important pathway of removal from seawater. The oceanic residence times, defined as the total amount of the element present in the global ocean divided by the removal or supply rate, are 1 Myr and 10 Myr for Ca and Mg respectively. This implies that the modern ratio of Mg and Ca in seawater (5.2) may have varied on time scales of more than a million years (Wilkinson and Algeo, 1989). The ratio does not vary geographically or bathymetrically, however, because these residence times are much longer than the oceanic mixing time (about 1000 yr).

If the Mg/Ca paleo-temperature proxy is to be applied on longer geological time

scales, the Mg/Ca of seawater needs to be considered. Such reconstructions are fundamental to our understanding of the evolution and magnitude of the cryosphere. Previous studies accounted for past changes in seawater Mg/Ca by applying low-resolution geochemical models (Lear et al., 2000; Lear et al., 2002; Billups and Schrag, 2002; Stanley et al., 2002) based on our understanding of Mg^{2+} and Ca^{2+} fluxes into and out of the modern oceans, and records of oceanic crustal cycling and dolomite abundance (Wilkinson and Algeo, 1989; Stanley and Hardie, 1998). Although these processes in themselves are well understood, rates are probably highly variable. Geochemical models of a higher resolution indeed show that variability in Mg/Ca seawater is underestimated (Fantle and DePaolo, 2006), which has a direct and significant impact on Mg/Ca based temperature reconstructions (Medina-Elizalde et al., 2008, Medina-Elizalde and Lea, 2010). The models have been constrained mainly by data on fluid inclusions in halite and calcium carbonate veins in ocean ridge flank basalts, recording paleo-seawater Mg/Ca values with a low temporal resolution (Lowenstein et al., 2001; Horita et al., 2002, Coggon et al., 2010). These methods are well suited to reconstruct the Mg/Ca seawater history, although the discontinuity through time of such inclusions prevents a more or less continuous reconstruction.

We present a novel approach for reconstructing seawater Mg/Ca by combining Mg/Ca values of porcelaneous and hyaline foraminifera. Hyaline foraminifera produce tests with numerous pores and dominantly consist of low Mg calcite (Erez, 2003). Porcelaneous foraminifera produce smooth tests without pores consisting of high Mg calcite, and use a different calcification mechanism (Debenay et al., 1998; Erez, 2003; Bentov and Erez, 2006). The different test wall types have contrasting relations of Mg/Ca to temperature due to the dissimilar calcification mechanisms involved (Toyofuku et al., 2000, Erez, 2003, Bentov and Erez, 2006). Such species specific responses to environmental parameters can be used to disentangle different parameters influencing Mg/Ca. An example of this principle is given in this study by combining hyaline and porcelaneous Mg/Ca-temperature calibrations, which allows for quantifying past Mg/Ca of seawater, using the temperature dependent offset between different species from the same sample.

The potential use of porcelaneous *Pyrgo* species as a paleo-temperature proxy has been demonstrated over a small (1-3 °C) temperature range (Healey et al., 2008), but not over a larger temperature gradient. First a Mg/Ca-temperature calibration using the benthic porcelaneous species *Pyrgo depressa* and *Pyrgo murrhina* from a series of core tops is presented. This calibration is then combined with an existing calibration

for hyaline *Cibicidoides* species (Rosenthal et al., 1997), allowing the development of an independent proxy for past Mg/Ca values of seawater. Secondly, this proxy is then applied to a low resolution record Mg/Ca for the last 10 Myr from the Walvis Ridge (southeastern Atlantic Ocean).

5.2 Methods

Core top samples were taken with a classic Barnett multi-tube corer along a transect in the Bay of Biscay (Barnett et al., 1984) (Appendix 5.1), a semi-enclosed basin with a well developed stratification due to the occurrence of water masses with rather constant temperature and salinity (Table 5.1) (Ogawa and Tauzin, 1973; Fontanier et al., 2002), creating an ideal environment for a Mg/Ca-temperature calibration (Reichart et al., 2003). Temperature of the bottom waters was maintained using an insulation device and measurements were done in duplicate within 30 min after core recovery. Sediments were stored in 500 cm^3 bottles, with 95% ethanol and containing 1 g/l Rose Bengal stain. In the laboratory, samples were gently shaken for several minutes in order to get a homogenous mixture and sieved through 63 and 150 μm mesh screens (Fontanier et al., 2002). Samples were picked for the porcelaneous benthic foraminifers *Pyrgo depressa* and *Pyrgo murrhina*.

Upper Miocene-Pleistocene *Pyrgo* and *Cibicidoides* species (*C. wuellerstorfi* and *C. mundulus*) were obtained from cores collected at Site 1264 during Ocean Drilling Program (ODP) Leg 208 (Zachos et al., 2004). This site is located at a water depth of 2507 m near the crest of a north-south trending segment of the Walvis Ridge in the southeastern Atlantic Ocean. Sample depths are converted to the appropriate age using the shipboard age model (Zachos et al., 2004), based on magneto- and biostratigraphic datum levels, with the geomagnetic polarity time scale of Lourens et al. (2004).

Water Mass	Depth (m)	Temperature (°C)	Salinity
NACW [1]	150-800	11.9	35.60
MOW [2]	800-1200	10.5	35.80
IAW-PAW [3]	1200-3000	4.0	35.00
AABW [4]	3000-5000	3.0	34.95

Table 5.1 Depth, temperature and salinity of the different water masses in the Bay of Biscay after Ogawa and Tauzin (1973), Fontanier et al. (2002) and Fontanier et al. (2005). 1) North Atlantic Central Water , 2) Mediterranean Outflow Water, 3) Intermediate Atlantic Water and Polar Atlantic Water (both North Atlantic Deep Water masses), 4) Antarctic Bottom Water

Sample preparation for elemental analysis followed standard laboratory procedures. Samples were 8 times individually rinsed and sonically agitated with ultra pure water (6 times with 200 ml) and methanol (2 times with 200 ml) to remove any contamination caused by adhesive detrital particles and subsequently treated for 5 minutes with a buffered 1% H_2O_2 solution (200 ml) to remove any organic contaminants, following the approach of Barker et al. (2003). No acid leach cleaning steps were used for *Pyrgo* spp., as their porcelaneous high Mg-calcite test is highly susceptible to dissolution, and *Cibicidoides* spp. to maintain a uniform cleaning procedure.

Elemental concentrations were measured on multiple chambers per individual with laser ablation inductively coupled mass spectrometry (LA-ICP-MS), using ^{24}Mg, ^{26}Mg, ^{27}Al, ^{42}Ca, ^{43}Ca, ^{44}Ca, ^{55}Mn, ^{88}Sr and their relative natural abundances. Ablation took place with a deep-ultraviolet-wavelength laser (193 nm) using a Lambda Physik Excimer laser system with GeoLas 200Q optics at a pulse repetition of 6 Hz for approximately 60 seconds with an energy density of 1 J/cm^2 (Reichart et al., 2003). A He-gas flow transported the ablated material, which was mixed with Argon prior to injection into the plasma of the quadrapole ICP-MS instrument (Micromass Platform ICP). Elemental concentrations were calculated from raw counts using computer software (Glitter).

ICP-OES	Mg	Mn	Sr
Average	663	99	173
Standard deviation	35	0.40	4.3
Standard deviation (%)	5.2	0.41	2.5
N	3	3	3
LA-ICP-MS	Mg	Mn	Sr
Average	674	106	184
Standard deviation	61	7.2	15
Standard deviation (%)	9.1	6.9	8.0
N (4 year average)	643	643	643
Ratio	1.016	1.068	1.068

Table 5.2 Comparison between laser ablation (LA-ICP-MS) and solution (ICP-OES) based element data in ppm for in-house GJR calcite standard (Wit et al., 2010). Solution based data consists of three measurements of the in-house calcite standard, while the laser ablation data is derived from the 4 year average of the in-house standard during laser ablation ICP-MS measurements of foraminiferal calcite.

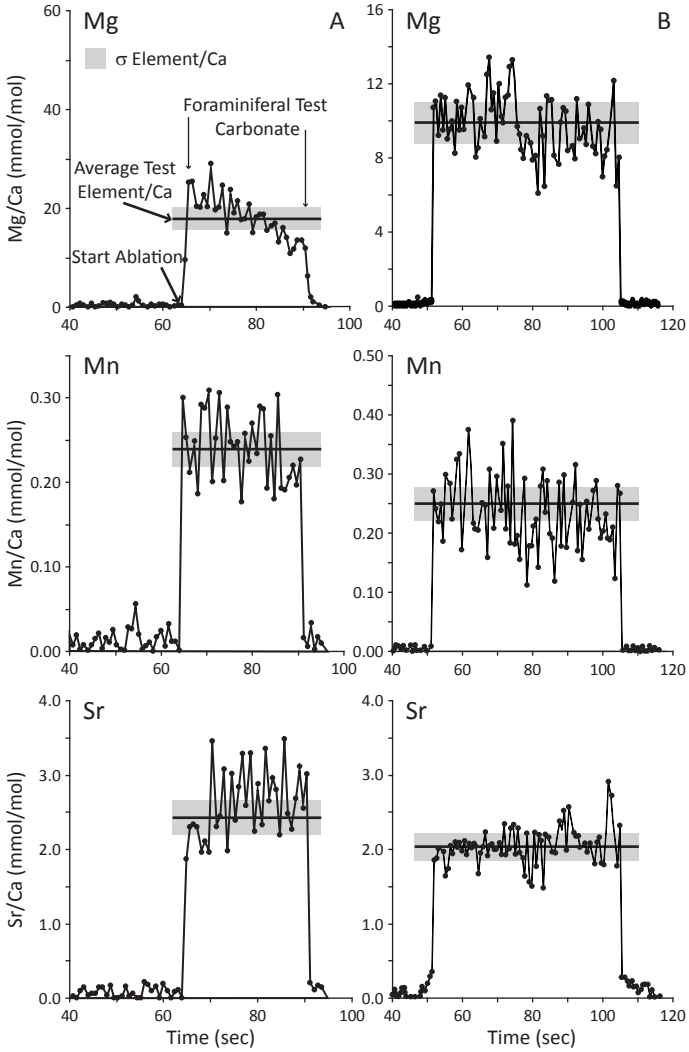

Figure 5.1 Laser Ablation Mg/Ca, Mn/Ca and Sr/Ca profiles through the test of two *Pyrgo* spp. specimens. *Pyrgo* spp. specimen A was retrieved from a sediment depth of 0-0.25 cm and a water depth of 1000 m, *Pyrgo* spp. specimen B was retrieved from Sample 1264A 12H of the Walvis Ridge and has an age of 9.24 Ma. The absence of Mn/Ca peaks at the start and end of each ablation indicates that Mn is incorporated in the foraminiferal test carbonate during test wall formation and does not result from post mortem overgrowth.

Elemental ratios with respect to Ca were based on the average of each ablation profile (Figure 5.1). Element/Ca ratios of individual foraminifera were determined by averaging 3-4 ablation profiles per single test. Furthermore, although element/Ca profiles show variability through individual foraminiferal shells, table 5.2 shows that there is no statistical difference between elemental concentrations measured on a in-house calcite standard by LA-ICP-MS and solution based ICP-OES attesting to the quality of the element/ratio measurements on foraminiferal tests by LA-ICP-MS (Table 5.2).

Measurements are calibrated against the US National Institute of Standards and Technology SRM N610 glass (4 J/cm^2) and an in-house calcite standard GJR (1 J/cm^2) with Ca as an internal standard. Within this range, changing energy density between standard and sample does not affect the quantification of the elemental analyzed (Table 5.2, Wit et al., 2010). Measurements were carefully checked for contamination by evaluating both Al and Mn of all individual test wall profiles. Contamination still adhering to the foraminiferal calcite despite the cleaning steps is identified by high Al concentrations in clay particles, whereas post depositional inorganic overgrowth is recognized through high Mn concentrations at the start of the ablation of the foraminiferal test. Since both phases potentially have high Mg concentrations compared to the test wall, these contaminations might also bias Mg measurements. Correcting for such contaminations seems not possible and samples with high Al and Mn concentrations were, therefore, excluded from further evaluation. All measured Mg/Ca data for *C. mundulus* was species normalized to *C. wuellerstorfi* using a 0.16 mmol/mol correction, based on the average difference between both species as measured at core 1264. This correction is comparable to the averaged difference of 0.28 mmol/mol between both species as found by Lear et al. (2000).

5.3 Results

Magnesium/Calcium values measured on *Pyrgo* spp. ranged from 7.05 to 50.12 mmol/mol (Figure 5.2). Samples used for the *Pyrgo* spp. based temperature calibration from the Bay of Biscay represent a temperature gradient from ~2.4-10.8 °C (Appendix 5.1). Individual *Pyrgo* specimens show an increase in Mg/Ca with increasing temperatures. The regression line between bottom water temperatures and Mg/Ca ratios is represented by equation 5.1. The R^2 of the regression line is 0.76, significant at the 99% level ($p<0.01$), although a large inter-individual variability is present (Appendix 5.1).

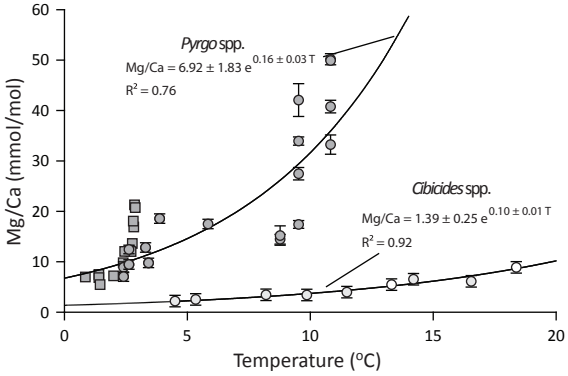

Figure 5.2 Mg/Ca-temperature calibration for *Pyrgo* spp. from the Bay of Biscay (light circle) and *Pyrgo* spp. species from Healey et al (2008) (dark square) with *Cibicidoides* spp. from the Little Bahama Bank (light). The data for *Cibicidoides* spp. is from Rosenthal et al. (1997). Error bars plotted for individual Mg/Ca values for *Pyrgo* spp. are based on the standard error of the mean ($\sigma/\sqrt{n}$). Regression lines and errors are calculated using the individual measurements. Uncertainties in the calibration (equation 5.1) are calculated for the 95% confidence limits. The two individual *Pyrgo* spp. at 8.75 ºC, may well have calcified at colder temperatures as they lived at the mixing depth of MOW and IAW (Table 5.2), as might be indicated by the relatively low Mg/Ca values.

$$Mg/Ca = 6.92 \pm 1.83 \cdot e^{(0.16 \pm 0.03 \cdot T)} \qquad (5.1)$$

Furthermore, we see a moderate positive correlation between size and Mg/Ca ($r = 0.589$, $p < 0.01$) and a positive correlation between size and temperature, indicating that individual *Pyrgo* spp. are larger at higher temperatures ($r = 0.423$, $p < 0.05$) (Table 5.3).

Mn/Ca varied between 0.04 and 0.41 mmol/mol. The Mn was not present in coatings adhering to the outside of the test (Figure 5.1), except for a few specimens. These were recognized as peak Mn values at the start of ablation, and subsequently excluded from the signal, before determining Mn/Ca values. Measured values for individual specimens of *Pyrgo* spp. co-vary positively with size (Table 5.2).

Mg/Ca in upper Miocene-Recent *Cibicidoides* spp. and *Pyrgo* spp. from Site 1264 varies between 1.12 and 1.64 mmol/mol, and 6.99 and 9.96 mmol/mol respectively. Both curves are not significantly correlated over the entire record ($r^2=0.04$), implying that the impact of changes in Mg/Ca_{SW} was larger than that of differences in bottom water temperature and CO_3^{2-} over the interval studied (Figure 5.3).

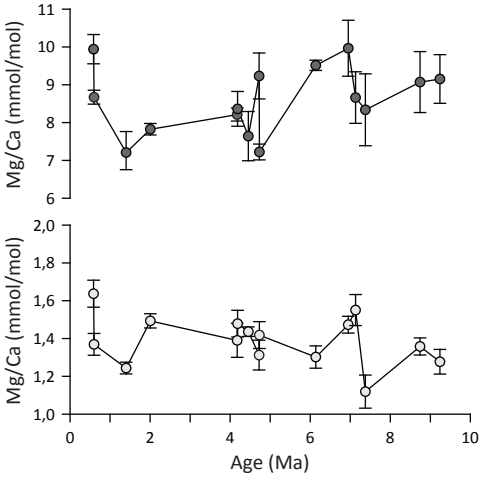

Figure 5.3 Mg/Ca values of *Pyrgo* spp. (dark) and *Cibicidoides* spp. (light) specimens from ODP Leg 208 Site 1264. Error bars are based on the standard error of the mean ($\sigma/\sqrt{n}$).

5.4 Discussion

5.4.1 Pyrgo spp. based Mg/Ca temperature calibration

The *Pyrgo* spp. based temperature calibration shows a 16 % change in Mg/Ca per °C. Calibrations for the high-Mg calcite foraminifer *Planoglabratella opercularis* and *Quinqueloculina yabei* (Toyofuku et al., 2000) show a much lower slope (2-3%), although the absolute Mg concentrations are 10 times higher compared to *Pyrgo* spp. These high Mg concentrations are of the same order of magnitude as those of inorganic calcite precipitation experiments (Morse et al., 2007). These experiments potentially represent the maximum amount of Mg incorporation under more or less open ocean conditions without any biological impact. The sensitivity of Mg incorporation as a function of temperature is in these experiments is 3% (Morse et al., 2007), which might explain the lower sensitivity in both *P. opercularis* and *Q. yabei*. A calibration of Mg incorporation in *Pyrgo murrhina* between 1.5-3 °C- showed a steeper slope than Mg/Ca-temperature calibrations over a larger temperature gradient, with Mg/Ca increasing 43 % per °C (Healey et al., 2008). This slope is somewhat higher but still comparable to the temperature sensitivity of 37 % per °C of this study for that same interval, although uncertainties are relatively large because of the small temperature range. Both datasets are of Mg/Ca values for *Pyrgo* spp. at low temperatures are, furthermore, similar to one another, indicating that both datasets are consistent. The large inter-specimen variability in the laser ablation ICP-MS based calibration adds

to this uncertainty. Existing temperature calibrations for the low Mg/Ca carbonate, hyaline, perforate, benthic species *Oridorsalis umbonatus* and the genus *Cibicidoides* show a 8.61-10.3% change per °C (Rosenthal et al., 1997; Lear et al., 2002; Rathmann et al., 2004), substantially lower than the *Pyrgo* spp. calibration.

The co-variation between test size and Mg/Ca suggests a potential ontogenetic effect (Table 5.3), which could impact the temperature calibration (Dueñas-Bohórquez et al., 2011) and should therefore be assessed before applying the Mg/Ca-temperature calibration of *Pyrgo* species down-core. Almost all coefficients for the correlations between size and the other parameters indicate that they are significant on the 0.01 or 0.05 level. Most coefficients are moderate (R^2 between 0.09-0.36), which implies that variability in size can only explain 9-36 % of the total observed variability in Mg/Ca. The relative contribution of size to the observed variability within these parameters is thus limited. Since each sample consists of *Pyrgo* spp. specimens of different sizes, this is even less important when comparing averages.

The correlation between test size and Mn incorporation suggests that larger *Pyrgo* spp. specimens live deeper infaunally, where they calcified under elevated pore water Mn concentrations. *Pyrgo* species indeed have an infaunal carbon isotope signature (Magana et al., 2010), but have been observed to migrate vertically, from living epifaunally on the sediment surface to infaunally to depths of 3 cm (Linke and Lutze, 1993). Possibly, larger specimens spend more time deeper in the sediment. Such a more infaunal habitat preference at larger test size potentially introduces a carbonate ion effect on Mg incorporation (Elderfield et al., 2006). Bottom waters at the sampled

Pearson coefficient	Size	Temperature
Size		0.423
Temperature	0.423	
Mg/Ca	0.589	0.782
Mn/Ca	0.525	0.545

Probability	Size	Temperature
Size		0.036
Temperature	0.036	
Mg/Ca	0.008	0.000
Mn/Ca	0.021	0.016

Table 5.3 Pearson correlation coefficients and probability (p-value), indicating whether the Pearson correlation coefficients can be caused by chance alone, for *Pyrgo* spp. from the Bay of Biscay.

sites are supersaturated with respect to calcite (Goyet et al., 2000), which implies that $[CO_3^{2-}]$ most likely decreases within the pore water of the uppermost few cm of the sediment (Jourabchi et al., 2005; Elderfield et al., 2006). This potentially would lower Mg concentrations of foraminiferal calcite (Elderfield et al., 2006; Dissard et al., 2010) of the larger specimen. The observed positive correlation between size and Mg/Ca indicates, however, that a carbonate ion effect is probably insignificant or, somehow, counter balanced by other effects. Since the overall impact of ontogeny, is minor, it is excluded from our further discussion, but limiting size range of analyzed specimens would improve future calibrations, although in practice scarcity of specimens may prevent this.

5.4.2 Reconstructing the Mg/Ca ratio of seawater

Combining the independent Mg/Ca to temperature calibrations for porcelaneous and hyaline foraminiferal species makes it possible to derive an equation for past Mg/Ca of seawater. Calibrations of $Mg/Ca_{calcite}$ versus temperature are commonly expressed through an exponential relationship (Equation 5.2).

$$Mg/Ca = a \cdot e^{(b \cdot T)} \tag{5.2}$$

, where T is the temperature in °C at the time of calcification, while $\boldsymbol{a}$ and $\boldsymbol{b}$ are empirically derived, species specific, constants. Equation 5.3 adds to this a factor R, which accounts for changes in the ratio of seawater Mg/Ca, compared to the present day ratio, over any geological time period.

$$Mg/Ca = a \cdot R \cdot e^{(b \cdot T)} \tag{5.3}$$

Mg-partitioning between seawater and carbonate (D_{Mg}), however, depends not only on temperature, but is also affected by seawater Mg/Ca, especially in high-Mg test-building species (Segev and Erez, 2006). The deviation from a linear relation between Mg/Ca seawater and calcite is only apparent at relatively high Mg/Ca seawater values. The linearity of this relation has been questioned by a number of studies investigating the relation between the Mg/Ca values of the solutions and the partition coefficients and suggested that a power relation between them would better fit the experimental data (Ries, 2004; Segev and Erez, 2006; Hasiuk and Lohmann, 2010). Raitzsch et al. (2010) investigated the relation between D_{Mg} and Mg/Ca_{sw} for high-Mg calcifier

Heterostegina depressa over a relatively smaller range (Mg/Ca_{SW} 5.08-6.20 mol/mol) (Equation 5.4).

$$D_{Mg} = 0.07 \cdot (Mg/Ca_{sw})^{-0.56} \quad (5.4)$$

Since this relation has been quantified only for *H. depressa* we assume here a fixed sensitivity (-0.56), albeit with a species-specific constant ***c*** (which is thus 0.07 for *H. depressa* at 24 °C), which is a function of temperature. Using the Mg/Ca-temperature calibration for *Pyrgo* spp. (equation 5.1) and the present-day Mg/Ca_{sw} of 5.2, ***c*** can be calculated for different temperatures for this species (equations 5-7). A factor 1000 is added to account for the strong discrimination against Mg by foraminifera, allowing Mg/Ca in seawater to be expressed in mol/mol and Mg/Ca in calcite in mmol/mol.

$$\frac{6.92 \cdot e^{0.16 \cdot T}}{Mg/Ca_{sw} \cdot 1000} = c \cdot (Mg/Ca_{sw})^{-0.56} \quad (5.5)$$

Solving this equation for ***c*** results in equation 5.6

$$c = 3.35 \cdot 10^{-3} \cdot e^{0.16 \cdot T} \quad (5.6)$$

Subsequently, ***c*** can be substituted in equation 4 to calculate D_{Mg} and thus Mg/Ca calcite for *Pyrgo* spp. at different Mg/Ca seawater values (equations 5.7-5.9).

$$D_{Mg} = 3.35 \cdot 10^{-3} \cdot e^{0.16 \cdot T} \cdot (Mg/Ca_{sw})^{-0.56} \quad (5.7)$$

This can be rewritten in terms of calcite and seawater Mg/Ca again:

$$\frac{Mg/Ca_c}{Mg/Ca_{sw} \cdot 1000} = 3.35 \cdot 10^{-3} \cdot e^{0.16 \cdot T} \cdot (Mg/Ca_{sw})^{-0.56} \quad (5.8)$$

Which simplifies into:

$$Mg/Ca_c = 3.35 \cdot (Mg/Ca_{sw})^{0.44} \cdot e^{0.16 \cdot T} \quad (5.9)$$

Defining R as the ratio between Mg/Ca_{sw} at the time of calcification and present day Mg/Ca_{sw}, equation 5.9 can be rewritten to include R (equation 5.10). Since present day Mg/Ca_{sw} is 5.2 this results in the following equation for *Pyrgo* spp:

$$Mg/Ca_c = 6.92 \cdot R^{0.44} \cdot e^{(0.16 \cdot T)} \tag{5.10}$$

This additional power function between Mg/Ca_{SW} ($R^{0.44}$) and the partitioning coefficient for Mg incorporation is not applied to the calibration for the hyaline foraminifera as no additional effect of changing Mg/Ca_{SW} was reported for hyaline species *Ammonia tepida* (Raitzsch et al., 2010). The relations between Mg/Ca, temperature and seawater Mg/Ca values in both hyaline and porcelaneous foraminifera can now be expressed as two equations in which *T* and *R* are the respective products. Equation 5.11 can then be used for the hyaline species, while equation 5.12 represents the porcelaneous species.

$$T = \frac{1}{b_h} LN\left(\frac{Mg/Ca_h}{a_h \cdot R}\right) \tag{5.11}$$

$$R^{0.44} = Mg/Ca_p \cdot a_p^{-1} \cdot e^{-(b_p \cdot T)} \tag{5.12}$$

In which $\boldsymbol{a_h}$ and $\boldsymbol{b_h}$ refer to the empirically derived constants for the temperature calibrations (equation 5.2) for a hyaline species of foraminifera and $\boldsymbol{a_p}$ and $\boldsymbol{b_p}$ for the constants from a porcelaneous Mg/Ca temperature calibration. Since, porcelaneous and hyaline taxa were picked from the same sample, and thus experienced identical T and R, equation 5.11 can be substituted into equation 5.12, resulting in equation 5.13.

$$R = {}^{(0.44-(\frac{b_p}{b_h}}\sqrt{Mg/Ca_p \cdot a_p^{-1} \cdot \left(\frac{Mg/Ca_h}{a_h}\right)^{(-\frac{b_p}{b_h})}} \tag{5.13}$$

in which *h* refers to hyaline and *p* to porcelaneous foraminifera.

Before applying the equation for Mg/Ca_{sw} derived above to the measured Mg/Ca values of site 1264, the potential impact of a carbonate ion effect on the Mg/Ca values of *Pyrgo* spp. and *Cibicidoides* spp. needs to be assessed. *Pyrgo* spp. has a more infaunal depth habitat making them less susceptible to a potential carbonate ion effect (Linke and Lutze, 1993, Elderfield et al., 2006, Rathmann and Kuhnert, 2008, Magana et

al., 2010). Mg/Ca values for *Cibicidoides* spp., however, show a small but significant carbonate ion effect, especially at bottom water temperatures below 4°C (Elderfield et al., 2006, Yu and Elderfield, 2008). Since Mg/Ca values for *Pyrgo* spp. and *Cibicidoides* spp. are not significantly correlating (Figure 5.3), a carbonate ion effect cannot be ruled out entirely, although we expect it to be minor. This potential effect will, therefore, be evaluated in the uncertainty analyses of the Mg/Ca seawater reconstruction.

Figure 5.4 shows reconstructed Mg/Ca values for the seawater based on using equation 5.13, the species-specific constants from equation 1 and Rosenthal et al. (1997) and Mg/Ca measured on *Cibicidoides* spp. and *Pyrgo* spp. from the Walvis Ridge (Appendix 5.2). The calibration of Rosenthal et al. (1997) was used as other calibrations for *Cibicidoides* spp. (Lear et al., 2002, Elderfield et al., 2006) resulted in Mg/Ca_{SW} values around 8 mol/mol at 0.5 Ma, while the current calibration results in a value of 4.8, which is close to the present-day value (5.2). Values for seawater Mg/Ca vary between 3.3 and 5.1, with large fluctuations on time scales shorter than or similar to the residence time of Mg and Ca respectively. The uncertainty on the reconstruction of Mg/Ca seawater is, however, relatively large. Uncertainties associated with the current reconstruction are mainly from four sources. The first uncertainty is caused by the used Mg/Ca-temperature calibration. If the species-specific constants of the calibrations of Lear et al (2002) or Elderfield et al (2006) are used in equation 5.13, Mg/Ca_{SW} varies between 6 and 10 mol/mol. Furthermore, the uncertainty (95

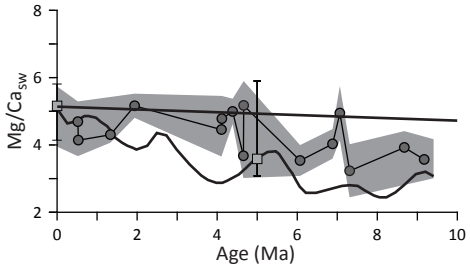

Figure 5.4 Fluctuations in Mg/Ca_{SW} over the last 10 Ma based on the Mg/Ca of *Pyrgo* spp. and *Cibicidoides* spp. (equation 5.13). The dark area is the uncertainty based on the standard error of the average resulting from the observed variability between individually measured foraminifera. This includes uncertainties derived from ontogenetic effects, foraminiferal migration through the sediment and age differences between the two used foraminiferal species. The bold sinuous line represents the Mg/Ca_{SW} values as modeled by Fantle and DePaolo (2006). The bold straight line is the Mg/Ca value of the seawater as reconstructed by Wilkinson and Algeo (1989). The squares represent Mg/Ca_{SW} values measured on fluid inclusions (Horita et al., 2002).

% confidence interval) in the here used Mg/Ca-temperature calibrations as seen in equation 5.1 and figure 5.2, including the variability in the relation between D_{Mg} and Mg/Ca seawater, results in an uncertainty in reconstructed Mg/Ca_{SW} with a maximum range of 7 mol/mol. The average variability in Mg/Ca_{SW} as a result of these uncertainties in the Mg/Ca-temperature calibration expressed as a standard deviation causes an average uncertainty on Mg/Ca_{SW} of 1-1.6 mol/mol. It is, therefore, vital to the accurate reconstruction of Mg/Ca_{SW} that the species-specific Mg/Ca-temperature calibrations are as accurate as possible. This uncertainty has, however, no effect on the reconstructed variability, as all points in the calibrations are affected equally by this factor, although the shift along the Mg/Ca_{SW} axes is largest for the uncertainty in the porcelaneous Mg/Ca-temperature calibration. The second uncertainty derives from the inter-individual variability when measuring Mg/Ca values of fossil foraminifera (Figure 5.3). This includes foraminiferal migration through the sediment during their lifetime, as it is not possible to quantify this for paleo-samples. Another component of this inter-individual variability is the variability between different species and morphotypes of the genus *Cibicidoides* (Rae et al., 2011). Although the exact contribution of each of these uncertainties to inter-individual variability is unknown, it still is part of the calculated uncertainty in Mg/Ca_{SW}. The third uncertainty derives from the assumption that the measured foraminifera have lived at the same time and thus temperature. This assumption might, however, no be valid, although its impact will be small since both foraminifera live in the deep sea where temperature fluctuations between climate changes are expected to be gradual and small. Finally, since a carbonate ion effect on the Mg/Ca values of the *Cibicidoides* spp. cannot be ruled out, we calculated the uncertainty in Mg/Ca_{SW}. We assumed a 60 mmol/kg gradual increase in CO_3^{2-} concentration for the last 10 Myr (Zeebe, 2012). The sensitivity of foraminiferal Mg/Ca to changes in CO_3^{2-} for *Cibicidoides* spp. is 0.0086 mmol/kg (Elderfield et al., 2006). The uncertainty in Mg/Ca_{SW} can be calculated using this sensitivity and the gradual increase in CO_3^{2-}, resulting in a uncertainty between 0.1-1.7 mol/mol, with an increasing uncertainty in the older samples. The sensitivity of 0.0086 is, however, determined using a global core-top data set. Dueñas-Bohórquez et al. (2011b) calibrated a sensitivity for *Ammonia tepida* of 0.0012 mmol/kg in a culturing study. When this sensitivity is used to calculate the uncertainty in Mg/Ca_{SW} it varies between 0.02-0.3 mol/mol.

Mg/Ca seawater shows an overall increase during the last 10 Myr, and values are generally in the same range as modeled in curves with lower time resolution (Wilkinson

and Algeo, 1989; Hardie, 1996). However, our values for the last 10 Myr are consistently lower then these low resolution models, and do show shorter time scale changes due to a higher resolution. A somewhat higher time-resolution model for the last 20 Myr is based on a simplified geochemical model of the Ca cycle, combined with seawater Mg values derived from numerical models for diagenesis, with reaction rates determined by measuring the isotopic composition and concentration of Sr in pore waters (Fantle and DePaolo, 2006). Our observed increasing trend ($R^2 = 0.22$, $p < 0.10$) appears to resemble their modeled increasing Mg/Ca_{sw} values ($R^2 = 0.68$, $p < 0.01$) for the last 10 Myr, although with an offset to higher values (Figure 5.5). This offset might be caused by uncertainties in our reconstruction, due to uncertainties in the used Mg/Ca-T calibrations and inter-individual variability, as well as by uncertainties in Fantle and DePaolo (2006), caused by their K_{Mg} values and variability therein. Our values are also in line with existing Mg/Ca_{sw} values measured in fluid inclusions (Lowenstein et al., 2001; Horita et al., 2002).

We have shown that Mg/Ca seawater can be calculated when equation 5.11 is substituted into equation 5.12. This resulted in equation 5.13 to calculate the Mg/Ca value of seawater independent of temperature. Equation 5.12 can, however, also be substituted into equation 5.11 (equation 5.14), resulting in a Mg/Ca-temperature equation, which is basically independent of changes in Mg/Ca seawater, following the same lines of reasoning as demonstrated for equation 5.13.

$$T = \frac{LN\left(\frac{Mg/Ca_h}{a_h\left(Mg/Ca_p \cdot a_p^{-1}\right)^{2.27}}\right)}{\left(b_h - 2.27 \cdot b_p\right)} \qquad (5.14)$$

Figure 5.5 shows the reconstructed temperatures (equation 5.14) independent from Mg/Ca_{SW}, for the last 10 Myr in comparison to the bottom water temperatures of the last 10 Myr as reconstructed by Lear et al (2000). The difference between the two reconstructions is appreciable, showing much lower temperatures in the current reconstruction. This offset is mainly due to the linear correction applied for Mg/Ca_{SW} by Lear et al. (2000). Previous studies corrected for Mg/Ca_{sw} (Lear et al., 2000; Billups and Schrag, 2002) using low-resolution geochemical models (Wilkison and Algeo, 1989; Hardie, 1996), which do not capture the shorter-term variability and suggest overall higher Mg/Ca_{sw} values for the last 10 Myr. This results in a significant underestimate of temperatures (Medina-Elizalde et al., 2008; 2010), and when such

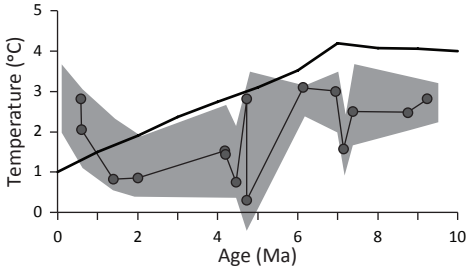

Figure 5.5 Fluctuations in temperature over the last 10 Ma based on the Mg/Ca of *Pyrgo* spp. and *Cibicidoides* spp. (equation 5.14). The dark area is the uncertainty based on the standard error of the average resulting from the observed variability between individually measured foraminifera. This includes uncertainties derived from ontogenetic effects, foraminiferal migration through the sediment and age differences between the two used foraminiferal species. The bold line represents temperature as reconstructed by Lear et al. (2000). The difference in temperature between both reconstructions is mainly due to the used Mg/Ca_{SW} correction by Lear et al. (2000).

temperature estimates are combined with stable oxygen isotope data to deconvolve ice volume, resulting in its underestimation. Recognition of the changes in Mg/Ca_{sw} on shorter timescales is, therefore, of vital importance to reliably apply the Mg/Ca temperature proxy further back in geological time. Our record does not go back in time further than 10 Myr, but it suggests that the simplified, low resolution curve of Mg/Ca_{sw} as e.g. published in Stanley and Hardie (1998) is not correct, as our curve shows Mg/Ca_{sw} values higher than 3 since the early Miocene, rising monotonically afterwards.

5.5. Conclusions

The Mg/Ca in the tests of the porcelaneous foraminiferal genus *Pyrgo* records bottom water temperature. Combining this calibration with an existing calibration for *Cibicidoides* spp. and Mg/Ca values of this taxon in the same samples as used for measurements on *Pyrgo* allows the deconvolution of Mg/Ca seawater values for the last 10 Myr. The use of species-specific responses to disentangle different parameters influencing a proxy is, therefore, a promising approach to further improve reconstructions of past climates. Applying the inverse relation, which reconstructs temperature without any influence of Mg/Ca_{SW}, shows that existing time series of Mg/Ca-based temperature reconstructions for the middle Pleistocene and earlier significantly underestimate absolute temperature, demonstrating the vital importance of tracking

Mg/Ca_{sw} changes through time.

Acknowledgements

We would like to thank David Naafs for providing the necessary measurements needed for the correction between to *C. wuellerstorfi* and *C. mundulus*. We appreciate the assistance of Paul Mason, Helen de Waard and Gijs Nobbe with laser ablation analyses. The manuscript benefitted from the constructive comments of 3 anonymous reviewers, for which we are grateful. This research is funded by the Utrecht University and the Darwin Centre for Geobiology project "Biological validation of proxies for temperature, salinity, oxygenation and pCO_2 based on experimental evidence using benthic foraminiferal cultures".

Chapter 6

Development and Application of a Novel, Direct Proxy for Paleo-Salinity

J.C. Wit[1], L.J. de Nooijer[1], G.J. de Lange[1], G.J. Reichart[1,2]

1 Department of Geochemistry, Faculty of Geosciences, Utrecht University, Budapestlaan 4 3584 CD Utrecht, The Netherlands

2 Marine Biogeosciences, Alfred Wegener Institute for Polar and Marine Research, Am Handelshafen 12, D-27570 Bremerhaven, Germany

Abstract

On geological timescales, seawater salinity varies with changes in continental ice volume, river discharge and evaporation/precipitation balance. Changes in salinity, in turn, impact CO_2 uptake capacity of seawater, ocean circulation pattern and subsequent temperature distribution (Broecker, 1990. Broecker et al., 1990). Accordingly, knowledge of present and past salinity is vital for understanding ocean circulation. Unfortunately, until now an independent quantitative proxy for past seawater salinity is missing. Here we present a novel tool for the direct reconstruction of past seawater salinity using the incorporation of the dominant seawater cation sodium (Na) in foraminiferal shells. Elemental analyses of shell carbonate from foraminifera cultured under controlled conditions show that Na/Ca values increase linearly with salinity. The values of this foraminiferal Na/Ca-salinity proxy appear to depend only on the sodium concentration in seawater, whereas temperature and $[Ca^{2+}]$ have no appreciable effect. Application of this novel proxy to fossil foraminiferal shells from a humid climate period with reported reduced seawater salinity (sapropel S5 ~125 ka, Eastern Mediterranean) shows a drop in salinity of 5 units. This is the first direct evidence for major surface water freshening of the Eastern Mediterranean during sapropel formation. This novel proxy not only allows a direct reconstruction of salinity itself, but also enables calculation of salinity-corrected values for seawater $\delta^{18}O$ and for Mg/Ca-based temperature reconstructions.

6.1 Introduction

Although salinity is a key parameter in paleoceanography, no independent proxy for salinity existed until now. Several approaches have been suggested to estimate salinity by combining proxies for seawater temperature (e.g. foraminiferal Mg/Ca or $U^{k'}_{37}$) with foraminiferal $\delta^{18}O$ or the hydrogen isotope composition (δD) of long-chained ketones, allowing calculation of the oxygen or hydrogen isotopic composition of seawater (Elderfield and Ganssen, 2000, Schouten et al., 2006). This may subsequently be translated into salinity using the present-day relation between salinity and the isotopic composition of seawater. Application on geological time scales is based on the assumption that this relation has remained constant. Variations through time and between locations in this relationship, however, are inevitable and limit the accuracy of such an approach. At best the relation between salinity and seawater isotope composition can be modeled, but this still involves assumptions on precipitation, evaporation and/or river runoff, introducing relatively large uncertainties in reconstructed salinities (Rohling and Bigg, 1998). Ideally, a proxy for past salinity should target one of the major constituents of the dissolved sea salt rather than an indirect variable as discussed above.

6.2 Methods

To test the effect of salinity on the element incorporation in foraminiferal shell calcite, specimens of the benthic, shallow-water species *Ammonia tepida* were cultured at four salinities (30.0, 32.5, 36.1, 38.6, ± 0.1 for all salinities) (Kester et al., 1967). In our experiment, as well as in natural systems, $[Na^+]$ co-varies with salinity (Kester et al., 1967) and cultured foraminifers were therefore analyzed for the amount of Na incorporated in their calcite. To exclude the impact of other parameters, the culturing experiment was conducted at constant temperature (20 ± 0.5 °C), pH (8.14 ± 0.05) and alkalinity (2505 ± 41 µmol/kg). Within 8 weeks, juveniles initially having ≤ 3 chambers, added 8-10 new ones at all four salinity conditions. After the experiments, shells were cleaned with 5% sodiumhypochloride to remove organic material, rinsed three times with MilliQ, twice with methanol, and three times again with MilliQ. Specimens were analyzed with Laser-Ablation-ICP-MS to determine the Na/Ca composition of individual chambers (Reichart et al., 2003, Wit et al., 2010).

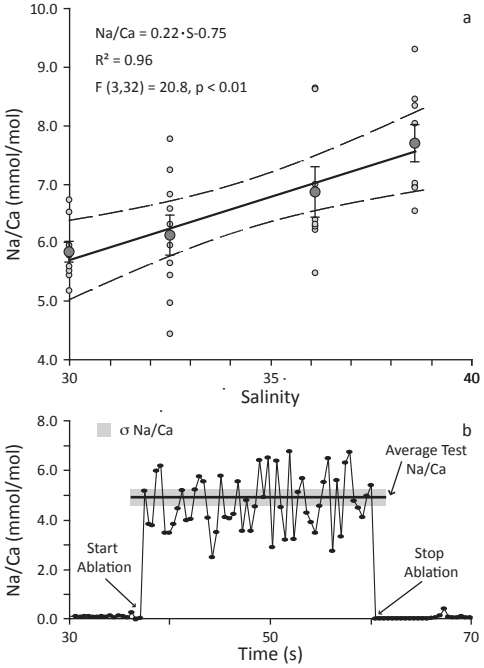

Figure 6.1 a, Na/Ca values for individual foraminifers of species *A. tepida* versus salinity in which they were cultured. The regression line is based on the averaged Na/Ca value per salinity experiment. The relation is tested with a one-way ANOVA and is statistically significant at the 99% level. The error bars are based on the standard error of the mean ($\sigma/\sqrt{n}$). All measurements on individual foraminifers can be found in appendix 6.1. **b**, Laser ablation Na/Ca profile of a cultured individual foraminifer of the species *A. tepida* at a salinity of 36.1. Average test Na/Ca was determined by averaging ~50 pulses of the ablation profile (Wit et al., 2010).

6.3 Results and Discussion

Results show a significant ($p < 0.01$), positive correlation between seawater salinity and calcite Na/Ca (Figure 6.1). Measured Na/Ca values do not vary systematically between consecutive foraminiferal shell chambers, excluding ontogenetic effects on Na incorporation. Inter-individual variability for Na/Ca values (relative standard deviation of 9-17%) is similar as previously recorded for Mg/Ca values measured on individual specimens and may be caused by biological impacts on the calcification mechanism (Sadekov et al., 2008, Wit et al., 2010, Dueñas-Bohórquez et al., 2011). To relate foraminiferal Na/Ca values to those obtained in previous studies, calcitic Na/Ca values are expressed as partition coefficients. The partition coefficient (D_{ele-}

$_{ment}$) is the amount of a minor or trace element incorporated into calcite compared to the concentration of that element in seawater. The rather similar D_{Na} found for foraminifera in our study($0.12\text{-}0.16\cdot10^{-3}$) and for inorganically precipitated calcites in previous studies ($0.07\text{-}0.20\cdot10^{-3}$) (Kitano et al., 1975, Ishikawa and Ichikuni, 1984) suggests that the biological control on Na incorporation in foraminifera is likely to be minor. Moreover, D_{Na} for other foraminiferal species is within the same range ($0.11\text{-}0.17\cdot10^{-3}$) (Delaney et al., 1985, Lea et al., 1999), suggesting that incorporation of Na is similar across species.

Previous studies reporting partition coefficients for Na in biogenic and inorganically precipitated calcium carbonates could not distinguish between lattice-bound Na and Na present in microscopic seawater inclusions (Rucker and Valentine, 1961, Gordon et al., 1970, Kitano et al., 1975, Ishikawa and Ichikuni, 1984). Although chloride is also incorporated in calcium carbonate, this occurs at a 20-40 times lower concentration than Na (Kitano et al., 1975). This suggests that Na is structurally bound in the calcite lattice, which is in line with the relatively constant concentrations of Na throughout shell wall profiles (Figure 6.1).

Some cations (e.g. Mg^{2+} or Sr^{2+}) are incorporated into calcite by substituting for calcium ions. For those elements seawater element/Ca values are correlated to calcitic element/Ca values. Sodium, however, does not substitute for Ca but is incorporated at interstitial sites in the calcite lattice (Ishikawa and Ichikuni, 1984). The incorporation of Na in calcium carbonate is therefore independent of seawater Ca concentration, and hence not necessarily correlated to seawater Na/Ca. Instead, foraminiferal Na/Ca depends primarily on the activity of Na in seawater, which is a function of the sodium concentrations and, to a lesser extent, its activity coefficient (Ishikawa and Ichikuni, 1984). Increasing salinity (and hence $[Na^+]$) increases the activity of Na, while the associated decrease in its activity coefficient because of the higher salinity, might explain the offset from a 1:1 relation between foraminiferal Na/Ca and salinity (Figure 6.1) (Zeebe and Wolf-Gladrow, 2001). Since the activity coefficient of Na in seawater is only slightly affected by temperature over the relevant range, the effect of temperature on Na incorporation is negligible (Ishikawa and Ichikuni, 1984, Delaney et al., 1985, Lea et al., 1999, Zeebe and Wolf-Gladrow, 2001). Our experimentally derived foraminiferal Na/Ca thus represents a robust and direct proxy for determining seawater salinity.

To test the applicability of our novel salinity-proxy, foraminiferal Na/Ca was determined on fossil specimens of the planktonic foraminifer *Globigerinoides ruber* over

sapropel S5 (~125 ka) from core MS66PC (Boere et al., 2011). This 625 cm long core is located in the Eastern Mediterranean under the direct influence of the Nile outflow (33°1.9'N, 31°47.9'E, Figure 6.2) and contains several dark organic layers known as sapropels. Timing of these sapropels correlate to a combination of precession minima and eccentricity maxima (Hilgen, 1991) and their formation is thought to be related to enhanced precipitation and river run-off in the circum-Mediterranean leading to a strongly stratified water column. The consequential, enhanced primary production, and the concomitant, improved preservation, has resulted in the formation of these organic-rich units (Calvert, 1983, De Lange and Ten Haven, 1983, Rohling and Gieskes, 1989, Emeis et al., 2003, De Lange et al., 2008).

Planktonic foraminiferal Na/Ca values indicate that salinity decreased from ~38 to ~35 at the onset of sapropel formation at 583 cm (Figure 6.2). The reconstructed major decrease in surface water salinity thus coincides with an increase in organic matter production or in its preservation due to lower deepwater oxygen conditions. After this rapid change in sea surface salinity, freshening continued (salinity dropping to 33), coinciding with considerably enhanced primary production and low oxygen deepwater conditions (Figure 6.2). The observed rapid decrease in salinity offshore the river Nile implies a major influx of freshwater, resulting in an overall lowering of Eastern Mediterranean surface water salinities. Since the formation of deep water in

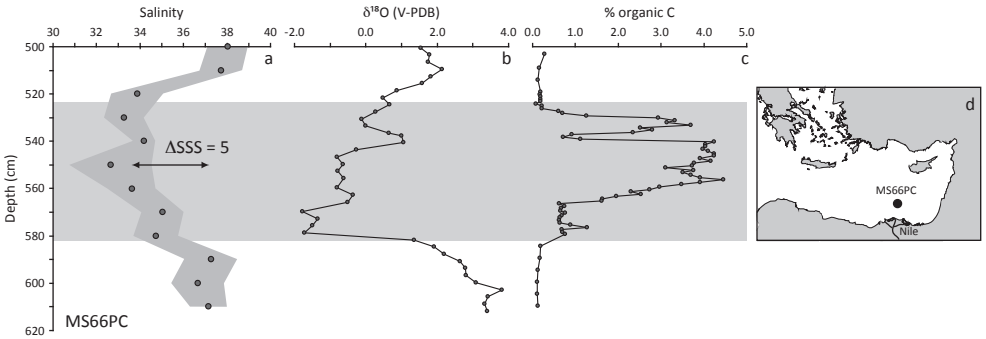

Figure 6.2 a, Reconstructed salinity using calcitic Na/Ca values of G. ruber for the S5 interval (Grey area) in core MS66PC (Boere et al., 2011). Salinity is calculated using the relation between Na/Ca and salinity (Figure 6.1a). Measured Na/Ca values for individual *G. ruber* can be found in appendix 6.2. **b**, Oxygen isotopes for the S5 interval. Oxygen isotopes are measured on bulk sediment with a SIRA24 coupled to an isocarb preparation station at Utrecht University. **c**, Organic carbon content (%) of the sediment over S5. Organic carbon was determined on a Fison instruments NCS NA 1500 analyzer (Van Santvoort et al., 1996). **d**, core location for MS66PC.

the eastern Mediterranean critically relies on high salinity conditions, this initially impaired circulation in the basin, possibly followed by an actual basin-wide stagnation of the water column, enhanced sapropel formation. At the end of the humid climate period precipitation decreased and consequently salinity increased gradually to pre-sapropel values of ~38.

Na/Ca and bulk carbonate oxygen isotope records strongly co-vary between onset and termination of sapropel S5 (Figure 6.2). This implies that the freshwater added to the Mediterranean surface waters had a lighter oxygen isotope composition (Rohling, 1994). The recorded decrease in $\delta^{18}O$ is more rapid and pronounced than the decrease in Na/Ca based salinity. This is explained by the fact that bulk sediment $\delta^{18}O$ represents a combination of surface water isotope composition, temperature and disappearance of the enriched benthic $\delta^{18}O$ component (due to colder bottom waters) of the bulk carbonate isotopes due to bottom water anoxia. Timing of the salinity changes during S5 based on foraminiferal Na/Ca match those based on the δD composition of alkenones (Van der Meer et al., 2007).

6.4 Conclusions

Unlike salinities derived indirectly via the isotopic composition of seawater, calibration and application of our novel method results in the first direct evidence for a reduction in surface water salinity during sapropel formation. This new proxy directly reflects salinity fully independent of $\delta^{18}O$ and δD, foraminiferal Mg/Ca, or other combined salinity/temperature proxies. Being independent from temperature also implies that foraminiferal Na/Ca values can be used to correct foraminiferal Mg/Ca-based temperature reconstructions for the hitherto unaccounted for salinity impact (Nürnberg et al., 1996). Combining such corrected temperatures with foraminiferal $\delta^{18}O$ then would allow reconstruction of seawater $\delta^{18}O$ to salinity relationships. Since such relationships are a function of mixing between open ocean and freshwater isotopic values, this reflects changes in the local and global hydrological cycle. Salinity reconstructions based on foraminiferal Na/Ca thus permits for the first time to independently reconstruct past changes in deep ocean circulation and formation of deepwater.

Chapter 7

Sea surface conditions during deposition of Mediterranean sapropel S5

J.C. Wit[1], L.J. de Nooijer[1], M. Wolthers[1], G.J. de Lange[1], G.J. Reichart[1,2]

1 Department of Geochemistry, Faculty of Geosciences, Utrecht University, Budapestlaan 4 3584 CD Utrecht, The Netherlands

2 Marine Biogeosciences, Alfred Wegener Institute for Polar and Marine Research, Am Handelshafen 12, D-27570 Bremerhaven, Germany

Abstract

Deposition of sapropels has been linked to increased outflow of the river Nile and precipitation over the Mediterranean basin, resulting in overall freshening of eastern Mediterranean surface waters. Still, the relative contribution of Nile water as such to this freshening remains unclear. Tracing the origin of the freshwater input and quantification of the amounts relies on the ability to accurately reconstruct salinity, temperature and $\delta^{18}O_w$. Combined measurements of single-specimen foraminiferal Mg/Ca, Na/Ca and $\delta^{18}O$ may allow reconstruction of these parameters. Since temperatures derived from foraminiferal Mg/Ca are impacted by salinity we quantified the independent effect of salinity on foraminiferal Mg/Ca. This effect was calibrated using a culturing experiment in which salinity impacts calcitic Mg/Ca by changes in the speciation for free Mg and Ca as a function of salinity. Corrected Mg/Ca temperatures were applied in combination with Na/Ca-based salinity reconstruction and $\delta^{18}O$ from specimens of the planktonic foraminifer *G. ruber* over the formation of Mediterranean sapropel S5 (~125 kyr BP). Post and pre-sapropel sea surface $\delta^{18}O_w$ values fall on a different $\delta^{18}O_w$ -salinity mixing line than during the time of sapropel deposition. This change in mixing line during sapropel formation can only be explained by the presence of a more "Atlantic" Mediterranean that experienced less evaporation and more precipitation than the Mediterranean during non-sapropel formation. This result implies that Sapropel formation is not primarily caused by an increased Nile outflow. Reduced evaporation and/or increased precipitation over the Mediterranean itself appear the main mechanisms that resulted in sapropel formation, linking the formation of sapropels not only to precession but also to orbital changes in obliquity.

7.1. Introduction

The Mediterranean sedimentary record of at least the last 10 Ma is characterized by periodical deposition of organic rich layers known as sapropels (Schenau et al., 1999). These sapropels mark periods of enhanced productivity and reduced ventilation, causing anoxia at the deeper parts of the basin. The resulting increased organic matter preservation together with the enhanced primary sea surface productivity resulted in deposition of organic rich layers (Calvert, 1983, De Lange and Ten Haven, 1983, Rohling and Gieskes, 1989, Rohling, 1994, Emeis et al., 2003, De Lange et al., 2008). Deposition of these sapropels shows a regular pattern through time, which has been linked to orbital controlled changes in solar insolation via its impact on the Indian Ocean summer monsoon and storm track position of Atlantic depressions over the Mediterranean (Hilgen, 1991, Rohling, 1994). The climate mechanism suggested for sapropel deposition was, therefore, primarily linked to increased river run-off via the river Nile (influenced by the Indian Ocean summer monsoon) and enhanced precipitation over the Mediterranean (storm track) (Rossignol Strick et al., 1982, Rohling, 1994). Sapropel formation is indeed accompanied by a depletion in stable oxygen isotopes of foraminiferal calcite, caused by an increased input of isotopically depleted water during these events. The source of this isotopically light water is hypothesized to be derived from increased river run off or intensified precipitation over the Mediterranean (Calvert, 1983, De Lange and Ten Haven, 1983, Rohling and Gieskes, 1989, Rohling, 1994, Emeis et al., 2003, De Lange et al., 2008). Increased contribution from either source resulted in a decrease of sea surface salinities in the eastern Mediterranean, reducing and possibly stopping deep-water formation and thus ventilation of the seafloor (Rohling, 1994).

Reconstructing ventilation, sapropel formation and associated environmental changes in the Mediterranean relies on the ability to determine sea surface temperature, salinity and the isotopic composition of seawater. An independent temperature proxy (e.g. foraminiferal Mg/Ca or $U^{k'}_{37}$) combined with foraminiferal oxygen isotope values allows calculation of the oxygen isotopic composition of seawater ($\delta^{18}O_w$). This, in turn, can be used in isotopic mixing models to investigate freshwater input and its origin (O'Neil et al., 1969, Shackleton, 1974). The reliability of this method, however, relies on the accuracy of each of the proxies involved. For example, reconstructions of $\delta^{18}O_w$ may be complicated by variability in growth season between foraminifera (hence determining their $\delta^{18}O_{cc}$) and coccolithophores (affecting the $U^{k'}_{37}$). Seasonal or microhabitat effects may be even more important during periods of surface water

freshening, as suggested happens during sapropel formation, by increasing the vertical salinity gradient and potential niche separation. One way to circumvent such offsets is by measuring calcitic Mg/Ca (for temperature) and oxygen isotopes (for seawater $\delta^{18}O$) on the same, single specimen.

Incorporation of Mg into foraminiferal test calcite, however, does not solely depend on temperature, but is also influenced by seawater salinity (Nürnberg et al., 1996, Kisakürek et al., 2008, Dueñas-Bohórquez et al., 2009, Dissard et al., 2010). Within these studies salinity varied by evaporating or adding water, causing at the same time changes in the carbonate chemistry of the seawater, which is known to affect foraminiferal Mg/Ca values as well (Elderfield et al., 2006). The independent relation between salinity and foraminiferal Mg/Ca is, therefore, still unknown.

The independent effect of salinity on foraminiferal Mg/Ca was determined by a culturing experiment in which inorganic carbon chemistry was kept constant. Specimens of the benthic foraminifer *Ammonia tepida* were kept at a range of salinities (30.0-38.6), and monitored for addition of calcite. The determined effect of salinity on magnesium incorporation can then be used to correct Mg/Ca-based temperature reconstructions when salinity is known. Reconstruction of salinity can be done via the recently developed proxy using Na incorporation in foraminiferal test carbonate (Chapter 6).

Combining the corrected Mg/Ca temperatures with $\delta^{18}O$ and Na/Ca measured on the same individuals now allows accurate reconstruction of seawater temperature, salinity and $\delta^{18}O_w$ during sapropel formation. Here we applied this approach on sapropel S5, deposited ~125 kyr BP, as this is one of the most pronounced sapropels in an inter-glacial period (Rohling et al., 2004).

7.2 Methods

Specimens of *Ammonia tepida* were collected from an intertidal mudflat at the Wadden Sea near Den Oever, The Netherlands. *A. tepida* is a typical inhabitant of rapidly changing environments (Murray, 1968, Hayward et al., 2004), making it an suitable species for culture studies as they can grow in a wide range of environmental conditions (De Nooijer et al., 2007; Dueñas-Bohórquez et al., 2011a). Individual foraminifera were picked and placed in natural seawater at 20 °C and salinity of 35 and monitored for asexual reproduction. Shortly after reproduction juvenile specimens consisting of 2-3 chambers were handpicked and placed into the different experi-

ments.

Culture media consisting of artificially prepared seawater was made following the recipe of Kester et al. (1967). A range in salinities was obtained in the culture media by varying the amount of salts added to each solution (Table 7.1). Amounts of added $NaHCO_3$ and $B(OH)_3$ were kept constant for each batch of culture media in order to keep alkalinity and dissolved inorganic carbon (DIC) concentration constant. Subsequently, all prepared artificial seawater batches were mixed with an equal amount of natural seawater of salinity 35. Experiments were set at salinities of 30.0, 32.5, 36.1 and 38.6, covering a large part of the range in salinities found in the open ocean. Temperature, salinity, alkalinity and DIC were monitored over the course of each experiment (Table 7.2). Subsamples of each experiment were measured for elemental composition on an ICP-OES (Spectro Arcos) in order to check the concentrations in each salinity experiment. Alkalinity and DIC were used to calculate the carbonate system of the culture media, using CO2SYS (Lewis and Wallace, 1998) (Table 7.2). Experiments ran for 6-8 weeks to ensure sufficient foraminiferal chambers to be added. Benthic foraminifera were harvested and sieved over a 125 μm mesh. Size of individual foraminifera was determined using a microscope camera and calibrated computer software. Since the spiral growth mode of *A. tepida* produces outlines that are not perfectly circular, the diameter of each individual foraminifer was measured 4 times to calculate the average diameter.

Core MS66pc was selected for sampling the interval around sapropel S5. This core was taken at a depth of 1650 meters in the Eastern Mediterranean (33°1.9'N, 31°47.9'E)

Salinity	30.0	32.5	36.1	38.6
NaCl (g)	17.0509	20.4611	25.2353	28.6455
Na_2SO_4 (g)	2.8563	3.4276	4.2273	4.7986
KCl (g)	0.4825	0.5790	0.7140	0.8105
$NaHCO_3$ (g)	0.1960	0.1960	0.1960	0.1960
KBr (g)	0.0698	0.0838	0.1034	0.1173
$B(OH)_3$ (g)	0.0260	0.0260	0.0260	0.0260
NaF (g)	0.0021	0.0026	0.0032	0.0036
1M $MgCl_2$ (ml)	37.6280	45.1536	55.6894	63.2150
1M $CaCl_2$ (ml)	7.3403	8.8084	10.8640	12.3320
1M $SrCl_2$ (ml)	0.0713	0.0855	0.1060	0.1200

Table 7.1 Used amounts of salts for 1 liter of artificial seawater following the recipe of Kester et al. (1967). Artificial seawater is mixed with one liter of natural seawater at salinity 35.

during 2004 MIMES cruise on the R/V *Pelagia* (Boere et al., 2011). Specimens of *Globigerinoides ruber* were picked from the size interval from 300 to 450 µm and placed in 5% Sodiumhypochloride (NaOCl) to remove organic matter attached to the surface of the foraminiferal test. Afterwards individual foraminifera were rinsed 6 times with MilliQ and twice with Methanol with a sonic agitation step between each rinse to prepare the samples for trace metal or oxygen isotope analysis (Wit et al., 2010).

Element to calcium ratios were measured with Laser Ablation Inductively Coupled Mass Spectrometry (LA-ICP-MS), using ^{23}Na, ^{24}Mg, ^{26}Mg, ^{27}Al, ^{43}Ca, ^{44}Ca, ^{55}Mn and ^{88}Sr and their relative natural abundances (Reichart et al., 2003, Wit et al., 2010). Elemental ratios with respect to Ca were based on the average of each ablation profile. The same fossil specimens were subsequently used for analyzing stable oxygen isotopes. Oxygen isotopes were measured on 10-15 crushed specimens of *G. ruber* on a Mat Finnigan 253 gas-source mass spectrometer with an automated Kiel type carbonate preparation line. Results were calibrated against the Vienna Pee Dee Belemnite standard (V-PBD) using NBS-19 with an internal reproducibility for $\delta^{18}O$ of 0.08 ‰.

7.3 Results

Culture solution parameters were stable within and between experiments, with the exception of salinity, while Mg/Ca values of the culture solution increases slightly with salinity (Table 7.2). Values for Mg/Ca measured on the calcite test of benthic foraminifer *Ammonia tepida* correlate positively with salinity ($R^2 = 0.99$, $p < 0.01$) (Appendix 7.1, Figure 7.1). Inter-individual variability per experiment varies between 13-16% (relative standard deviation) and is similar between the different

Experiment	Salinity	DIC (µmol/kg)	Alkalinity (µmol/kg)	CO_3^{2-} (µmol/kg)	$\Omega_{Calcite}$	Mg/Ca (mol/mol)
S 30.0	30.0 ± 0.1	2131 ± 17	2462 ± 32	246 ± 15	6.10 ± 0.4	4.98 ± 0.02
S 32.5	32.5 ± 0.2	2222 ± 25	2543 ± 46	238 ± 50	5.81 ± 1.2	5.08 ± 0.03
S 36.1	36.1 ± 0.2	2188 ± 24	2526 ± 23	244 ± 32	5.80 ± 0.8	5.15 ± 0.04
S 38.6	38.6 ± 0.1	2126 ± 7	2493 ± 21	258 ± 40	6.01 ± 0.4	5.19 ± 0.04
µ	34.3	2161	2502	248	5.97	5.10
σ	3.8	41	40	13	0.44	0.09

Table 7.2 Experiment water data. Carbonate ion concentration and Omega Calcite are calculated using the CO2SYS software (Lewis and Wallace, 1998). Standard deviations are based on the monitoring measurements over the course of each experiment.

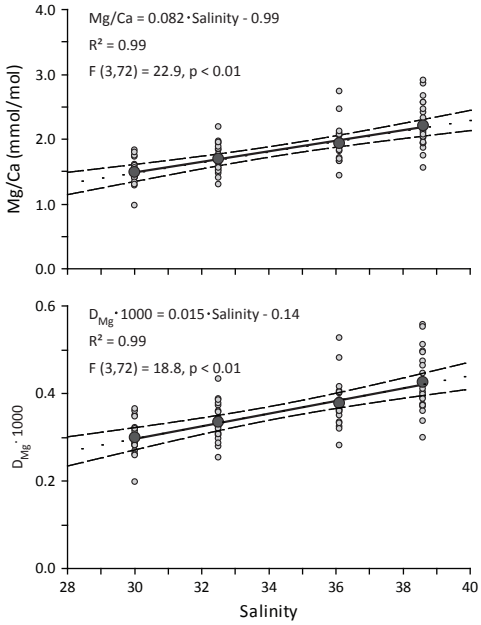

Figure 7.1 Foraminiferal Mg/Ca values (Upper panel) or D_{Mg} (Lower Panel) as measured on *A. tepida* versus the salinity of the culture solutions. Correlation coefficients are based on the averaged values. A one way analyses of variance (ANOVA) was performed with all data points to test the experimental effect of salinity for its significance.

experiments. The total range for all experiments in Mg/Ca is 0.98-2.57 mmol/mol. Foraminiferal test size significantly increases with salinity ($R^2 = 0.97$, $p < 0.01$) (Appendix 7.1, Figure 7.2).

Before, during and after deposition of sapropel S5 average Mg/Ca values of fossil planktonic foraminifer *G. ruber*, calculated for the different depth levels, varied between 3.12 and 6.13 mmol/mol (Appendix 7.2). Intra-test Variability varied between 18 and 49 % (relative standard deviation). Stable oxygen isotopes for *G. ruber* changes from 2.49 before, to -2.14 during and 0.72 ‰ (V-PDB) after deposition of the sapropel.

7.4 Discussion

7.4.1 Mg/Ca and Salinity

The Mg/Ca values of cultured benthic foraminifer *A. tepida* correlate well with salinity ($R^2 = 0.99$, $p < 0.01$) (Appendix 7.1, Figure 7.1). However, the small change in

Mg/Ca_{SW} between experiments potentially influences the correlation of foraminiferal Mg/Ca with salinity (Table 7.2). The effect of changes in Mg/Ca_{SW} can, however, be corrected for when expressing the foraminiferal Mg/Ca as its partition coefficient (D_{Mg}) (Figure 7.1). The partition coefficient of Mg (D_{Mg}) is the magnesium to calcium ratio in calcite compared to the concentration of the magnesium to calcium ratio in seawater. The correlation between D_{Mg} and salinity is highly significant ($R^2 = 0.99$, $p < 0.01$), indicating that the effect of variability in seawater Mg/Ca is negligible within this experiment. Changes in seawater Mg/Ca have been suggested to impact D values as well, albeit for high Mg carbonate test building species (Segev and Erez, 2006). Even for these species the changes in D_{Mg} related to Mg/Ca_{SW} would be only very

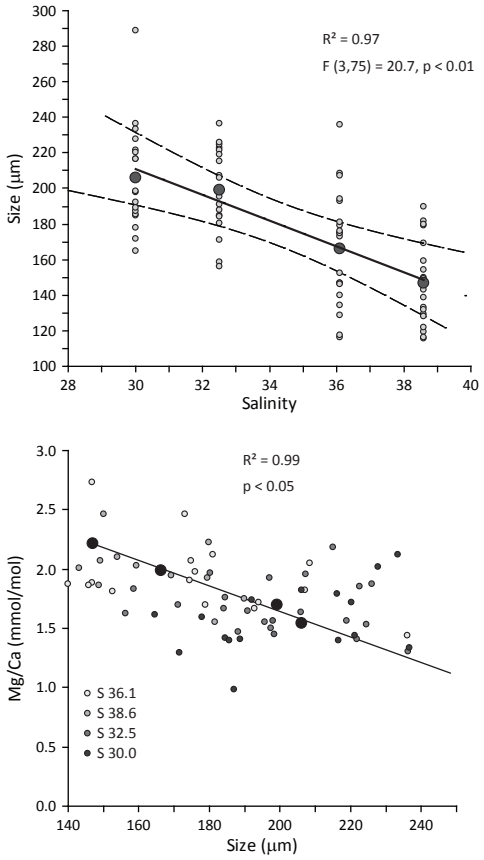

Figure 7.2 Individual size (Upper panel) or foraminiferal Mg/Ca values (Lower Panel) as measured on *A. tepida* versus the salinity of the culture solutions. Correlation coefficients are based on the averaged values. A one way analyses of variance (ANOVA) was performed with all data points to test the experimental effect of salinity for its significance.

minor (0.0001) over the measured range.

It has been shown that the incorporation of elements into foraminiferal test calcite of some species is correlated to ontogeny, i.e. depending on test size, (Nürnberg et al., 1996, Wit et al., 2010, Dueñas-Bohórquez et al., 2011b). Since in our experiment test size varied among culture conditions (Appendix 7.1), the relation between foraminiferal Mg/Ca and salinity may be indirect. To test this possibility, size and foraminiferal Mg/Ca within every of the four salinity experiments were analyzed. The experiments at a salinity of 30 and 32.5 do not show a significant correlation between size and Mg/Ca ($R^2 = 0.02$, $p > 0.10$ and $R^2 = 0.03$, $p > 0.10$ respectively, figure 7.3). However, experiments at higher salinities (36.1 and 38.6) show a small but significant effect of size on foraminiferal Mg/Ca ($R^2 = 0.22$, $p < 0.05$ and $R^2 = 0.45$, $p < 0.01$ respectively), indicating that part of the correlation between foraminiferal Mg/Ca and salinity may be attributed to the relation between size and test Mg/Ca. If the relation between salinity and foraminiferal Mg/Ca would be exclusively caused by ontogeny, no relation between foraminiferal Mg/Ca of a single chamber number (whorl position) and salinity would be present. However, chamber 3-13 (Figure 7.4) all show a significant correlation between Mg/Ca and salinity, although some variation in the relation is present. It is, therefore, concluded that the correlation between foraminiferal Mg/Ca and test size is primarily caused by co-variation of both parameters with salinity and that the relation between Mg/Ca and salinity for *A. tepida* found here is not

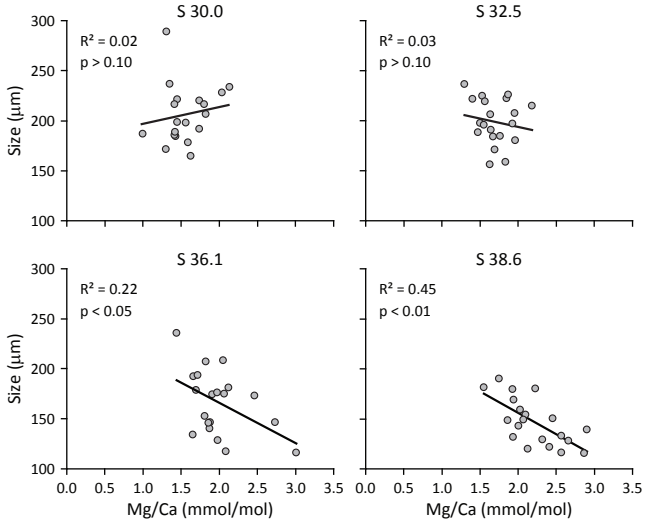

Figure 7.3 Measured Mg/Ca values of individual foraminifera versus size for the 4 salinity experiments. All relations are tested for significance with a one way ANOVA.

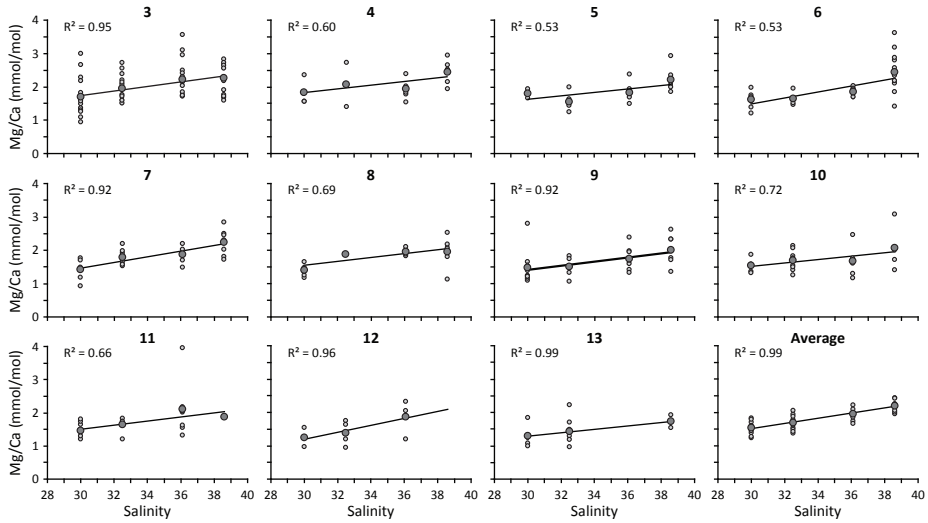

Figure 7.4 Salinity versus individual Mg/Ca values for each individual chamber. Chamber position is determined by counting the chambers in the whirl, starting at the youngest chambers. Correlation coefficients are determined on the averaged values per experiment.

significantly impacted by ontogeny. Still, a small effect may be present due to the variability in the relation between salinity and single chamber Mg/Ca. When measuring multiple chambers per individual foraminifera, as done here, this is not affecting the calibration.

Previous studies reported similar effects of salinity on the Mg content of both benthic and planktonic foraminifera (Kisakürek et al., 2008, Dueñas-Bohórquez et al., 2009, Dissard et al., 2010). The slope of the relation reported here (0.08) is similar to then one reported for *G. sacculifer* (0.11) (Dueñas-Bohórquez et al., 2009). Within the experiment of Dueñas-Bohórquez et al. (2009) the change in CO_3^{2-} was compensated, but alkalinity and DIC co-varied with salinity. The relative change per salinity unit is of the same order of magnitude as the response to changes in salinity of *G. ruber* in which alkalinity and DIC were not constant (Kisakürek et al., 2008). Since the response of Mg/Ca reported here is similar, while alkalinity and DIC were kept constant, we infer that alkalinity and DIC have a minor effect on foraminiferal Mg/Ca over this range. Dissard et al. (2010) also investigated the effect of salinity on Mg incorporation of *A. tepida*. Their calibration is characterized by relatively low Mg/Ca values and a low sensitivity of the relation between salinity and Mg/Ca (0.035 and 0.028). Within their experiment alkalinity, DIC and CO_3^{2-} co-varied with salinity,

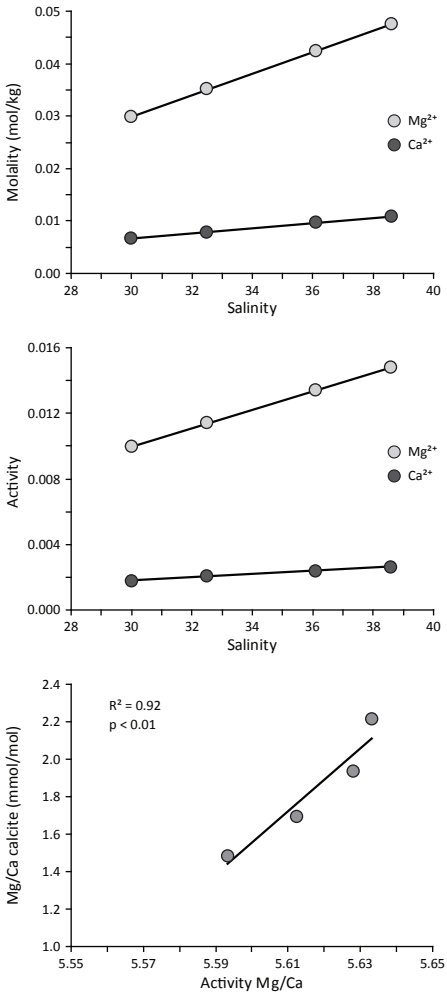

Figure 7.5 Salinity versus modeled Molality (Upper panel), Activity (Middle panel) and Free seawater Mg/Ca (Lower panel). Parameters were modeled using Phreeqc.

while adding Ca to the culture solution compensated for changes in the calcium carbonate saturation state. This decreases the Mg/Ca value of the culture solutions and hence Mg/Ca values of foraminiferal calcite and thus sensitivity to changes in salinity, resulting in similar D_{Mg} values for their and our experiment.

Similarity of the relations between salinity and foraminiferal Mg/Ca for both benthic and planktonic species indicates that alkalinity and DIC have no or a small impact on foraminiferal Mg/Ca. The similarity between the Mg/Ca to salinity relations, for all

different culture setups, analytical approaches and species, hints at a general control of salinity on the incorporation of Mg into foraminiferal calcite. The relation between salinity and foraminiferal Mg/Ca could, therefore, be related to purely a-biotic differences in element speciation related to changes in seawater salinity. Speciation of elements in seawater was modeled using PhreeqC (Lawrence Livermore National Laboratory database) with the different concentrations of salts used in our experiments. Model results show that molality and activity of for free Mg and Ca increase linearly with salinity and are an order of magnitude larger for free Mg^{2+} than that of free Ca^{2+} (Figure 7.5). This results in a change in the free Mg to free Ca ratios of the culture medium with increasing salinity, providing a mechanistic link between salinity and foraminiferal Mg/Ca.

7.4.2 Reconstructing sea surface conditions during sapropel formation

The effect of salinity on Mg/Ca significantly impacts reconstructed temperatures in areas that experienced relatively large changes in salinity. Variability of 1 salinity unit results in an offset of 0.20-1.5 °C in reconstructed Mg/Ca-based temperatures, depending on the sensitivity of the used temperature calibration (Wit et al., 2012). Therefore, large changes in salinity should be corrected for in order to accurately reconstruct seawater temperatures. To correct for the effect of salinity on foraminiferal Mg/Ca, the relation established between *Ammonia tepida* and salinity, the sensitivity of which was shown to be generally applicable to different species, was transferred to the temperature calibration of *G. ruber* (Elderfield and Ganssen, 2000). The Elderfield and Ganssen (2000) calibration is based on open ocean core top samples, for which here a general salinity of 35 is assumed.

$$Mg/Ca = 0.52\, e^{(0.10T)} + 0.08\,(S-35) \qquad (7.2)$$

Salinity can be reconstructed using a novel proxy based on the Na/Ca values of foraminiferal test calcite (Chapter 6). Hence, analyses of Na/Ca and Mg/Ca on the same foraminiferal tests allows correcting Mg/Ca-based temperatures for changes in salinity. During sapropel formation salinity is thought to change strongly, which always complicated the direct application of present day Mg/Ca-temperature calibrations. However, combining reconstructed salinities (Chapter 6) with Mg/Ca measured on the same individuals in equation 7.2 makes it possible to correct for salinity and accurately determine changes in temperature associated with sapropel formation.

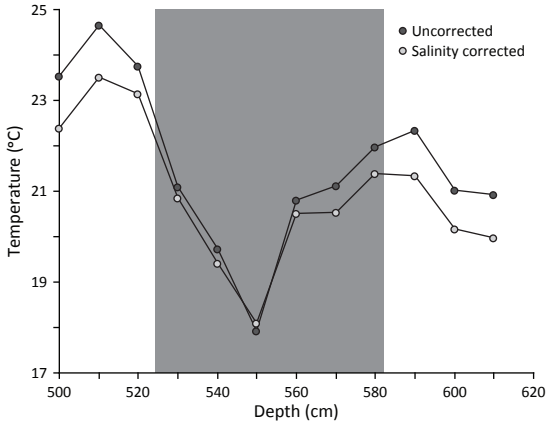

Figure 7.6 Mg/Ca based temperatures versus core depth. Mg/Ca values were converted to temperatures using the Mg/Ca-temperature calibration of Elderfield and Ganssen (2000) for planktonic species *G. ruber*. Corrected temperatures are calculated using equation 2 and the Na/Ca based salinities (Chapter 6).

Reconstructed temperatures during deposition of sapropel 5 show a 0.20-1.2 °C offset compared to temperatures not corrected for salinity (Figure 7.6). Sea surface temperatures during sapropel deposition decreased from 21 °C to 18 °C. This temperature decrease is similar to that based on $U^{k'}_{37}$, with lower temperatures before sapropel formation and higher afterwards (Rohling et al., 2004, Van der Meer et al., 2007). A deepening of the depth habitat of *G. ruber* may cause these lower temperatures during sapropel formation based on foraminifera, but this is unlikely due to the preference of this species for seawater with a relatively low salinity at the surface (Rohling et al., 2004). The preference of *G. ruber* for low salinities could, however, result in preferential recording of conditions of the season with highest fresh water input. Since the fresh surface water layer is most dominant during winter, this could explain the overall somewhat lower temperatures during sapropel formation. The changes in seawater temperatures during formation of S5 and the potential shift in the growth season of *G. ruber* is, furthermore, similar to observed changes in both temperature and blooming season during the formation of S1 in the Adriatic Sea, although absolute temperatures are somewhat higher during S5 (Sangiorgi et al., 2003).

Sea surface temperatures, corrected for changes in salinity, can subsequently be combined with the oxygen isotopes measured on the same specimens, allowing the calculation of the oxygen isotopic composition of the surface water ($\delta^{18}O_w$) (Figure 7.7). Figure 7.7 shows reconstructed temperatures based on Mg/Ca with the con-

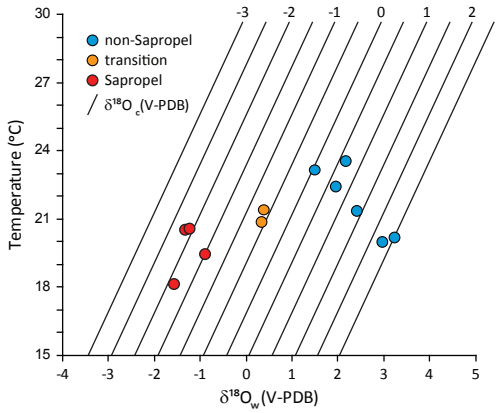

Figure 7.7 Oxygen isotopic composition of seawater calculated from the Mg/Ca based temperatures and measured $\delta^{18}O_c$. Values are calculated using the equation of O'Neil et al. (1969) as refitted by Shackleton (1974). Transitional and sapropel samples are much more depleted in oxygen isotopes, than samples from the pre- and post-sapropel period.

comitant values for the oxygen isotopic composition of calcite and that calculated for the surface water. The oxygen isotope composition of surface waters decreases at the onset of sapropel formation, coinciding with a reduction in sea surface salinity. This implies that the freshwater added to the sea surface during these events is light in oxygen isotope composition, as is the case for seawater diluted by river outflow and/or precipitation. Oxygen isotopic composition of surface water represents mixing between a freshwater and a high salinity Mediterranean seawater end-member. If the high salinity Mediterranean end-member is assumed fixed, the relative addition of freshwater at a certain point thus controls the $\delta^{18}O$ of seawater at that location. Modern Mediterranean seawater without the influence of the Nile River has an oxygen isotope composition of about 1.6 ‰ and a salinity of 39 (Pierre, 1999, Conkright et al., 2002), while the river Nile had a pre-Aswan dam signature of -2 ‰ and a salinity of 0 (El-Asrag, 2005). The $\delta^{18}O_w$ values at our core location should thus plot on this mixing line, since mixing between these two end-members determines salinity. Figure 7.8 shows reconstructed salinities versus reconstructed $\delta^{18}O_w$ from core MS66pc. Pre- and post-sapropel values all plot on this mixing line, confirming the dominant impact of river Nile outflow on salinity. Samples from the transition and from the sapropel itself, however, do not plot on this mixing line. This suggests that the $d^{18}O$ and salinity of one or both end members (the freshwater and/or Mediterranean seawater end-member) changed. Since the isotopic composition of the high salinity-

endmember is exclusively controlled by on-going evaporation it is likely to remain relatively stable. This implies that for the values observed during sapropel deposition discharge from the river Nile or enhanced Mediterranean precipitation should be approximately -20 ‰ (Figure 7.8). Such values, however, are reported for precipitation at higher latitudes only and have never been observed for rainfall over the Mediterranean or the Nile catchment (Bowen, 2012). Increased precipitation and/or Nile outflow can, therefore, not explain the observed combination of salinity and $\delta^{18}O_w$ values during formation of sapropel S5. Hence, the end-member representing the high salinity Mediterranean surface water during sapropel formation must have been impacted by a different source.

The Mediterranean climate during these periods was not only characterized by enhanced precipitation, but also more humid conditions have been reported (Rossignol-Strick, 1999). Such more humid conditions shifted Mediterranean surface waters towards lower salinity and lower $\delta^{18}O_w$. In general the overall composition changed towards a more Atlantic signal (lower salinity (37) and $\delta^{18}O_w$ (-1 ‰), while the $\delta^{18}O_w$ decreased to -4 ‰ due to an amount effect (El-Asrag, 2005). Samples from the period of sapropel formation are closer to the $\delta^{18}O_w$-salinity mixing line, when an Atlantic signature is assumed also for Mediterranean seawater. This indicates that not

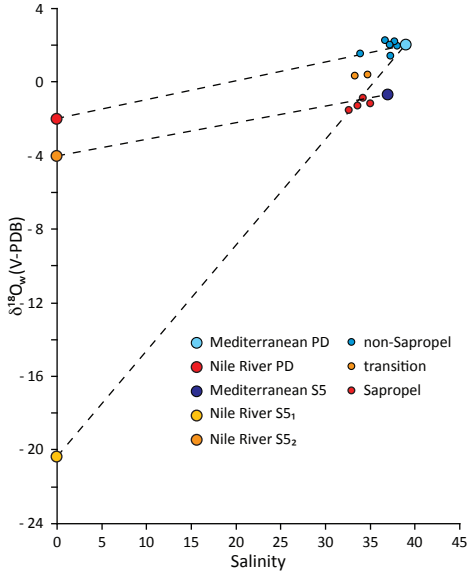

Figure 7.8 Reconstructed salinity versus $\delta^{18}O_w$. The dotted lines, represent different mixing lines for the Mediterranean basin during sapropel formation and in a present-day setting.

the enhanced input of freshwater by the Nile River and/or precipitation is primarily controlling formation of sapropels, but that lower evaporation in the entire Mediterranean basin resulted in less saline surface water, hence reducing Mediterranean overturning circulation.

A significant effect of higher latitude climate has been suggested by the impact of obliquity on sapropel formation (Lourens et al., 1996). When sapropels would be exclusively low latitude forced, one would expect only precession to impact sapropel formation. The influence of obliquity has been confirmed through numerical climate models, showing a clear link between African/Mediterranean precipitation and obliquity (Tuenter et al., 2003). A shift in the storm tracks of Atlantic depression over Europe could mechanistically link obliquity and Mediterranean climate. Changes in these storm tracks are predominantly related to atmospheric variations between high and low pressure areas over the North Atlantic basin, such as the North Atlantic Oscillation (NAO) (Hurrell, 1995). The position and strength over longer timescales of these high and low-pressure areas is influenced by changes in obliquity (Tuenter et al., 2006). The data presented here show that decreased evaporation and/or increased local precipitation resulted in sapropel formation, independently providing a climatic link between sapropel formation and obliquity.

7.5 Conclusions

The effect of salinity on foraminiferal Mg/Ca values appears to be mainly controlled by a change in speciation between free Mg and Ca with increasing salinity. This effect can be corrected for when Mg/Ca measurements are combined with an independent proxy for salinity, such as foraminiferal Na/Ca values. Combining salinity corrected temperatures with the calcite oxygen isotopic composition allows calculating the oxygen isotopic composition of seawater. When applied to Mediterranean sapropel S5, the resulting reconstruction suggests that samples from a sapropel period follow a different $\delta^{18}O_w$ -salinity mixing line than pre- and post-sapropel samples. The change from evaporative basin to a more precipitation-dominated basin is instrumental for sapropel formation and furthermore provides a mechanistic link between sapropel formation and obliquity.

References

Anand, P., Elderfield, H., 2005, Variability of Mg/Ca and Sr/Ca between and within the planktonic foraminifers *Globigerina bulloides* and *Globorotolia truncatulinoides*, *Geochem. Geophys. Geosys.,* **6**, 1-15.

Anand, P., Elderfield, H., Conte, M.H., 2003, Calibration of Mg/Ca thermometry in planktonic foraminifera from a sediment trap time series, *Paleoceanography,* **18**, 1050-1064.

Bárcena, M.A., Flores, J.A., Sierro, F.J., Pérez-Folgado, M., Fabres, J., Calafat, A., Canals, M., (2004), Planktonic response to main oceanographic changes in the Alboran Sea (Western Mediterranean) as documented in sediment traps and surface sediments, *Mar. Micropaleontol.,* **53**, 423-445.

Bard, E., Arnold, M., Duprat, J., Moyes, J., Duplessy, J.C., 1987, Bioturbation effects on abrupt climatic changes recorded in deep sea sediments. Correlation between $\delta^{18}O$ profiles and accelerator ^{14}C dating, in "*Abrupt Climate Change*" by Berger, W.H., Labeyrie, L.D., D. Reidel publishing Company, Dordrecht, 263-278.

Barker, S., Greaves, M., Elderfield, H., 2003, A study of cleaning procedures used for foraminiferal Mg/Ca paleothermometry, *Geochem., Geophys., Geosys.,* **4**, 1-20.

Barker, S., Broecker, W., Clark, E., Hajdas, I., 2007, Radiocarbon age offsets of foraminifera resulting from differential dissolution and fragmentation within the sedimentary bioturbated zone, *Paleoceanography*, **22**, 1-11.

Barnett P.R.O., Watson J. and Connely D., 1984, A multiple corer for taking virtually undisturbed sample from shelf, bathyal and abyssal sediments, *Oceanol. Acta*, **7**, 399-408.

Barras, C., Duplessy, J.-C., Geslin, E., Michel., E., Jorissen, F.J., 2010, Calibration of $\delta^{18}O$ of cultured benthic foraminiferal calcite as a function of temperature, *Biogeosciences*, **7**, 1349-1356.

Bemis, B.E., Spero, H.J., Bijma, J., Lea, D.W., 1998, Reevaluation of the oxygen isotopic composition of planktonic foraminifera: Experimental results and revised paleotemperature equations, *Paleoceanography*, **13**, 150-160.

Bentov S. and Erez J., 2006, Impact of biomineralization processes on the Mg content of foraminiferal shells: A biological perspective, *Geochem., Geophys., Geosyst.*, **7**, 1-11.

Bernhard, J.M., Blanks, J.K., Hintz, C., Chandler, T.G., 2004, Use of the fluorescent marker Calcein to label foraminiferal tests, J. Foram. Res., **34**, 96-101.

Bijma, J., Hemleben, C, Huber, B.T., Erlenkeuser, H., Kroon, D., 1998, Experimental determenation of ontogenetic stable isotope variability in two morphotypes of *Globigerinella siphonifera* (d'Orbigny), *Mar. Micropaleontol.*, **35**, 141-160.

Billups K. and Schrag D.P., 2002, Paleotemperatures and ice volume of the past 27 Myr revisited with paired Mg/Ca and $^{18}O/^{16}O$ measurements on benthic foraminifera, *Paleoceanography*, **17**, 1-11.

Billups, K., Spero, H., 1996, Reconstructing the stable isotope geochemistry and paleotemperatures of equatorial Atlantic during the last 150,000 years: Results from individual foraminifera, *Paleoceanography*, **11**, 217-238.

Bluman, A. G., 2004, Elementary Statistics: a step by step approach, McGraw-Hill, New York, 810 p.

Boere, A.C., Rijpstra, W.I.C., De Lange, G.J., Sinninghe Damsté, J.S., Coolen, M.J.L., 2011, Preservation potential of ancient plankton DNA in Pleistocene marine sediments, *Geobiology* , **9**, 377-393.

Bowen, G., 2012, www.waterisotopes.org, http://wateriso.eas.purdue.edu/waterisotopes/media/IsoMaps/jpegs/o_Global/oma_global.jpg

Boyle, E.A., 1992, Cadmium and $d^{13}C$ paleochemical ocean distribution during stage 2 Glacial Maximum, *Ann. Rev. Earth Planet. Sci.*, **20**, 245-287.

Bradley, R.S., 1999, Paleoclimatology: Reconstructing Climates of the Quaternary, International Geophysics Series Vol. 68, Elsevier Academic Press, London, 614 p.

Broecker, W.S., 1990, Salinity history of the northern Atlantic during the last deglaciation, *Paleoceanography*, **5**, 459-467.

Calvert, S.E., 1983, Geochemistry of Pleistocene sapropels and associated sediments from the eastern Mediterranean, *Oceano. Acta*, **6**, 255-267.

Caron, D.A., Anderson, R.O., Lindsey, J.L., Faber Jr, W.W., Lin Lim, E., 1990, Effects of Gametogenisis on Test Structure and Dissolution of Some Spinose Planktonic Foraminifera and Implications for Test Preservation, *Mar. Micropaleontol.,* **16**, 93-116.

Clark, F.W., Wheeler, W.C., 1922, The inorganic constituents of marine invertebrates, *US. Geol. Surv. Prof. Papers*, **124**, 62p.

Conkright, M.E., Locarnini, R.A., Garcia, H.E., O'Brien, T.D., Boyer, T.P., Stephens, C., Antonov, J.I., 2002, World Ocean Atlas 2001: Objective Analysis, Data Statistics, and Figures, CD-ROM, Documentation, National Oceanographic Data Center, Silver Spring.

De Lange, G.J., Ten Haven, H.L., 1983, Recent sapropel formation in the eastern Mediterranean, *Nature*, **305**, 797-798.

De Lange, G.J., Thomson, J., Reitz, A., Slomp, C.P., Speranza Principato, M., Erba, E., Corselli, C., 2008, Synchronous basin-wide formation and redox-controlled preservation of a Mediterranean sapropel, *Nat. Geosc.*, **1**, 606-610.

De Nooijer, L.J., Hathhorne, E., G.J. Reichart, Langer, G., Bijma, J., under review, Variability in calcitic Mg/Ca and Sr/Ca ratios in clones of the benthic foraminifer *Ammonia tepida*, *Geochem. Geophys. Geosys.*

De Nooijer, L.J., Langer, G., Nehrke, G., Bijma, J., 2009a, Physiological controls on seawater uptake and calcification in the benthic foraminifer *Ammonia tepida*, *Biogeosciences*, **6**, 2669-2675.

De Nooijer, L.J., Toyofuku, T., Kitazato, H., 2009b, Foraminifera promote calcification by elevating their intracellular pH, *PNAS*, **106**, 15374-15378.

De Rijk, S., Troelstra, S.R., Rohling, E.J., 1999, Benthic foraminiferal distribution in the Mediterranean Sea, *J. Foraminiferal Res.,* **29**, 93-103.

Debenay J.P., Guillou J.J., Geslin E., Lesourd M. and Redois F., 1998, Processus de cristallisation de plaquettes rhomboédriques à la surface d'un test porcelané de foraminifère actuel, *Geobios.* **31**, 295-302.

Dekens, P.S., Lea, D.W., Pak, D.K., Spero, H.J., 2002, Core top calibration of Mg/Ca in tropical foraminifera: Refining paleotemperature estimation, *Geochem. Geophys. Geosys.,* **3**, 1-29.

Delaney, M.L., Bé, A.W.H., Boyle, E.A., 1985, Li, Sr, Mg and Na in foraminiferal calcite shells from laboratory culture, sediment traps, and sediment cores, *Geochim. Cosmochim. Acta*, **49**, 1327-1341.

DeMenocal, P., Ortiz, J., Guilderson, T., Sarnthein, M., 2000, Coherent High- and Low-Latitude Climate Variability During the Holocene Warm Period, *Science*, **288**, 2198-2202.

Denton, G.H., Alley, R.B., Comer, G.C., Broecker, W.S., 2005, The role of seasonality in abrupt climate change, *Quat. Sci. Rev.*, **24**, 1159-1182.

Dickson J.A.D., 2002, Fossil Echinoderms As Monitor of the Mg/Ca Ratio of Phanerozoic Oceans. *Science*, **298**, 1222-1224.

Dickson J.A.D., 2004, Echinoderm skeletal preservation: Calcite-Aragonite seas and the Mg/Ca ratio of phanerozoic oceans, *J. of Sed. Res.*, **74**, 355-365.

Dissard, D., Nehrke, G., Reichart, G.J., Nouet, J., Bijma, J., 2009, Effect of the fluorescent indicator calcein on Mg and Sr incorporation into foraminiferal calcite, *Geochem., Geophys. Geosyst.*, **10**, 1-13.

Dissard D., Nehrke G., Reichart G.J. and Bijma J., 2010, Impact of seawater pCO_2 on calcification and Mg/Ca and Sr/Ca ratios in benthic foraminifera calcite: results from culturing experiments with *Ammonia tepida*, *Biogeosci*., **7**, 81-93.

Dissard, D., Nehrke, G., Reichart, G.J., Bijma, J., 2010, The impact of salintiy on the Mg/Ca and Sr/Ca ratio in the benthic foraminifera *Ammonia tepida*: Results from culture experiments, *Geochim. Cosmochim. Acta*, **74**, 928-940.

Dueñas-Bohórquez A., da Rocha R.E., Kuroyanagi A., Bijma J. and Reichart G. J., 2009, Effect of salinity and seawater calcite saturation state on Mg and Sr incorporation in cultured planktonic foraminifera, *Mar. Micropaleo.*, **73**, 178-189.

Dueñas-Bohórquez A., da Rocha R.E., Kuroyanagi A., De Nooijer L.J., Bijma J. and Reichart G. J., 2011, Interindividual variability and ontogenetic effects on Mg and Sr incorporation in the planktonic foraminifer *Globigerinoides sacculifer*, *Geochim. Cosmochim. Acta*, **75**, 520-532.

Dueñas-Bohórquez A., Raitzsch, M., De Nooijer, L.J., Reichart, G.J., 2011, Independent impacts of calcium and carbonate ion concentration on Mg and Sr incorporation in cultured benthic foraminifera, *Mar. Micropal.*, **81**, 122-130.

El-Asrag, A.M., 2005, Effect of synoptic and climatic situations on fractionation of stable isotopes in rainwater over Egypt and East Mediterranean, *Isotopic composition of precipitation in the Mediterranean Basin in relation to air circulation patterns and climate: Final report of a coordinated research project 2000-2004*, IAEA-TECDOC-1453, 230 p.

Elderfield, H., Ganssen G.M., 2000, Past temperatures and $\delta^{18}O$ of surface waters inferred from foraminiferal Mg/Ca ratios, *Nature*, **405**, 442-445.

Elderfield H., Yu J., Anand P., Kiefer T. and Nyland B., 2006, Calibrations for benthic foraminferal Mg/Ca paleothermometry and the carbonate ion hypothesis, *Earth Planet. Sci. Let.*, **250**, 633-649.

Emeis, K.C., Schultz, H., Struck, U., Rossignol-Strick, M., Erlenkeuser, H., Howell, M.W., Kroon, D., Mackensen, A., Ishizuka, S., Oba, T., Sakamoto, T., Koizumi, I., 2003, Eastern Mediterranean surface water temperatures and $\delta^{18}O$ composition during deposition of

sapropels in the late Quaternary, *Paleoceanography*, **18**, 1-18.

Emiliana, C., 1955, Pleistocene temperatures, *J. Geology*, **53**, 538-578.

Epstein, S., Buchsbaum, R., Lowenstam, Urey, H.C., (1951), Carbonate-water isotopic temperature scale, *Geo.l Soc. Am. Bull.,* **62**, 417-426.

Epstein, S., Buchsbaum, R., Lowenstam, H.A, Urey, H.C., 1953, Revised carbonate-water isotopic temperature scale, *Geo.l Soc. Am. Bull.*, **64**, 1315-1325.

Erez J., 2003, The source of ions for biomineralization in foraminifera and their implications for paleoceanographic proxies, *Rev. Miner. Geochem.* **54**, 115-149.

Fairbanks, R.G., Sverdlove, M., Free, R., Wiebe, P.H., Be, A.W.H., 1982, Vertical distribution and isotopic fractionation of living planktonic foraminifera from the Panama Basin, *Nature*, **298**, 841-844.

Fantle M.S. and DePaolo D.J., 2006, Sr isotopes and pore fluid chemistry in carbonate sediment of the Ontong Java Plateau: Calcite recrystallization rates and evidence for a rapid rise in seawater Mg over the last 10 million years, *Geochim. Cosmochim. Acta*, **70**, 3883-3904.

Ferguson, J.E., Henderson, G.M., Kucera, M., Rickaby, R.E.M., 2008, Systematic change of foraminiferal Mg/Ca ratios across a strong salinity gradient, *Earth Planet. Sci. Lett.,* **265**, 153-166.

Field, A., 2009, Discovering statistics using SPSS, SAGE, London, 822 p.

Filipsson, H.L., Berhard, J.M., Lincoln, S.A., McCorkle, D.C., 2010, A culture-based calibration of benthic foraminiferal paleotemperature proxies: $\delta^{18}O$ and Mg/Ca results, *Biogeosciences*, **7**, 1335-1347.

Fontanier C., Jorissen F.J., Licari L., Alexandre A., Anschutz P. and Carbonel P., 2002, Live benthic foraminiferal faunas from the Bay of Biscay: faunal density, composition, and microhabitats, *Deep-Sea Res. I*, **49**, 751-785.

Fontanier, C., Jorissen, F.J., Chaillou, G., David, C., Anschutz, P. et Lafon, V. 2003. Seasonal and interannual variability of benthic foraminiferal faunas at 550 m depth in the Bay of Biscay. *Deep-Sea Res.*, I, **50**, 457-494.

Fontanier C., Jorissen F.J., Chaillou G., Anschutz P., Grémare A. and Griveaud C., 2005, Live foraminiferal faunas from a 2800 m deep lower canyon station from the Bay of Biscay: Faunal response to focusing of refractory organic matter, *Deep-Sea Res. I*, **52**, 1189-1227.

Fontanier, C., Jorissen, F.J., Anschutz, P. and Chaillou, G., 2006, Seasonal variability of benthic foraminiferal faunas at 1000 m depth in the Bay of Biscay. *J. Foram. Res.*, **36**, 61-76.

Ganssen, G.M., Kroon, D., 2000, The isotopic signature of planktonic foraminifera from NE Atlantic surface sediments: implications for the reconstructions of past oceanic conditions, *J.Geol. Soc. London,* **157**, 693-699.

Ganssen, G.M., Brummer, G.J.A., Jung, S.J.A., Kroon, D., Peeters, F.J.C., 2005, The oxygen isotope composition in planktic foraminifera shells as recorder of maximum seasonal SST variation, *Geophys. Res. Abs.*, **7**, 01775.

Ganssen, G., Peeters, F., Metcalfe, B., Anand, P., Jung, S., Kroon, D., Brummer, G.J., 2011, Quantifying sea surface temperatures ranges of the Arabian Sea for the past 20000 years, *Clim. Past*, **7**, 1337–1349.

Gooday, A.J., 2003. Benthic foraminifera (Protista) as tools in deep-water palaeoceanography: environmental influences on faunal characteristics. *Adv. Mar. Bio.*, **46**, 1-90.

Gordon, C.M., Carr, R.A., Larson, R.E., 1970, The influence of environmental factors on the sodium and manganese content of barnacle shells, *Limnol. Ocean.*, **15**, 461-466.

Goyet C., Healy R.J. and Ryan J.P., 2000, Global distribution of total inorganic carbon and total alkalinity below deepest winter mixed layer depths, ORNL/CDIAC-127, NDP-076.

Guinasso Jr, N.L., Schink, D.R., 1975, Quantitative estimates of biological mixing rates in abyssal sediments. *J. Geophys. Res.,* **80**, 3032-3043.

Hardie L.A., 1996, Secular variation in seawater chemistry: An explanation for the coupled secular variation in the mineralogies of marine limestone and potash evaporites over the past 600 my, *Geology*, **24**, 279-283.

Hasiuk, F.J., Lohmann, K.C., 2010, Application of calcite Mg partitioning functions to the reconstruction of paleocean Mg/Ca, *Geochim. Cosmochim. Acta*, **74**, 6751-6763.

Hathorne, E.C., James, R.H., Savage, P., Alard, O., 2008, Physical and chemical characteristics of particles produced by laser ablation of biogenic calcium carbonate, *J. Analyt. Atom. Spectro.*, **23**, 240-243.

Hathorne, E.C., James, R.H., Lampitt, R.S., 2009, Environmental versus biomineralization controls on the intratest variation in the trace element composition of the planktonic foraminifera *G. inflata* and *G. scitula*, *Paleoceanography*, **24**, 1-14.

Hay, W.W., DeConto, R.M., Wold, C.N., 1997, Climate: Is the past the key to the future?, *Geologische Rundschau*, **86**, 471-491.

Hayward, B.W., Holzmann, M., Grenfell, H.R., Pawlowski, J., Triggs, C.M., 2004, Morphological distinction of molecular types in Ammonia – towards a taxonomic revision of the world's most commonly misidentified foraminifera, *Mar. Micropal.* **50**, 237-271.

Healey S.L., Thunell R.C. and Corliss B.H., 2008, The Mg/Ca-temperature relationship of benthic foraminiferal calcite: New core-top calibrations in the <4°C temperature range, *Earth Planet. Sci. Let.*, **272**, 523-530.

Hemleben, C., Spindler, M., Anderson, O.R., 1989, Modern planktonic foraminifera, Springer, New York, 363 p.

Hemleben, C., 2002, Short Cruise Report; R.V. Meteor Cruise 51, Leg 3, 4p.

Hemleben, C., Spindler, M., Anderson, O.R., 1989, Modern Planktonic Foraminifera, Springer, New York, 363 p.

Hess, S., and Jorissen, F.J., 2009. Distribution patterns of living benthic foraminifera from Cap Breton Canyon, Bay of Biscay: faunal response to sediment instability. *Deep-Sea Res., I*, **56**, 1555-1578.

Hilgen, F.J., 1991, Astronomical calibration of Gauss to Matuyama sapropels in the Mediterranean and implication for the Geomagnetic Polarity Time Scale, *Earth Planet. Sci. Let.*, **104**, 226-244.

Hintz, C. J., Shaw, T.J., Bernhard, J.M., Chandler, G.T., McCorckle, D.C., Blanks, J.K., 2006, Trace/minor element:calcium ratios in cultured benthic foraminifera. Part II: Ontogenetic variation, *Geochim. Cosmochim. Acta*, **70**, 1964-1976.

Holland H.D. and Zimmerman H., 2000, The dolomite problem revisited, *Int. Geol. Rev.*, **42**, 481-490.

Holland H.D., 2005, Sea level, sediments and the composition of seawater, *Americ. J. Sci.*, **305**, 220-239.

Holzmann, M., Habura, A., Giles, H., Bowser, S.S., Pawlowski, J., 2003, Freshwater foraminiferans revealed by analysis of environmental DNA samples, *J. of Eukary. Microbiol.*, **50**, 135-139.

Hopkins, T.S., (1991), The GIN-sea, a synthesis of its physical oceanography and literature review 1972–1985, *Earth Sci. Rev.,* **30**, 175-318.

Horita J., Zimmerman H. and Holland H.D., 2002, Chemical evolution of seawater during the Phanerozoic: Implications from the record of marine evaporites, *Geochim. Cosmochim. Acta*, **66**, 3733-3756.

Hübscher, C., 2002, Short Cruise Report; R.V. Meteor Cruise M52/2, 5.

Hurrell, J.W., 1995, Decadal Trends in the North Atlantic Oscillation: Regional Temperatures and Precipitation, *Science,* **269**, 676-679.

Hut, G., 1987, Stable isotope reference samples for geochemical and hydrological investigations. Consultant Group Meeting, 16-18.09.1985., Int. At. Energy Agency (I.A.E.A.), Vienna, Austria, 42p.

Hutson, W.H., 1980, Bioturbation of deep-sea sediments: Oxygen isotopes and stratigraphic uncertainties, *Geology*, **8**, 127-130.

Imbrie, J., Kipp, N.G., 1971, A new micropaleontological method for paleoclimatology: Application to a Late Pleistocene Caribbean core. *In* "The Late Cenozoic Glacial Ages" (K.K. Turekian Ed.), Yale University Press, New Haven, Connecticut, 71-181.

IPCC, 2007, Climate Change 2007: Synthesis report. Contributions of working groups I, II and III to the fourth Assessment Report of Intergovermental Panel on Climate Change. Technical Report.

Ishikawa, M., Ichikuni, M., 1984, Uptake of sodium and potassium by calcite, *Chem. Geol.*, **42**, 137-146.

Jorissen, F.J., 1987, Benthic foraminifera from the Adriatic Sea; principles of phenotypic variation, *Utrecht Micropaleontological Bulletins*, **37**, 176 p.

Jorissen, F.J., Barmawidjaja, D.M., Puskaric, S., Van der Zwaan, G.J., 1992, Vertical distribution of benthic foraminifera in the northern Adriatic Sea: The relation with the organic flux, *Mar. Micropal.*, **19**, 131-146.

Jorissen, F.J., Wittling,, I., Peypuquet, J.P., Rabouille, C., Relexans, J.C., 1998, Live benthic foraminiferal faunas off Cape Blanc, NW-Africa: Community structure and microhabitats, *Deep-Sea Res. I: Ocean. Res. Papers*, **45**, 2157-2188.

Jourabchi P., Van Capellen P. and Regnier P., 2005, Quantitative interpretation of pH distributions in aquatic sediments: A reaction-transport modeling approach, *Americ. J. Sci*., **305**, 919-956.

Keigwin, L.D., 1996, The Little Ice Age and Medieval Warm Period in the Sargasso Sea, *Science*, **274**, 1504-1508.

Keigwin, L.D., Guilderson, T.P., 2009, Bioturbation artifacts in zero-age sediments, *Paleoceanography*, **24**, 1-6.

Kester, D.R., Duedall, I.W., Connors, D.N., Pytkowicz, R.M., 1967, Preperation of artificial seawater, *Limonol. Ocean.*, **12**, 176-179.

Kisakürek, B., Eisenhauer, A., Böhm, D., Garbe-Schönberg, Erez, J., 2008, Controls on shell Mg/Ca and Sr/Ca in cultured plankyonic foraminifera, *Globigerinoides ruber* (white), *Earth Planet. Sci. Lett.*, **273**, 260-269.

Kitano, Y., Okumura, M., Idogaki, 1975, M. Incorporation of sodium, chloride and sulfate with calcium carbonate, *Geochem. J.*, **9**, 75-84.

Koho, K.A., García, R., de Stigter, H.C., Epping, E., Koning, E., Kouwenhoven, T.J., van der Zwaan, G.J., 2008, Sedimentary labile organic carbon and pore water redox control on species distribution of benthic foraminifera: A case study from Lisbon-Setúbal Canyon (southern Portugal), *Prog. Oceanography*, **79**, 55-82.

Koutavas, A., deMenocal, P.B., Olive, G.C., Lynch-Stieglitz, J., 2006, Mid-Holocene El Niño-Southern Oscillation (ENSO) attenuation revealed by individual foraminifera in eastern tropical Pacific sediments, *Geology,* **34**, 993-996.

Kroon, D., Darling, K., 1995, Size and upwelling control of stable isotope composition of *Neogloboquadrina dutertrei* (d'Orbigny), *Globigerinoides ruber* (d'Orbigny) and *Globigerina bulloides* (d'Orbigny): Examples from the Panama basin and Arabian Sea, *J. Foraminiferal Res.,* **25**, 39-52.

Lea, D.W., Mashiotta, T.A., Spero, H.J., 1999, Controls on magnesium and strontium uptake in planktonic foraminifera determined by live culturing, *Geochim. Cocmochim. Acta,* **63**, 2369-2379.

Lear C.H., Elderfield H. and Wilson P.A., 2000, Cenozoic Deep-Sea temperatures and Global ice volumes from Mg/Ca in benthic foraminiferal calcite, *Science*, **287**, 269-272.

Lear C.H., Rosenthal Y. and Slowey N., 2002, Benthic foraminiferal Mg/Ca-paleothermometry: A revised core-top calibration, *Geochim. Cosmochim. Acta*, **66**, 3375-3387.

Lewis, E., Wallace, D., 1998, Program developed for CO_2 system calculations, 38 p.

Linke P. and Lutze G. F., 1993, Microhabitat preferences of benthic foraminifera – a static concept or a dynamic adaptation to optimize food acquisition?, *Mar. Micropaleontol.*, **20**, 215-234.

Lourens, L.J., Antonarakou, A., Hilgen, F.J., Van Hoof, A.A.M., Vergnaud-Grazzini, C., Zachariasse, W.J., 1996, Evaluation of the Plio-Pleistocene astronomical timescale, *Paleoceanography*, **11**, 391-413.

Lourens L.J., Hilgen F.J., Laskar J. and Shackleton N.J., Wilson D. (2004). The Neogene Period. In Gradstein F.M., Ogg J.G. and Smith A.G. (Eds.), *A Geologic Time Scale 2004* (pp. 409-440). Cambridge University Press.

Lowenstein T.K., Timofeff M.N., Brennan S.T., Hardie L.A. and Demicco D.V., 2001, Oscillations in Phanerozoic Seawater Chemistry: Evidence from Fluid Inclusions, *Science*, **294**, 1086-1088.

Magana A. L., Southon J. R., Kennett J. P., Roark E. B., Sarnthein M. and Stott L. D., 2010, Resolving the cause of large differences between deglacial benthic foraminifera radiocarbon measurements in Santa Barbara Basin, *Paleoceanography*, **115**. 1-12.

Martin P.A., Lea D.W., Rosenthal Y., Shackleton N.J., Sarntheim M. and Papenfuss T., 2002, Quaternary deep sea temperature history derived from benthic foraminiferal Mg/Ca, *Earth Planet. Sci. Let.*, **198**, 193-209.

McManus, J.F., Francois, R., Gherhardi, J.M., Keigwin, L.D., Brown-Leger, S., 2004, Collapse and rapid resumption of Atlantic meridional circulation linked to deglacial climate changes, *Nature*, **428**, 834-837.

Medina-Elizalde, M., Lea, D.W., Fantle, M.S., 2008, Implications of seawater Mg/Ca variability for Plio-Pleistocene tropical climate reconstruction, *Earth Planet. Sci. Let.*, **3-4,** 585-595.

Medina-Elizalde, M., Lea, D.W., 2010, Late Pliocene equatorial Pacific, *Paleoceanography*, **25**, 1-10.

Millot, C., 1987, Circulation in the western Mediterranean, *Oceanol. Acta,* **10**, 143-149.

Morse, J.W., Arvidson, R.S., Lüttge, A., 2007, Calcium carbonate formation and dissolution, Chemic. Rev., **107**, 342-381.

Murray, J.W., 1968, Living foraminifers of lagoons and estuaries, *Micropal.*, **14**, 435-455

Nürnberg, D, Bijma, J., Hemleben, C., 1996, Assessing the reliability of magnesium in foraminiferal calcite as a proxy for water mass temperature, *Geochim. Cosmochim. Acta*, **60**, 803-814.

O'Neil, J.R., Clayton, R.N., Mayeda, T.K., 1969, Oxygen isotope fractionation in divalent metal carbonates, *J. Chem. Phys.*, **51**, 5547-5558.

Ogawa N. and Tauzin P., 1973, Contribution à l'étude hydrologique et géochimique du golfe de cap-breton, *Bulletin de l'institut Géologique du Bassin d'Aquitaine Bordeaux*, **14**, 19-46.

Ottens, J.J., 1991, Planktonic foraminifera as North Atlantic water mass indicators, *Oceanol. Acta,* **14**, 123-140.

Ovchinnikov, I.M., 1966, Circulation in the surface and intermediate layers of the Mediterranean. *Oceanology,* **6**, 48–59.

Pawlowski, J., Holzmann, M., Berney, C., Fahrni, J., Gooday, A.J., Cedhagen, T., Habura, A., Bowser, S.S., 2003, The evolution of early Foraminifera, *PNAS*, **100**, 11494-11498.

Peng, T.H., Broecker, W.S., 1984, The impacts of bioturbation on the age difference between benthic and planktonic foraminifera in deep sea sediments, *Nuc. Instrum. Meth. Phys. Res. B*, **5**, 346-352.

Peng, T.H., Broecker, W.S., Berger, W.H., 1979, Rates of benthic mixing in deep-sea sediment as determined by radioactive tracers, *Quat. Res.*, **11**, 141-149.

Petit, J.R., Jouzel, J., Raynaud, D., Barkov, N.I., Barnola, J.-M., Basile, I., Bender, M., Chappellaz, J., Davis, M., Delaygue, G., Delmotte, M., Kotlyakov, V.M., Legrand, M., Lipenkov, V.Y., Lorius, C. Pépin, L., Ritz, C., Saltzman, E., Stievenard, M., 1999, Climate and atmospheric history of the past 420,000 years from the Vostok ice core, Antarctica, *Nature*, **399**, 429-436.

Pierre, C., 1999, The oxygen and carbon isotope distribution in the Mediterranean water masses, *Mar. Geol.*, **153**, 41-55.

Pujol, C., Vergnaud-Grazzini, C., 1995, Distribution patterns of live planktic foraminifers as related to regional hydrography and productive systems of the Mediterranean Sea, *Mar. Micropaleontol.,* **25**, 187-217.

Raitzsch M., Dueñas-Bohórquez A., Reichart G.-J., de Nooijer L.J. and Bickert T., 2010, Incorporation of Mg and Sr in calcite of cultured benthic foraminifera: impact of calcium concentration and associated calcite saturation state, *Biogeosci.*, **7**, 869-881.

Rathmann S. and Kuhnert H., 2008, Carbonate ion effect on Mg/Ca, Sr/Ca and stable isotopes on the benthic foraminifera *Oridorsalis umbonatus* off Namibia, *Mar. Micropaleontol.*, **66**, 120-133.

Rathmann S., Hess S., Kuhnert H. and Mulitza S., 2004, Mg/Ca ratios of the benthic foraminifera *Oridoralis umbonatus* obtained by laser ablation from core top sediments: Relationship to bottom water temperature, *Geochem. Geophys. Geosyst.*, **5**, 1-10.

Reichart G-J., Jorissen F., Anschutz P. and Mason P.R.D., 2003, Single foraminiferal test chemistry records the marine environment, *Geology*, **31**, 355-358.

Ries, J.B., 2004, Effect of ambient Mg/Ca ratio on Mg fractionation in calcareous marine invertebrates: A record of the oceanic Mg/Ca ratio over the Phanerozoic, *Geology*, **32**, 981-984.

Rohling, E.J., Gieskes, W.W.C., 1989, Late Quaternary changes in Mediterranean intermediate water density and formation rate, *Paleoceanography*, **4**, 531-545.

Rohling, E.J., 1994, Review and new aspects concerning the formation of eastern Mediterranean sapropels, *Mar. Geol.*, **122**, 1-28.

Rohling, E.J., Bigg, G.R., 1998 Paleosalinity and $\delta^{18}O$: A critical assessment, *J. Geophys. Res.*, **103**, 1307-1318.

Rohling, E.J., 1999, Environmental control on Mediterranean salinity and $\delta^{18}O$, *Paleoceanography,* **14**, 706-715.

Rohling, E.J., Sprovieri, M., Cane, T., Casford, J.S.L., Cooke, S., Bouloubassi, I., Emeis, K.C., Schiebel, R., Rogerson, M., Hayes, A., Jorissen, F.J., Kroon, D., 2004, Reconstructing past planktic foraminiferal habitats using stable isotope data: a case history for Mediterranean sapropel S5, *Mar. Micropal.*, **50**, 89-123.

Rosenthal Y., Boyle E.A. and Slowey N., 1997, Temperature control on the incorporation of magnesium, strontium, fluorine, and cadmium into benthic foraminiferal shells from Little Bahama Bank: Prospects for thermocline paleoceanography, *Geochim. Cosmochim. Acta*, **61**, 3633-3643.

Rosenthal, Y., Morley, A., Barras, C., Katz, M.E., Jorissen, F.J., Reichart, G.J., Oppo, D.W., Linsley, B.K., 2011, Temperature calibration of Mg/Ca ratios in the intermediate water benthic foraminifer *Hyalinea balthica*, *Geochem., Geophys., Geosys.*, **12**, 1-17.

Rossignol-Strick, M., Nesteroff, W., Olive, P., Vergnaud-Grazzini, C., 1982, After the deluge : Mediterranean stagnation and sapropel formation, *Nature*, **295**, 105-110.

Rossignol-Strick, M., 1985, Mediterranean Quaternary sapropels, an immediate response of the African monsoon to variation of insolation, *Palaeogeogr., Palaeoclimatol., Palaeoecol,*, **49**, 237-263.

Rossignol-Strick, M., 1999, The Holocene climatic optimum and pollen records of sapropel 1 in the eastern Mediterranean, 9000-6000 BP, *Quat. Sci. Rev.*, **18**, 515-530.

Rucker, J.B., Valentine, J.W., 1961, Salinity response of trace elements concentration in *Crassostrea virginica*, *Nature*, **190**, 1099-1100.

Rupke, N.A., Stanley, D.J., Stuckenrath, R., 1974, Late Quaternary rates of abbysal mud deposition in the western Mediterranean Sea, *Mar. Geol.*, **17**, M9-M16.

Russell, A.D., Spero, H.J., 2000, Field examination of the oceanic carbonate ion effect on stable isotopes in planktic foraminifera, *Paleoceanography,* **15**, 43-52.

Russell, A.D., Hönisch, B., Spero, H.J., Lea, D.W., 2004, Effects of seawater carbonate ion concentration and temperature on shell U, Mg, and Sr in cultured planktonic foraminifera, *Geochim. Cosmochim. Acta*, **68**, 4347-4361.

Rutten, A., Lange, de G.J., Ziveri, P., Thomson, J., Santvoort, van P.J.M., Colley, S., Corselli, C., 2000, Recent terrestrial and carbonate fluxes in the pelagic eastern Mediterranean; a comparison between sediment trap and surface sediment, *Palaeogeogr., Palaeoclimatol., Palaeoecol.,* **158**, 197-213.

Sadekov, A., Eggins, S., De Deckker, P., Kroon, D., 2008, Uncertainties in seawater thermometry deriving from intratest and intertest Mg/Ca variability in *Globigerinoides ruber*, *Paleoceanography,* **23**, 1215-1226.

Sangiorgi, F., Capotondi, L., Combourieu Nebout, N., Vigliotti, L., Brinkhuis, H., Giunta, S., Lotter, A.F., Morigi, C., Negri, A., Reichart, G.J., 2003, Holocene seasonal sea-surface temperature variations in the southern Adriatic Sea inferred from a multi-proxy approach, *J. Quat. Res.*, **18**, 723-732.

Schenau, S.J., Antonarakou, A., Hilgen, F.J., Lourens, F.J., Nijenhuis, I.A., van der Weijden, C.H., Zachariasse, W.J., 1999, Organic-rich layers in the Metochia section (Gavdos, Greece) : evidence for a single mechanism of sapropel formation during the past 10 My, *Mar. Geol.*, **153**, 117-135.

Schiebel, R., Hemleben, C., 2005, Modern Planktic Foraminifera, *Palaeontologische Zeitschrift,* **79**, 135-148.

Schilman, B., Bar-Matthews, M., Almogi-Labin, A., Luz, B., 2001, Global climate instability reflected by Eastern Mediterranean marine records during the late Holocene, *Palaeogeogr., Palaeoclimatol., Palaeoecol.,* **176**, 157-176.

Schink, D.R., Guinasso Jr, N.L., 1977, Modelling the influence of bioturbation and other processes on carbonate dissolution at the sea floor. In "*The Fate of Fossil Fuel CO_2". in the Oceans,* (N.R. Andersen and A. Malahoff, eds.), 375-399.

Schmidt, G.A., G. R. Bigg and E. J. Rohling., 1999, "Global Seawater Oxygen-18 Database". http://data.giss.nasa.gov/o18data/

Schouten, S., Ossebaar, J., Schreiber, K., Kienhuis, M.V.M., Langer, G., Benthien, A., Bijma, J., 2006, The effect of temperature, salinity and growth rate on stable hydrogen isotopic composition of long chain alkenones produces by *Emiliana huxleyi* and *Gephyrocapsa oceanica*, *Biogeosciences*, **3**, 113-119.

Schweizer, M., Pawlowksi, J., Kouwenhoven, T.J., Guiard, J., Van der Zwaan, G.J., 2008, Molecular phylogeny of Rotaliida (Foraminifera) based on complete small subunit rDNA sequences, *Mar. Micropal.*, **66**, 233-246.

Schweizer, M., Pawlowski, J., Duijnstee, I.A.P., Kouwenhoven, T.J., Van der Zwaan, G.J., 2005, Molecular phylogeny of the foraminiferal genus *Uvigerina* based on the ribosomal DNA sequences, *Mar. Micropal.*, **57**, 51-67.

Segev, E., Erez, J., 2006, Effect of Mg/Ca ratio in seawater on shell composition in shallow benthic foraminifera, *Geochem. Geophys. Geosys.*, **7**, 1-8.

Shackleton, N.J., 1974, Attainment of isotopic equilibrium between ocean water and benthonic foraminifera genus *Uvigerina*: isotopic changes in the oceans during the last glacial, *Cent. Natl. Rech. Sci. Colloq. Int.*, **219**, 203-210.

Spero, H.J., Williams, D.F., 1988, Extracting environmental information from planktonic foraminiferal $d^{13}C$ data, *Nature*, **335**, 717-719.

Spero, H.J., Williams, D.F., 1989, Opening the carbon isotope "vital effect" black box. 1. Seasonal temperatures in the euphotic zone, *Paleoceanography*, **4**, 593-601.

Spero, H.J., 1992, Do planktic foraminifera accurately record shifts in the carbon isotopic compostition of seawater ΣCO_2, *Mar. Micropaleont.,* **19**, 275-285.

Spero, H.J., Lea, D.W., 1993, Intraspecific stable isotope variability in the planktic foraminifera *Globigerinoides sacculifer*: results from laboratory experiments, *Mar. Micropaleont*, **22**, 221-234.

Spero, H.J., Lea, D.W., 1996, Experimental determination of stable isotope variability in *Globigerina bulloides*: implications for paleoceanographic reconstructions, *Mar. Micropaleontol.,* **28**, 231-246.

Spero, H.J., Bijma, J., Lea., D.W., Bemis, B.E., 1997, Effect of seawater carbonate concentration on foraminiferal carbon and oxygen isotopes, *Nature,* **390**, 497-500.

Stanley S.M. and Hardie L.A., 1998, Secular oscillations in the carbonate mineralogy of reef-building and sediment-producing organisms driven by tectonically forced shifts in seawater chemistry, *Palaeogeogr. Palaeoclimatol. Palaeoecol.*, **144**, 3-19.

Stanley S.M., Ries J.B. and Hardie L.A., 2002, From the Cover: Low-magnesium calcite produced by coralline algae in seawater of Late Cretaceous composition, *PNAS*, **99**, 15323-15326

Tadjiki, S., Erten, H.N., 1994, Radiochronology of sediments from the Mediterranean Sea using natural ^{210}Pb and fallout ^{137}Cs, *J. Radioanal. Nuclear Chem.*, **181**, 447-459.

Tans, P., NOAA/ESRL, (www.esrl.noaa.gov/gmd/ccgg/trends/), Keeling, R., Scripps Institution of Oceanography (scrippsco2.ucsd.edu/), 2012.

Ter Kuile, B.H., Erez, J., Padan, E., 1989, Carbon budgets for two species of benthonic symbiont-bearing foraminifera, *Mar. Biology*, **103**, 241-251.

Toyofuku T., Kitazato H., Kawahata H., Tsuchiya M. and Nohara M., 2000, Evaluation of Mg/Ca thermometry in foraminifera: Comparison of experimental results and measurements in nature, *Paleoceanography*, **15**, 456-464.

Toyofuku, T., Suzuki, M., Suga, H., Sakai, S., Suzuki, A., Ishikawa, T., de Nooijer, L.J., Schiebel, R., Kawahata, H., Kitazato, H., 2011, Mg/Ca and δ^{18}O in the brackish shallow-water benthic foraminifer *Ammonia beccarii*, *Mar. Micropal.*, **78**, 113-120.

Tuenter, E., Weber, S.L., Hilgen, F.J., Lourens, L.J., 2003, The response of the African summer monsoon to remote and local forcing due to precession and obliquity, *Global Planet. Ch.*, **36**, 219-235.

Urey, H.C., Lowenstam, H.A., Epstein, S., McKinney, C.R., 1951, Measurement of paleotemperatures and temperatures of the upper Cretaceous of England, Denmark, and the Southeastern United States, *Bull. Geol. Soc. Am.*, **62**, 399-416.

Van der Meer, M.T.J., Baas, M., Rijpstra, W.I.C., Marino, G., Rohling, E.J., Sinnighe Damsté, J.S., Schouten, S., 2007, Hydrogen isotopic compositions of long-chain alkenones record freshwater flooding of the Eastern Mediterranean at the onset of sapropel deposition, *Earth Planet. Sci. Let.*, **262**, 594-600.

Van der Zwaan, G.J., Jorissen, F.J., Verhallen, P.J.J.M., von Daniels, C.H., 1986, Atlantic-European Oligocene to Recent *Uvigerina*: taxonomy, paleoecology and paleobiogeography, *Utrecht Micropaleontological Bulletins*, **35**, 240 p.

Van Santvoort, P.J.M., de Lange, G.J., Thomson, J., Cussen, H., Wilson, T.R.S., Krom, M.D., Ströhle, K., 1996, Active post-depositional oxidation of the most recent sapropel (S1) in sediments of the eastern Mediterranean Sea, *Geochim. Cosmochim. Acta*, **60**, 4007-4024.

Weiner, S., Dove, P.M., 2003, An overview of biomineralization processes and the problem of the vital effect, *Rev. Mineral Geochem.*, **54**, 1-29.

Wilkinson B.H. and Algeo T.J., 1989, Sedimentary carbonate record of calcium-magnesium cycling, *Americ. J. Sci.*, **289**, 1158-1194.

Wit J.C., Reichart G.-J., Jung S.J.A. and Kroon D., 2010, Approaches to unravel seasonality in sea surface temperatures using paired single specimen foraminiferal $d^{18}O$ and Mg/Ca analyses, *Paleoceanography*, **25**, 1-15.

Wit, J.C., de Nooijer, L.J., Barras, C., Jorissen, F., Reichart, G.J., 2012, A reappraisal of the vital effect in benthic foraminifera on Mg/Ca ratios: species specific uncertainty relationships, *Biogeosci. Disc.* **9**, 4947-4977.

Wit, J.C., Haig, J., Jorissen, F.J., Thomas, E., Reichart, G.J., under review, Reconstructing ancient seawater Mg/Ca: implications for temperature reconstructions based on foraminiferal Mg/Ca values, *Geochim. Comsochim. Acta*.

Yu J. and Elderfield H., 2008, Mg/Ca in the benthic foraminifera *Cibicidoides wuellerstorfi* and *Cibicidoides mundulus*: Temperature versus carbonate ion saturation, *Earth Planet. Sci. Let.*, **276**, 129-139.

Zachos J.C., Kroon D. and Blum P., 2004*,* Initial Reports Leg 208, *Proc. Ocean Dril. Prog.*, **208**, 73.

Zeebe, R.E., Wolf-Gladrow, D., 2001, CO_2 in Seawater: Equilibrium, Kinetics, Isotopes, *Elsevier Oceanography Series 65*, Halpern, D. (ed), Elsevier, Amsterdam, 346 p.

Zeebe, R.E., 2012, History of seawater carbonate chemistry, atmospheric CO2, and ocean acidification, *Annu. Rev. Earth Planet. Sci.*, **40**, 141-165

Ziegler, M., Nürnberg, D., Karas, C., Tiedemann, R., Lourens, L.J., 2008, Persistent summer expansion of the Atlantic Warm Pool during glacial abrupt cold events, *Nature Geoscience,* **1**, 601-605.

Appendices

T88/11	$\delta^{18}O$ (V-PDB)
1	0.36
2	0.66
3	0.68
4	0.84
5	0.92
6	0.96
7	0.97
8	0.99
9	1.01
10	1.02
11	1.03
12	1.07
13	1.08
14	1.09
15	1.10
16	1.11
17	1.13
18	1.15
19	1.15
20	1.18
21	1.20
22	1.22
23	1.22
24	1.23
25	1.23
26	1.24
27	1.27
28	1.38
29	1.41
30	1.43
31	1.43
32	1.49
33	1.56
34	1.58
35	1.64

Amplitude	11.09
Width	0.59
Height	499.99
Transform	0.12
Peak Position	1.26

SS^2
16.64

Bin (V-PDB)	Frequency Measured	Modeled[1]	Fit
0.0	0	0.12	0.02
0.2	0	0.13	0.02
0.4	1	0.14	0.74
0.6	0	0.37	0.13
0.8	2	1.86	0.02
1.0	5	6.27	1.62
1.2	13	10.88	4.48
1.4	7	9.43	5.92
1.6	6	4.11	3.59
1.8	1	0.97	0.00
2.0	0	0.21	0.05
2.2	0	0.13	0.02
2.4	0	0.12	0.02
2.6	0	0.12	0.02
2.8	0	0.12	0.02

1: $\text{Frequency} = \text{Transform} + \text{Height}^{-0.5\left(\frac{\text{Bin-Peak Position}}{\text{Width}}\right)^2} \bullet \text{Amplitude}$

2: $SS = (\text{Measured Frequency} - \text{Modeled Frequency})^2$

Appendix 2.1 Simple Excel spread sheet model for generating frequency distributions and the subsequent modeled Gaussian curve. SS = Sum of Squares.

$\delta^{18}O$ (V-PDB)	T88/2	T88/3	T88/11	T86/8	T86/11
1	1.49	1.79	0.99	1.26	1.13
2	1.83	1.41	1.07	0.90	2.44
3	1.64	1.46	1.18	0.94	0.91
4	1.23	0.74	1.08	1.05	1.98
5	1.25	1.58	1.27	1.20	2.57
6	1.58	1.59	1.64	1.02	1.19
7	1.84	1.57	1.56	1.09	0.88
8	1.70	1.78	1.11	0.87	1.29
9	2.06	1.53	1.15	1.11	0.93
10	1.51	1.05	0.97	1.09	0.68
11	1.48	1.42	0.92	0.94	1.10
12	1.59	2.20	0.68	1.24	0.91
13	1.66	1.69	1.13	0.87	2.20
14	1.78	1.50	1.58	1.21	1.17
15	1.59	1.67	1.20	1.20	2.20
16	1.49	1.40	1.43	1.26	0.87
17	1.32	1.52	1.03	1.04	1.02
18	1.51	1.72	1.22	1.14	2.07
19	1.71	1.80	1.09	1.08	0.76
20	1.01	1.40	1.41	2.16	2.41
21	1.66	1.91	0.66	0.57	1.33
22	1.63	1.41	1.43	0.95	0.54
23	1.29	1.80	1.01	0.81	1.90
24	3.10	1.79	1.15	0.65	1.87
25	1.44	1.74	1.23	1.19	1.09
26	2.17	1.39	0.84	1.02	1.98
27		1.30	1.10	1.08	0.76
28		1.56	1.38	2.18	0.80
29		1.69	1.02	0.86	1.50
30		1.61	0.36	0.77	1.22
31		1.80	1.23	0.78	1.58
32		1.78	1.24	0.93	1.76
33		1.91	0.96	0.60	1.89
34		1.81	1.49	1.32	0.81
35		1.80	1.22	1.11	0.67
36		2.06		1.24	2.22
37		1.79		0.86	0.73
38				0.95	0.85
39					0.80
40					1.07

Appendix 2.2 Single specimen oxygen isotope values per station for *G. inflata*

Sample	$\delta^{18}O$ (VPDB)	Sample	$\delta^{18}O$ (VPDB)	Sample	$\delta^{18}O$ (VPDB)	Sample	$\delta^{18}O$ (VPDB)	Sample	$\delta^{18}O$ (VPDB)	Sample	$\delta^{18}O$ (VPDB)
T86/11S-4	0.43	T87/49	0.57	T83/23	-0.33	M40-4-88-1	-0.06	M51-3-563	1.05	T83/63	0.48
T86/11S	-0.42	T87/49	0.21	T83/23	0.38	M40-4-88-1	0.77	T87/83	0.87	T83/63	-0.23
T86/11S	1.11	T87/49	0.85	T83/23	-0.39	M40-4-88-1	1.06	T87/83	0.75	T83/63	1.09
T86/11S-6	2.12	T87/49-7	0.83	T83/23	0.34	M40-4-88-1	0.88	T87/83	-0.85	T83/63	1.50
T86/11S-10	0.38	T87/49-9	-0.03	T83/23	0.00	M40-4-88-1	0.60	T87/83	-0.19	T83/63	1.52
T86/11S-11	-0.98	T87/49-15	-0.83	T83/23	-0.66	M40-4-88-1	0.39	T87/83	0.33	T83/63	1.08
T86/11S-13	0.51	T87/49-17	0.57	T83/23	-0.18	M40-4-88-1	0.69	T87/83	0.40	T83/63	0.63
T86/11S-16	0.80	T87/49-26	-0.64	T83/23	-0.56	M40-4-88-1	0.06	T87/83	-0.24	T83/63	1.01
T86/11S	-0.31	T87/49-18	-0.20	T83/23	-0.40	M40-4-88-1	-0.90	T87/83	1.34	T83/63	0.94
T86/11S	-0.22	T87/49-48	0.73	T83/23	0.23	M40-4-88-1	0.39	T87/83	1.30	T83/63	1.12
T86/11S	0.50	T87/49-50	0.35	T83/23	0.16	M40-4-88-1	-0.12	T87/30	0.16	T87/114	0.29
T86/11S	0.61	T87/49-51	0.02	T87/132	-0.48	M40-4-88-1	-0.70	T87/30	0.91	T87/114	0.66
T86/11S	0.06	T87/49-57	0.82	T87/132	0.07	M51-3-562	0.88	T87/30	0.06	T87/114	-0.25
T86/11S	1.54	T87/49-58	0.99	T87/132	-0.48	M51-3-562	0.76	T87/30	0.74	T87/114	0.10
T86/11S	-0.72	T87/49-59	0.51	T87/132	0.04	M51-3-562	1.47	T87/30	0.14	T87/114	0.24
T86/11S	-0.60	T87/49-60	0.84	T87/132	-0.05	M51-3-562	-0.69	T87/30	1.72	T87/114	0.24
T86/11S	0.18	T87/49-63	-0.75	T87/132	-0.43	M51-3-562	0.90	T87/30	1.65	T87/114	1.01
T86/11S-20	-0.38	T87/49-66	0.65	T87/132	-0.34	M51-3-562	0.95	T87/30	0.30	T87/114	0.00
T86/11S-21	-0.28	T87/49-47	0.28	T87/132	0.00	M51-3-562	1.47	T87/30	-0.88	T87/114	0.48
T86/11S	0.00	T87/49-52	1.16	T87/132	-0.73	M51-3-562	0.08	T87/30	0.57	T87/114	-0.01
T86/11S	-1.21	T87/49-55	0.34	T87/132	0.62	M51-3-562	-0.25	T87/30	1.07	T87/114	0.43
T86/11S	0.55	T83/23	0.74	T87/132	-0.42	M51-3-562	1.28	T87/30	0.24	T87/114	0.83
T86/11S	-0.52	T83/23	0.30	T87/132	-0.06	M51-3-562	1.08	T87/30	0.35	T87/114	-0.71
T86/11S	0.74	T83/23	1.56	T87/132	0.42	M51-3-562	0.08	T87/30	0.84	T87/114	-0.58
T86/11S	-0.89	T83/23	0.06	T87/132	0.24	M51-3-562	0.10	T87/30	0.18	T87/114	0.69
T86/11S	-0.93	T83/23	-0.48	T87/132	0.56	M51-3-562	-0.08	T87/14	0.12	T87/61	0.28
T87/49-1	0.17	T83/23	0.73	T87/132	-0.71	M51-3-562	-0.06	T87/14	0.10	T87/61	1.02
T87/49-10	1.04	T83/23	0.09	M51-3-569	0.33	M51-3-562	0.82	T87/14	-0.12	T87/61	-0.40
T87/49-14	-0.42	T83/23	1.16	M51-3-569	-0.87	M51-3-563	-0.26	T87/14	0.30	T87/61	0.41
T87/49	-0.09	T83/23	-0.20	M51-3-569	0.93	M51-3-563	0.98	T87/14	0.70	T87/61	-0.09
T87/49	0.62	T83/23	1.55	M51-3-569	1.01	M51-3-563	-0.39	T87/14	1.72	T87/61	0.85
T87/49	0.60	T83/23	1.26	M51-3-569	0.28	M51-3-563	2.20	T87/14	1.47	T87/61	0.24
T87/49	0.06	T83/23	0.44	M51-3-569	0.81	M51-3-563	-0.52	T87/14	1.47	T87/61	-0.24
T87/49	0.12	T83/23	-0.32	M51-3-569	-0.24	M51-3-563	0.30	T83/63	0.59	T87/61	0.27
T87/49	0.57	T83/23	0.86	M51-3-569	0.81	M51-3-563	0.64	T83/63	0.56	T87/61	0.03
T87/49	0.34	T83/23	0.53	M51-3-569	0.32	M51-3-563	1.19	T83/63	0.72	T87/61	0.18
T87/49	-0.06	T83/23	0.40	M51-3-569	1.43	M51-3-563	0.45	T83/63	1.08	T87/61	1.22
T87/49	0.37	T83/23	0.33	M40-4-88-1	0.07	M51-3-563	0.40	T83/63	0.44	T87/61	0.29
T87/49	0.86	T83/23	-0.03	M40-4-88-1	0.29	M51-3-563	0.08	T83/63	1.36	T87/61	0.11
T87/49	-0.54	T83/23	-0.88	M40-4-88-1	-0.09	M51-3-563	0.72	T83/63	-0.25	T87/61	-0.46
T87/49	0.44	T83/23	-0.26	M40-4-88-1	0.52	M51-3-563	1.41	T83/63	-0.07		
T87/49	0.67	T83/23	-0.16	M40-4-88-1	0.14	M51-3-563	1.50	T83/63	1.01		

Appendix 3.1 *G. ruber* $\delta^{18}O$ values. Samples measured for paired $\delta^{18}O$-Mg/Ca analyses are listed with an additional number, matching the sample name from appendices 3.2 and 3.3.

Sample	Chamber	Mg/Ca (mmol/mol)	Sample	Chamber	Mg/Ca (mmol/mol)	Sample	Chamber	Mg/Ca (mmol/mol)
T86/11S-4-01	F-1	5.28 ± 0.50	T86/11S-20-01	F-2	6.28 ± 0.67	T87/49-68-1	F-2	2.56 ± 0.29
T86/11S-4-02	F-4	6.60 ± 0.50	T86/11S-20-02	F-1	5.17 ± 0.56	T87/49-69-1	F-2	2.77 ± 0.32
T86/11S-4-03	F	2.53 ± 0.19	T86/11S-20-03	F	3.67 ± 0.40	T87/49-70-1	F-2	2.21 ± 0.25
T86/11S-4-04	F-2	6.75 ± 0.51	T86/11S-21-01	F-1	3.37 ± 0.39	T87/49-70-2	F-1	2.13 ± 0.25
T86/11S-6-01	F-2	3.61 ± 0.28	T86/11S-21-02	F-3	2.89 ± 0.34	T87/49-71-1	F-2	2.47 ± 0.29
T86/11S-6-02	F	3.04 ± 0.23	T86/11S-21-03	F	1.87 ± 0.22	T87/49-72-1	F-2	3.06 ± 0.36
T86/11S-7-01	F-1	3.75 ± 0.29	T86/11S-22-01	F-2	7.55 ± 0.87	T87/49-36-1	F-1	2.28 ± 0.11
T86/11S-7-03	F	2.67 ± 0.21	T86/11S-22-02	F-1	5.74 ± 0.67	T87/49-36-2	F-2	1.50 ± 0.08
T86/11S-9-01	F-1	3.22 ± 0.26	T86/11S-22-03	F	3.81 ± 0.45	T87/49-1-1	F-1	2.76 ± 0.14
T86/11S-9-02	F-2	3.67 ± 0.29	T87/49-47-1	F-2	4.36 ± 0.37	T87/49-2-1	F-1	5.12 ± 0.25
T86/11S-9-03	F	2.46 ± 0.20	T87/49-47-2	F-1	4.52 ± 0.39	T87/49-2-2	F-2	4.37 ± 0.22
T86/11S-10-01	F-2	5.14 ± 0.42	T87/49-48-1	F-1	2.95 ± 0.25	T87/49-5-1	F-1	3.60 ± 0.19
T86/11S-10-02	F-1	6.28 ± 0.51	T87/49-50-1	F-2	1.85 ± 0.16	T87/49-6-1	F-1	2.68 ± 0.14
T86/11S-11-01	F-2	5.81 ± 0.50	T87/49-51-1	F-2	1.35 ± 0.12	T87/49-7-1	F-2	3.35 ± 0.18
T86/11S-11-02	F-1	5.17 ± 0,45	T87/49-51-2	F-2	1.47 ± 0.13	T87/49-8-1	F-1	7.60 ± 0.41
T86/11S-12-01	F-1	3.15 ± 0.27	T87/49-52-1	F-1	1.63 ± 0.15	T87/49-9-1	F-1	2.48 ± 0.14
T86/11S-12-03	F	2.64 ± 0.23	T87/49-53-1	F-1	4.24 ± 0.39	T87/49-10-1	F-1	2.93 ± 0.16
T86/11S-13-01	F-3	3.22 ± 0.28	T87/49-54-1	F-1	2.74 ± 0.25	T87/49-12-1	F-1	2.99 ± 0.17
T86/11S-13-02	F-1	4.08 ± 0.36	T87/49-55-1	F-2	3.46 ± 0.32	T87/49-13-1	F-2	2.65 ± 0.15
T86/11S-13-03	F-2	3.00 ± 0.27	T87/49-57-1	F-2	3.02 ± 0.29	T87/49-14-1	F-1	4.64 ± 0.27
T86/11S-13-04	F	1.58 ± 0.15	T87/49-57-2	F-1	3.93 ± 0.38	T87/49-15-1	F-2	2.73 ± 0.16
T86/11S-14-01	F-1	3.10 ± 0.29	T87/49-58-1	F-2	2.69 ± 0.26	T87/49-16-1	F-1	6.33 ± 0.38
T86/11S-14-02	F	3.36 ± 0.31	T87/49-59-1	F-1	4.13 ± 0.40	T87/49-17-1	F-2	2.99 ± 0.18
T86/11S-15-01	F-1	2.79 ± 0.26	T87/49-60-1	F-2	4.00 ± 0.41	T87/49-18-1	F-1	1.89 ± 0.12
T86/11S-15-02	F-2	2.23 ± 0.21	T87/49-61-1	F-2	2.13 ± 0.22	T87/49-19-2	F-1	4.18 ± 0.27
T86/11S-15-03	F	2.07 ± 0.20	T87/49-62-1	F-2	5.24 ± 0.54	T87/49-23-1	F-2	3.84 ± 0.25
T86/11S-16-01	F-2	4.80 ± 0.46	T87/49-63-1	F-2	4.62 ± 0.48	T87/49-24-1	F-1	2.85 ± 0.20
T86/11S-16-02	F-1	4.83 ± 0.46	T87/49-63-2	F-1	3.87 ± 0.41	T87/49-26-1	F-2	3.67 ± 0.26
T86/11S-17-01	F-1	2.75 ± 0.27	T87/49-64-1	F-2	5.88 ± 0.64	T87/49-27-1	F-1	2.73 ± 0.20
T86/11S-17-02	F-2	1.89 ± 0.19	T87/49-65-1	F-2	4.27 ± 0.47	T87/49-29-1	F-1	4.86 ± 0.35
T86/11S-17-03	F	1.67 ± 0.17	T87/49-66-1	F	2.55 ± 0.29	T87/49-30-1	F-1	5.67 ± 0.42
T86/11S-17-04	F-3	2.41 ± 0.25	T87/49-67-1	F-2	3.06 ± 0.34			

Appendix 3.2 Mg/Ca values of *G. ruber.* Values are listed with one standard deviation.

Sample	$\delta^{13}C$ (VPDB)	Sample	$\delta^{13}C$ (VPDB)	Sample	$\delta^{13}C$ (VPDB)	Sample	$\delta^{13}C$ (VPDB)	Sample	$\delta^{13}C$ (VPDB)	Sample	$\delta^{13}C$ (VPDB)
T86/11S-4	0.88	T87/49	1.62	T83/23	1.50	M40-4-88-1	1.34	M51-3-563	0.07	T83/63	1.89
T86/11S	1.34	T87/49	0.90	T83/23	1.45	M40-4-88-1	1.20	T87/83	1.00	T83/63	1.65
T86/11S	0.49	T87/49	1.00	T83/23	1.27	M40-4-88-1	0.67	T87/83	0.55	T83/63	1.91
T86/11S-6	0.64	T87/49-7	0.98	T83/23	1.00	M40-4-88-1	0.85	T87/83	1.28	T83/63	0.98
T86/11S-10	0.26	T87/49-9	1.42	T83/23	0.87	M40-4-88-1	1.27	T87/83	0.64	T83/63	1.51
T86/11S-11	-0.02	T87/49-15	0.98	T83/23	0.65	M40-4-88-1	1.66	T87/83	1.91	T83/63	1.81
T86/11S-13	0.14	T87/49-17	0.80	T83/23	0.67	M40-4-88-1	1.28	T87/83	1.65	T83/63	1.36
T86/11S-16	0.15	T87/49-26	0.79	T83/23	0.80	M40-4-88-1	1.38	T87/83	1.31	T83/63	1.93
T86/11S	1.13	T87/49-18	1.29	T83/23	1.39	M40-4-88-1	1.69	T87/83	0.28	T83/63	1.16
T86/11S	0.80	T87/49-48	0.53	T83/23	1.09	M40-4-88-1	1.05	T87/83	1.38	T83/63	1.89
T86/11S	0.60	T87/49-50	1.21	T83/23	1.43	M40-4-88-1	1.22	T87/30	0.61	T87/114	1.25
T86/11S	1.14	T87/49-51	0.41	T87/132	1.63	M40-4-88-1	1.42	T87/30	1.43	T87/114	1.29
T86/11S	0.72	T87/49-57	1.27	T87/132	0.93	M51-3-562	0.99	T87/30	0.65	T87/114	1.48
T86/11S	0.47	T87/49-58	0.82	T87/132	1.06	M51-3-562	1.46	T87/30	0.63	T87/114	1.52
T86/11S	0.01	T87/49-59	1.60	T87/132	1.19	M51-3-562	1.35	T87/30	1.33	T87/114	1.51
T86/11S	0.48	T87/49-60	0.72	T87/132	0.72	M51-3-562	1.03	T87/30	2.33	T87/114	2.04
T86/11S	0.57	T87/49-63	1.47	T87/132	1.57	M51-3-562	0.88	T87/30	2.16	T87/114	0.71
T86/11S-20	0.86	T87/49-66	1.23	T87/132	0.43	M51-3-562	0.82	T87/30	1.21	T87/114	1.30
T86/11S-21	0.59	T87/49-47	0.00	T87/132	0.23	M51-3-562	2.20	T87/30	2.47	T87/114	1.22
T86/11S	0.65	T87/49-52	0.51	T87/132	1.49	M51-3-562	1.08	T87/30	1.03	T87/114	1.61
T86/11S	-0.85	T87/49-55	0.19	T87/132	1.16	M51-3-562	0.69	T87/30	1.97	T87/114	1.49
T86/11S	0.61	T83/23	1.84	T87/132	1.37	M51-3-562	2.10	T87/30	1.49	T87/114	0.99
T86/11S	0.53	T83/23	1.21	T87/132	1.57	M51-3-562	1.71	T87/30	1.45	T87/114	1.29
T86/11S	0.95	T83/23	1.72	T87/132	0.75	M51-3-562	1.03	T87/30	1.17	T87/114	1.56
T86/11S	0.88	T83/23	0.77	T87/132	1.09	M51-3-562	1.13	T87/30	0.72	T87/114	0.51
T86/11S	1.67	T83/23	1.12	T87/132	0.84	M51-3-562	0.47	T87/14	0.84	T87/61	1.51
T87/49-1	1.23	T83/23	0.86	T87/132	1.42	M51-3-562	0.72	T87/14	0.85	T87/61	0.86
T87/49-10	0.86	T83/23	1.63	M51-3-569	1.51	M51-3-562	1.20	T87/14	1.47	T87/61	0.96
T87/49-14	1.22	T83/23	2.11	M51-3-569	0.46	M51-3-563	1.27	T87/14	1.61	T87/61	0.79
T87/49	1.38	T83/23	1.24	M51-3-569	1.15	M51-3-563	0.94	T87/14	0.74	T87/61	1.45
T87/49	1.19	T83/23	1.69	M51-3-569	0.14	M51-3-563	0.98	T87/14	1.62	T87/61	1.32
T87/49	1.03	T83/23	1.29	M51-3-569	0.95	M51-3-563	2.29	T87/14	0.71	T87/61	0.91
T87/49	1.99	T83/23	1.34	M51-3-569	0.98	M51-3-563	1.55	T87/14	0.72	T87/61	1.40
T87/49	1.96	T83/23	1.64	M51-3-569	1.14	M51-3-563	0.86	T83/63	1.54	T87/61	1.51
T87/49	1.54	T83/23	1.77	M51-3-569	1.25	M51-3-563	1.19	T83/63	1.41	T87/61	1.45
T87/49	1.97	T83/23	1.72	M51-3-569	0.80	M51-3-563	1.02	T83/63	1.07	T87/61	1.27
T87/49	1.32	T83/23	1.52	M51-3-569	1.83	M51-3-563	0.98	T83/63	0.49	T87/61	1.05
T87/49	0.46	T83/23	1.93	M40-4-88-1	1.10	M51-3-563	0.83	T83/63	1.28	T87/61	0.76
T87/49	1.20	T83/23	1.13	M40-4-88-1	0.95	M51-3-563	0.66	T83/63	1.69	T87/61	1.28
T87/49	1.49	T83/23	1.23	M40-4-88-1	0.72	M51-3-563	1.03	T83/63	1.01	T87/61	1.47
T87/49	1.25	T83/23	1.23	M40-4-88-1	1.36	M51-3-563	1.76	T83/63	1.34		
T87/49	0.94	T83/23	1.20	M40-4-88-1	1.57	M51-3-563	0.62	T83/63	1.45		

Appendix 3.3 *G. ruber* $\delta^{13}C$ values. Samples measured for paired $\delta^{13}C$-Mg/Ca analyses are listed with an additional number, matching the sample name from appendices 3.1 and 3.2.

Sample Nr	Temperature (°C)	Mg/Ca (mmol/mol)	Average Mg/Ca (mmol/mol)	Sample Nr	Temperature (°C)	Mg/Ca (mmol/mol)	Average Mg/Ca (mmol/mol)
1	4.1	1.30		37	10.2	1.38	
2	4.1	1.78		38	10.2	1.30	
3	4.1	1.87		39	10.2	1.44	
4	4.1	1.60		40	10.2	2.22	
5	4.1	1.48		41	10.2	1.85	
6	4.1	1.24		42	10.2	2.50	
7	4.1	1.25		43	10.2	1.91	
8	4.1	1.15	**1.46 ± 0.09**	44	10.2	2.18	
9	6.0	1.80		45	10.2	1.50	
10	6.0	1.64		46	10.2	1.42	
11	6.0	0.91		47	10.2	1.68	
12	6.0	1.30		48	10.2	2.03	**1.78 ± 0.11**
13	6.0	0.75		49	11.3	2.22	
14	6.0	1.47		50	11.3	1.97	
15	6.0	1.25		51	11.3	1.73	
16	6.0	1.34		52	11.3	1.37	**1.82 ± 0.18**
17	6.0	1.19	**1.30 ± 0.11**	53	12.7	1.63	
18	7.9	1.73		54	12.7	1.61	
19	7.9	1.77		55	12.7	1.98	
20	7.9	1.39		56	12.7	2.06	
21	7.9	1.77		57	12.7	1.65	
22	7.9	1.72		58	12.7	1.17	
23	7.9	1.61		59	12.7	1.71	
24	7.9	1.98		60	12.7	1.72	
25	7.9	1.24		61	12.7	1.57	**1.68 ± 0.09**
26	7.9	1.11		62	14.0	2.31	
27	7.9	1.14		63	14.0	2.33	
28	7.9	1.29		64	14.0	1.91	
29	7.9	1.46		65	14.0	2.11	
30	7.9	1.65		66	14.0	1.87	
31	7.9	1.70		67	14.0	2.72	
32	7.9	1.84		68	14.0	2.26	
33	7.9	2.13		69	14.0	2.32	
34	7.9	2.77	**1.67 ± 0.10**	70	14.0	2.91	**2.31 ± 0.11**
35	9.3	1.15					
36	9.3	1.24	**1.19 ± 0.04**				

Appendix 4.1 Sample number with single specimen Mg/Ca value for *B. marginata*. Mg/Ca values for individual foraminifers are based on 1-4 laser ablation profiles. The error in averaged Mg/Ca values per temperature experiment is based on the standard error of the average ($\sigma/\sqrt{n}$)

Depth (m)	Temperature (°C)	Size (µm)	Mg/Ca (mmol/mol)	Mn/Ca (mmol/mol)
550	10.80	1203	50.12 ± 1.10	0.32 ± 0.011
550	10.80	634	33.21 ± 1.91	0.30 ± 0.004
550	10.80	1431	49.87 ± 0.80	0.41 ± 0.020
550	10.80	650	40.74 ± 1.25	0.26 + 0.002
1000	9.50	1041	33.91 ± 0.82	0.15 ± 0.002
1000	9.50	976	42.03 ± 3.25	0.18 ± 0,021
1000	9.50	1528	27.44 ± 1.23	0.24 + 0.011
1000	9.50	520	17.39 ± 0.77	0.23 ± 0.007
1195	5.80	520	17.48 ± 0.30	0.03 ± 0.003
1200	8.75	911	14.46 ± 0.96	0.14 ± 0.009
1200	8.75	878	15.19 ± 1.92	0.15 ± 0.010
2000	3.85	683	18.55 ± 0.48	0.17 ± 0.010
2005	3.40	846	9.77 ± 0.46	0.05 ± 0.008
2800	2.60	618	12.43 ± 0.85	0.16 ± 0.008
2800	2.60	618	9.45 ± 0.28	0.26 ± 0.002
2850	3.27	585	12.78 ± 0.24	0.13 ± 0.020
4800	2.38	488	7.05 ± 0.42	0.13 + 0.007
4800	2.38	390	8.90 ± 1.07	0.06 ± 0.005

Appendix 5.1 Depth, site temperature, size, Mg/Ca and Mn/Ca value of the used *Pyrgo* spp. specimens for the Mg/Ca-temperature calibration based on samples from the Bay of Biscay. Mg/Ca and Mn/Ca values are averaged over 3-4 ablation craters per individual foraminifer. Uncertainties in Mg/Ca and Mn/Ca are based on the standard error of the average ($\sigma/\sqrt{n}$) and depend on the standard deviation and number of ablation profiles.

Age (Ma)	Species	Mg/Ca (mmol/mol)	Average (mmol/mol)	Age (Ma)	Species	Mg/Ca (mmol/mol)	Average (mmol/mol)
0.59	*Cibicidoides* spp.	1.43 ± 0.08		0.59	*Pyrgo* spp.	9.66 ± 0.19	
0.59	*Cibicidoides* spp.	1.84 ± 0.05		0.59	*Pyrgo* spp.	10.60 ± 0.63	
0.59	*Cibicidoides* spp.	1.71 ± 0.09		0.59	*Pyrgo* spp.	9.56 ± 0.23	**9.94 ± 0.33**
0.59	*Cibicidoides* spp.	1.55 ± 0.03		0.60	*Pyrgo* spp.	8.41 ± 0.51	
0.59	*Cibicidoides* spp.	1.43 ± 0.32		0.60	*Pyrgo* spp.	8.57 ± 0.40	
0.59	*Cibicidoides* spp.	1.28 ± 0.22	**1.54 ± 0.08**	0.60	*Pyrgo* spp.	9.02 ± 0.16	**8.67 ± 0.18**
0.60	*Cibicidoides* spp.	1.53 + 0.14		1.40	*Pyrgo* spp.	7.73 ± 0.79	
0.60	*Cibicidoides* spp.	1.21 ± 0.05	**1.37 ± 0.16**	1.40	*Pyrgo* spp.	6.74 ± 0.20	
1.40	*Cibicidoides* spp.	1.25 ± 0.01		1.40	*Pyrgo* spp.	6.18 ± 0.57	
1.40	*Cibicidoides* spp.	1.24 ± 0.12	**1.24 ± 0.01**	1.40	*Pyrgo* spp.	8.17 ± 0.54	**7.21 ± 0.45**
2.01	*Cibicidoides* spp.	1.55 ± 0.03		2.01	*Pyrgo* spp.	7.86 ± 0.22	
2.01	*Cibicidoides* spp.	1.46 ± 0.03		2.01	*Pyrgo* spp.	7.83 ± 0.44	
2.01	*Cibicidoides* spp.	2.40 ± 0.09		2.01	*Pyrgo* spp.	7.86 ± 0.57	
2.01	*Cibicidoides* spp.	0.99 ± 0.05		2.01	*Pyrgo* spp.	7.74 ± 0.17	**7.82 ± 0.03**
2.01	*Cibicidoides* spp.	0.99 ± 0.05		4.18	*Pyrgo* spp.	7.99 ± 0.05	
2.01	*Cibicidoides* spp.	1.47 ± 0.20	**1.48 ± 0.21**	4.18	*Pyrgo* spp.	8.55 ± 0.54	
4.18	*Cibicidoides* spp.	1.33 ± 0.10		4.18	*Pyrgo* spp.	8.09 ± 0.14	**8.21 ± 0.17**
4.18	*Cibicidoides* spp.	2.03 ± 0.05		4.19	*Pyrgo* spp.	7.90 ± 0.02	
4.18	*Cibicidoides* spp.	1.37 ± 0.06		4.19	*Pyrgo* spp.	8.82 ± 0.58	**8.36 ± 0.46**
4.18	*Cibicidoides* spp.	1.28 ± 0.09		4.46	*Pyrgo* spp.	8.93 ± 0.17	
4.18	*Cibicidoides* spp.	0.93 ± 0.05	**1.39 ± 0.18**	4.46	*Pyrgo* spp.	7.11 ± 0.18	
4.19	*Cibicidoides* spp.	1.70 ± 0.10		4.46	*Pyrgo* spp.	6.87 ± 0.21	**7.64 ± 0.65**
4.19	*Cibicidoides* spp.	1.30 ± 0.05		4.72	*Pyrgo* spp.	8.82 ± 0.77	
4.19	*Cibicidoides* spp.	1.19 ± 0.15		4.72	*Pyrgo* spp.	9.62 ± 0.42	
4.19	*Cibicidoides* spp.	1.72 ± 0.29	**1.48 ± 0.14**	4.72	*Pyrgo* spp.	9.25 ± 0.45	**9.23 ± 0.23**
4.46	*Cibicidoides* spp.	1.46 ± 0.09		4.73	*Pyrgo* spp.	7.50 ± 0.54	
4.46	*Cibicidoides* spp.	1.22 ± 0.13		4.73	*Pyrgo* spp.	7.63 ± 0.38	
4.46	*Cibicidoides* spp.	1.51 ± 0.34		4.73	*Pyrgo* spp.	6.73 ± 0.28	
4.46	*Cibicidoides* spp.	1.51 ± 0.17		4.73	*Pyrgo* spp.	7.02 ± 0.55	**7.22 ± 0.21**
4.46	*Cibicidoides* spp.	1.48 ± 0.29	**1.44 ± 0.05**	6.14	*Pyrgo* spp.	9.20 ± 0.31	
4.72	*Cibicidoides* spp.	1.42 ± 0.02		6.14	*Pyrgo* spp.	9.28 ± 0.15	
4.72	*Cibicidoides* spp.	1.21 ± 0.03	**1.31 ± 0.10**	6.14	*Pyrgo* spp.	10.06 ± 0.32	**9.51 ± 0.27**
4.73	*Cibicidoides* spp.	1.45 ± 0.09		6.95	*Pyrgo* spp.	10.70 ± 0.16	
4.73	*Cibicidoides* spp.	1.55 ± 0.11		6.95	*Pyrgo* spp.	9.22 ± 0.09	**9.96 ± 0.74**
4.73	*Cibicidoides* spp.	0.98 ± 0.14		7.14	*Pyrgo* spp.	9.61 ± 0.23	
4.73	*Cibicidoides* spp.	1.59 ± 0.05		7.14	*Pyrgo* spp.	10.02 ± 0.19	
4.73	*Cibicidoides* spp.	1.52 ± 0.14	**1.42 ± 0.11**	7.14	*Pyrgo* spp.	7.22 ± 0.17	
6.14	*Cibicidoides* spp.	1.17 ± 0.25		7.14	*Pyrgo* spp.	7.79 ± 0.11	**8.66 ± 0.68**
6.14	*Cibicidoides* spp.	1.57 ± 0.05		7.38	*Pyrgo* spp.	6.92 ± 0.08	
6.14	*Cibicidoides* spp.	1.17 ± 0.09	**1.30 ± 0.13**	7.38	*Pyrgo* spp.	6.68 ± 0.17	
6.95	*Cibicidoides* spp.	1.16 ± 0.21		7.38	*Pyrgo* spp.	9.04 ± 0.15	
6.95	*Cibicidoides* spp.	1.42 ± 0.17		7.38	*Pyrgo* spp.	10.70 ± 0.26	**8.34 ± 0.95**
6.95	*Cibicidoides* spp.	1.81 ± 0.09		8.75	*Pyrgo* spp.	9.31 ± 0.32	
6.95	*Cibicidoides* spp.	1.50 ± 0.03	**1.47 ± 0.13**	8.75	*Pyrgo* spp.	8.36 ± 0.15	
7.14	*Cibicidoides* spp.	1.41 ± 0.17		8.75	*Pyrgo* spp.	9.54 ± 0.09	**9.07 ± 0.36**
7.14	*Cibicidoides* spp.	1.37 ± 0.11		9.24	*Pyrgo* spp.	7.66 ± 0.19	
7.14	*Cibicidoides* spp.	1.87 ± 0.13	**1.55 ± 0.16**	9.24	*Pyrgo* spp.	9.90 ± 0.31	
7.38	*Cibicidoides* spp.	0.96 ± 0.09		9.24	*Pyrgo* spp.	9.89 ± 0.26	**9.15 ± 0.74**
7.38	*Cibicidoides* spp.	1.28 ± 0.11	**1.12 ± 0.16**				
8.75	*Cibicidoides* spp.	1.50 ± 0.23					
8.75	*Cibicidoides* spp.	1.20 ± 0.12					
8.75	*Cibicidoides* spp.	1.21 ± 0.01					
8.75	*Cibicidoides* spp.	1.39 ± 0.21					
8.75	*Cibicidoides* spp.	1.59 ± 0.13					
8.75	*Cibicidoides* spp.	1.25 ± 0.07	**1.36 ± 0.07**				
9.24	*Cibicidoides* spp.	1.55 ± 0.20					
9.24	*Cibicidoides* spp.	1.30 ± 0.27					
9.24	*Cibicidoides* spp.	1.30 ± 0.03					
9.24	*Cibicidoides* spp.	0.96 ± 0.19	**1.28 ± 0.12**				

Appendix 5.2 Measured LA-ICP-MS Mg/Ca values with their standard deviations for fossil *Cibicidoides* spp. and *Pyrgo* spp. Standard deviations are based on 3-4 ablation profiles (Figure 1) per individual. Average Mg/Ca values and standard error ($\sigma/\sqrt{n}$) for each depth are calculated with the unweighted average of the individual measurements of that depth.

Salinity	Na/Ca (mmol/mol)	Average (mmol/mol)	Salinity	Na/Ca (mmol/mol)	Average (mmol/mol)
30.0	6.73 ± 0.96		36.1	6.39 ± 0.16	
30.0	6.52 ± 0.78		36.1	8.65 ± 0.67	
30.0	5.95 ± 0.31		36.1	8.61 ± 1.21	
30.0	5.78 ± 0.26		36.1	7.00 ± 0.88	
30.0	5.44 ± 0.34		36.1	6.21 ± 0.33	
30.0	5.52 ± 0.27		36.1	6.28 ± 0.21	
30.0	5.79 ± 0.34		36.1	5.48 ± 0.32	
30.0	5.17 ± 0.27		36.1	6.31 ± 0.45	**6.87 ± 0.41**
30.0	5.60 ± 0.31	**5.83 ± 0.17**	38.6	6.94 ± 0.76	
32.5	6.57 ± 0.73		38.6	9.29 ± 1.82	
32.5	5.44 ± 0.64		38.6	7.70 ± 1.89	
32.5	6.31 ± 0.58		38.6	8.34 ± 0.13	
32.5	7.24 ± 1.12		38.6	8.45 ± 0.34	
32.5	7.77 ± 1.32		38.6	7.00 ± 0.67	
32.5	5.95 ± 0.54		38.6	6.55 ± 0.17	
32.5	6.83 ± 0.32		38.6	8.02 ± 0.65	
32.5	5.66 ± 0.15		38.6	6.93 ± 0.45	**7.69 ± 0.30**
32.5	4.97 ± 0.50				
32.5	4.43 ± 0.30	**6.12 ± 0.33**			

Appendix 6.1 Individual Na/Ca values for cultured benthic foraminifer *A. tepida*. The uncertainty (±) in the individual measurements and the average (bold) are based on the standard error of the mean ($\sigma/\sqrt{n}$). Na/Ca values of individual foraminifers are based on the ablation profiles of 2-4 chambers.

Depth (cm)	Na/Ca (mmol/mol)	Salinity	Average	Depth (cm)	Na/Ca (mmol/mol)	Salinity	Average
500	7.94 ± 0.10	40.4		570	7.11 ± 0.45	36.6	
500	7.99 ± .023	40.7		570	7.22 ± 0.06	37.1	
500	6.58 ± 0.31	34.1		570	5.99 ± 0.42	31.3	
500	7.80 ± 0.09	39.8		570	5.62 ± 0.14	29.6	
500	8.27 ± 0.21	41.9		570	7.68 ± 0.28	39.2	
500	7.54 ± 0.01	38.5		570	6.62 ± 0.03	34.3	
500	6.76 ± 0.13	34.9		570	6.61 ± 0.34	34.2	
500	7.73 ± 0.20	39.4		570	7.05 ± 0.49	36.3	
500	7.18 ± 0.40.	36.9		570	7.44 ± 0.39	38.1	
500	6.51 ± 0.21	33.7	**38.0 ± 0.93**	570	6.54 ± 0.11	33.9	**35.1 ± 0.94**
510	7.51 ± 0.62	38.4		580	6.71 ± 0.33	34.7	
510	6.81 ± 0.31	35.1		580	7.08 ± 0.22	36.4	
510	6.73 ± 0.23	34.8		580	5.35 ± 0.32	28.4	
510	8.54 ± 0.21	43.2		580	6.83 ± 0.31	35.2	
510	7.24 ± 0.39	37.1		580	6.48 ± 0.23	33.6	
510	8.01 ± 0.31	40.7		580	7.07 ± 0.06	36.4	
510	6.92 ± 0.23	35.7		580	7.27 ± 0.01	37.3	
510	6.92 ± 0.39	35.6		580	6.23 ± 0.04	32.5	
510	7.62 ± 0.07	38.9	**37.7 ± 0.95**	580	7.48 ± 0.46	38.3	**34.8 ± 1.00**
520	6.41 ± 0.23	33.3		590	6.98 ± 0.11	35.9	
520	5.42 ± 0.33	28.7		590	8.10 ± 0.21	41.2	
520	7.18 ± 0.41	36.9		590	7.54 ± 0.25	38.6	
520	6.89 ± 0.05	35.5		590	7.12 ± 0.32	36.6	
520	6.45 ± 0.59	33.5		590	6.58 ± 0.31	34.1	**37.3 ± 1.21**
520	6.87 ± 0.23	35.4	**33.9 ± 1.18**	600	6.80 ± 0.21	35.1	
530	6.59 ± 0.31	34.1		600	6.36 ± 0.23	33.1	
530	6.21 ± 0.17	32.4	**33.3 ± 0.88**	600	7.68 ± 0.24	39.2	
540	6.22 ± 0.15	32.4		600	6.16 ± 0.07	32.1	
540	6.76 ± 0.18	34.9		600	6.18 ± 0.04	32.2	
540	6.55 ± 0.95	33.9		600	7.44 ± 0.05	38.1	
540	6.79 ± 0.12	35.1		600	7.48 ± 0.16	38.3	
540	6.69 ± 0.31	34.6	**34.2 ± 0.49**	600	8.07 ± 0.21	41.0	
550	5.87 ± 0.15	30.8		600	8.00 ± 0.23	40.7	**36.7 ± 1.19**
550	5.34 ± 0.13	28.3		610	7.56 ± 0.03	38.6	
550	7.00 ± 0.15	36.0		610	7.10 ± 0.19	36.5	
550	6.88 ± 0.12	35.5	**32.7 ± 1.87**	610	6.76 ± 0.01	34.9	
560	6.45 ± 0.14	33.5		610	6.79 ± 0.15	35.1	
560	6.85 ± 0.07	35.3		610	7.18 ± 0.07	369.0	
560	6.07 ± 0.27	31.7		610	8.14 ± 0.85	41.3	
560	6.38 ± 0.24	33.2		610	7.17 ± 0.15	36.9	**37.2 ± 0.84**
560	5.64 ± 0.28	29.7					
560	6.38 ± 0.59	33.2					
560	7.61 ± 0.09	38.9	**33.6 ± 1.09**				

Appendix 6.2 Individual Na/Ca values for planktonic foraminifer *G. ruber* from core MS66PC. The uncertainty (±) in the individual measurements and the average (bold) are based on the standard error of the mean ($\sigma/\sqrt{n}$). Na/Ca values of individual foraminifers are based on the ablation profiles of 2-4 chambers.

Sample	Experiment	Size (μm)	Mg/Ca (mmol/mol)	Average	Sample	Experiment	Size (μm)	Mg/Ca (mmol/mol)	Average
1	S 30.0	192	1.74 ± 0.19		39	S 36.1	208	2.05 ± 0.27	
2	S 30.0	198	1.45 ± 0.16		40	S 36.1	207	1.82 ± 0.17	
3	S 30.0	216	1.79 ± 0.88		41	S 36.1	193	1.66 ± 0.38	
4	S 30.0	220	1.72 ± 0.08		42	S 36.1	194	1.72 ± 0.28	
5	S 30.0	217	1.40 ± 0.28		43	S 36.1	173	2.46 ± 0.34	
6	S 30.0	237	1.33 ± 0.21		44	S 36.1	179	1.69 ± 0.02	
7	S 30.0	289	1.29 ± 0.32		45	S 36.1	175	2.07 ± 0.30	
8	S 30.0	198	1.56 ± 0.26		46	S 36.1	176	1.97 ± 0.29	
9	S 30.0	206	1.82 ± 0.40		47	S 36.1	181	2.12 ± 0.26	
10	S 30.0	172	1.29 ± 0.28		48	S 36.1	147	1.88 ± 0.29	
11	S 30.0	185	1.41 ± 0.20		49	S 36.1	174	1.91 ± 0.26	
12	S 30.0	186	1.40 ± 0.27		50	S 36.1	153	1.81 ± 0.12	
13	S 30.0	165	1.61 ± 0.16		51	S 36.1	147	2.74 ± 1.08	
14	S 30.0	187	0.98 ± 0.07		52	S 36.1	140	1.88 ± 0.31	
15	S 30.0	189	1.40 ± 0.11		53	S 36.1	128	1.98 ± 0.14	
16	S 30.0	178	1.59 ± 0.16		54	S 36.1	117	2.09 ± 0.41	
17	S 30.0	221	1.43 ± 0.19	**1.48 ± 0.05**	55	S 36.1	134	1.66 ± 0.31	
18	S 32.5	215	2.18 ± 0.45		56	S 36.1	146	1.86 ± 0.19	**1.94 ± 0.07**
19	S 32.5	197	1.50 ± 0.14		57	S 38.6	190	1.75 ± 0.11	
20	S 32.5	191	1.65 ± 0.37		58	S 38.6	182	1.55 ± 0.18	
21	S 32.5	206	1.63 ± 0.60		59	S 38.6	179	1.93 ± 0.23	
22	S 32.5	196	1.55 ± 0.24		60	S 38.6	180	2.22 ± 0.24	
23	S 32.5	225	1.53 ± 0.26		61	S 38.6	169	1.94 ± 0.17	
24	S 32.5	222	1.41 ± 0.24		62	S 38.6	154	2.10 ± 0.25	
25	S 32.5	219	1.56 ± 0.08		63	S 38.6	150	2.46 ± 0.33	
26	S 32.5	226	1.87 ± 0.24		64	S 38.6	159	2.03 ± 0.26	
27	S 32.5	207	1.96 ± 0.22		65	S 38.6	139	2.90 ± 0.31	
28	S 32.5	222	1.85 ± 0.47		66	S 38.6	149	2.07 ± 0.19	
29	S 32.5	185	1.76 ± 0.29		67	S 38.6	129	2.32 ± 0.14	
30	S 32.5	197	1.93 ± 0.51		68	S 38.6	149	1.87 ± 0.51	
31	S 32.5	171	1.69 ± 0.42		69	S 38.6	143	2.01 ± 0.54	
32	S 32.5	236	1.30 ± 0.21		70	S 38.6	116	2.86 ± 0.65	
33	S 32.5	188	1.47 ± 0.05		71	S 38.6	120	2.13 ± 0.10	
34	S 32.5	184	1.67 ± 0.12		72	S 38.6	133	2.57 ± 0.39	
35	S 32.5	159	1.83 ± 0.29		73	S 38.6	128	2.66 ± 0.11	
36	S 32.5	156	1.63 ± 0.25		74	S 38.6	131	1.93 ± 0.67	
37	S 32.5	180	1.97 ± 0.20	**1.70 ± 0.05**	75	S 38.6	122	2.41 ± 0.32	
38	S 36.1	236	1.44 ± 0.30		76	S 38.6	116	2.57 ± 0.22	**2.21 ± 0.08**

Appendix 7.1 : Mg/Ca and size data for the individual foraminifera of each salinity experiment. Averaged Mg/Ca for each experiment is given in bold text.

Depth (cm)	Mg/Ca (mmol/mol)	Average	Depth (cm)	Mg/Ca (mmol/mol)	Average
500	5.17 ± 1.11		570	3.34 ± 0.51	
500	4.97 ± 0.39		570	3.13 ± 0.50	
500	3.94 ± 0.42		570	2.55 ± 0.15	
500	5.26 ± 0.88		570	2.92 ± 0.15	
500	8.31 ± 0.90		570	4.49 ± 0.74	
500	7.23 ± 1.00		570	6.02 ± 0.32	
500	6.63 ± 1.40		570	3.94 ± 0.61	
500	4.05 ± 0.61		570	6.36 ± 0.85	
500	5.75 ± 1.19		570	4.77 ± 0.55	
500	3.44 ± 0.34	**5.48 ± 0.49**	570	5.45 ± 0.60	**4.30 ± 0.42**
510	5.24 ± 0.10		580	3.34 ± 0.17	
510	4.87 ± 0.26		580	6.03 ± 0.61	
510	4.12 ± 0.91		580	7.88 ± 0.32	
510	5.06 ± 0.32		580	5.54 ± 0.62	
510	4.47 ± 0.10		580	2.81 ± 0.23	
510	10.09 ± 1.23		580	6.12 ± 0.26	
510	4.74 ± 0.40		580	4.20 ± 0.82	
510	6.69 ± 0.34		580	3.02 ± 0.18	
510	9.88 ± 0.58	**6.13 ± 0.77**	580	3.17 ± 0.30	**4.68 ± 0.59**
520	5.17 ± 0.19		590	5.62 ± 0.19	
520	6.06 ± 0.39		590	3.02 ± 0.91	
520	3.66 ± 0.82		590	5.24 ± 0.20	
520	6.90 ± 0.27		590	5.77 ± 0.97	
520	6.46 ± 0.46		590	4.75 ± 0.81	
520	5.29 ± 0.47	**5.59 ± 0.47**	590	7.26 ± 1.45	
530	3.42 ± 1.36		590	3.21 ± 0.06	
530	6.69 ± 0.32		590	3.97 ± 0.29	**4.85 ± 0.50**
530	2.77 ± 0.81	**4.29 ± 1.21**	600	2.88 ± 0.42	
540	4.56 ± 0.31		600	3.04 ± 0.22	
540	3.55 ± 0.27		600	3.00 ± 0.55	
540	2.86 ± 0.11		600	2.76 ± 0.31	
540	3.43 ± 0.53		600	3.11 ± 0.47	
540	4.29 ± 0.36	**3.74 ± 0.31**	600	5.88 ± 0.14	
550	2.42 ± 0.09		600	6.06 ± 1.39	
550	2.58 ± 0.57		600	3.51 ± 0.42	
550	2.81 ± 0.24		600	8.11 ± 0.39	**4.26 ± 0.64**
550	4.69 ± 1.21	**3.12 ± 0.53**	610	6.20 ± 1.04	
560	3.81 ± 0.04		610	3.90 ± 0.71	
560	3.61 ± 0.21		610	3.20 ± 0.41	
560	5.46 ± 1.35		610	4.74 ± 0.52	
560	6.50 ± 0.89		610	4.19 ± 0.60	
560	2.65 ± 0.11		610	2.49 ± 0.32	
560	3.89 ± 0.20		610	4.76 ± 0.44	**4.21 ± 0.45**
560	3.22 ± 0.27	**4.16 ± 0.51**			

Appendix 7.2 Mg/Ca data for the individual foraminifera from core MSPC66. Averaged Mg/Ca per sample interval are given in bold text.

Summary

Atmospheric CO_2 concentrations are rapidly increasing over the last 150 years. Since atmospheric CO_2 is a potent greenhouse gas, it functions as a trap for heat in the Earth's atmosphere, subsequently causing a global rise in temperature. Future effects can be studied by the use of numerical climate models, capable of predicting climate changes on both regional and global scale. Verification of such models over longer timescales can only be achieved through comparison with past climate reconstructions. Such paleo-climate reconstructions rely on the use of proxies, representative of one or more climate parameters, and their preservation in continuous sedimentary archives. The chemistry of the calcite test of foraminifera is an often excellently preserved proxy for paleo-climate reconstructions. The use of these proxies is, however, often limited due to uncertainties or even absence in proxy-parameter calibrations. This thesis, therefore, focuses on the calibration, validation and application of foraminiferal carbonate based proxies as a tool to reconstruct past climates.

Several processes, such as bioturbation and/or reworking of sediments, hamper the use of foraminifera as proxy-carriers for the accurate reconstruction of past climates. Bioturbation mixes sediments of different ages. Short-term changes are, therefore, potentially smoothed in the sedimentary record. Bioturbation can be recognized by the use of $\delta^{18}O$ frequency distributions measured on individual foraminifera and interpreted by using simple spreadsheet end-member modeling. This allows unmixing of temperature records affected by bioturbation into multiple distributions, representing the original and bioturbated component within each sample. Simple spreadsheet modeling, furthermore, allows quantification of the average of each distribution, thereby correcting the measured $\delta^{18}O$ signal for the effects of bioturbation.

Temperature reconstructions are often based on the continuous analysis of many fossil foraminiferal specimens, representing the annual average temperature. Seasonal variability in sea surface temperatures is, however, orders of magnitude larger than the inter-annual variability reconstructed by these measurement practices. Analyzing single specimens from one sample, however, allows reconstructing a range of past temperatures potentially representative of the seasonal temperature contrast. The range in $\delta^{18}O$ and Mg/Ca derived temperature estimated from single specimen analysis resembles the range in seasonal temperature values at the sea surface (0–50 m) in the Mediterranean Sea and the Atlantic Ocean. This implies that it is possible to reconstruct the seasonal range in temperatures (seasonality) using single-specimen

analysis of (combined) Mg/Ca and $\delta^{18}O$.

Quantification of the inter-individual variability of Mg/Ca in foraminiferal calcite within one population of foraminifera is of vital importance to the accuracy of the Mg/Ca-thermometer. The inter-individual variability is mainly controlled by biological imperfections in the calcification mechanism of foraminiferal calcite. Culturing experiments under controlled conditions allows such quantifications of the uncertainty as a result of inter-individual variability. The magnitude of this uncertainty on the accuracy of foraminiferal Mg/Ca-temperature calibrations is mainly depending on the sensitivity of the used species-specific calibrations and the amount of individuals measured.

The large differences between sensitivities of species-specific Mg/Ca-temperature calibrations can be used to disentangle the effects of temperature and seawater Mg/Ca on foraminiferal Mg/Ca values. Although magnesium concentrations are relatively constant over shorter time scales, it fluctuates appreciably over longer time scales. Paleo-Mg/Ca_{sw} can now be reconstructed using the temperature-dependent offset in magnesium incorporation (sensitivity) between porcelaneous (high Mg) *Pyrgo* spp. and hyaline (low Mg) *Cibicidoides* spp. Applying this reconstructed Mg/Ca_{sw} to existing time series shows that Mg/Ca-based temperature reconstructions for the middle Pleistocene and earlier significantly underestimate absolute temperature.

The two major parameters controlling ocean circulation, and thereby global climate, are temperature and salinity. Several proxies have been developed to reconstruct past seawater temperatures. A proxy that allows the direct and reliable reconstruction of salinity remained among the most important challenges in current-day paleoceanography. The Na/Ca values of benthic foraminifer *Ammonia tepida*, cultured over a range of salinities, however, provides a robust and independent tool to accurately reconstruct seawater salinity. Application of this calibration over a sapropel (S5) from the Eastern Mediterranean showed that salinity decreased by 5 units during this interval, providing for the first time independent evidence for a major freshening of surface waters during sapropel formation. Foraminiferal Na/Ca values thus provide an accurate and novel tool to reliably reconstruct past changes in ocean salinity.

Sapropel formation in the Eastern Mediterranean Sea is always accompanied by a freshening of surface waters. The exact source of this increased freshwater input has, however, not been identified, due to a lack of independent proxies or ecological habitat separation of those proxies. Temperature reconstructions depending on

foraminiferal Mg/Ca values are, for instance, not independent of changes in seawater salinity. The incorporation of magnesium increases with salinity as a result of the increased activity of free magnesium-ions with respect to that of calcium-ions, thereby impacting Mg/Ca-temperature reconstructions. This effect of salinity can, however, be quantified and corrected for when using foraminiferal Na/Ca values in combination with Mg/Ca measurements. Corrected temperatures are then combined with records for salinity and foraminiferal $\delta^{18}O$, showing that the Mediterranean basin changed from an evaporation dominated basin with eastward increasing salinities to a basin with less evaporation and a more "Atlantic signal" during sapropel formation. This overall change in basin hydrology might be more important than the impact of the increased Nile outflow as a cause for sapropel formation.

Samenvatting

Atmosferische CO_2 concentraties zijn de afgelopen 150 jaar aanzienlijk toegenomen. CO_2 is een sterk broeikasgas dat als het ware warmte opsluit in de atmosfeer, waardoor de aarde in de toekomst steeds verder zal opwarmen. De lokale en globale effecten die een opwarmende aarde met zich mee brengen, kunnen bestudeerd worden met behulp van numerieke klimaatmodellen. Over langere tijdschalen kunnen deze modellen alleen geverifieerd worden door ze te vergelijken met reconstructies van vroegere klimaatsystemen. Deze reconstructies maken gebruik van zogenaamde proxies, die representatief zijn voor een of meerdere klimaatparameters. De chemische samenstelling van de schelp gemaakt door foraminiferen wordt vaak gebruikt als proxy bij het reconstrueren van vroegere klimaten. Dit proefschrift richt zich op de kalibratie, validatie en applicatie van op foraminiferen gebaseerde carbonaat proxies als middel om het klimaat van vroeger te reconstrueren.

Het gebruik van foraminiferen voor een nauwkeurige reconstructie van vroegere klimaten, hangt af van bioturbatie en/of de herwerking van sedimenten. Bioturbatie mixt sedimenten van verschillende ouderdommen, wat er bijvoorbeeld voor zorgt dat korte, snelle klimaatsveranderingen anders worden gearchiveerd in het sediment. Bioturbatie kan herkent worden door het gebruik van frequentieverdelingen van de zuurstofisotopen ($\delta^{18}O$) samenstelling van individueel gemeten foraminiferen. Interpretatie van deze verdelingen met behulp van simpele rekenbladmodellen, leidt tot het opdelen van de gemeten verdelingen in een origineel deel en een deel afkomstig van bioturbatie. De gemiddelde van deze verdelingen kunnen vervolgens gekwantificeerd worden, waardoor het gemeten $\delta^{18}O$ signaal gecorrigeerd kan worden voor bioturbatie.

Temperatuurreconstructies zijn vaak gebaseerd op de jaarlijkse gemiddelde temperatuur, die bepaald wordt door meerdere foraminiferen tegelijkertijd te meten. De seizoenale spreiding in zeewater temperatuur is echter een keer zo groot als de langdurige variatie in de gemiddelde jaarlijkse temperatuur. Het individueel meten van meerdere foraminiferen uit één monster maakt het mogelijk om een bereik van tempetaturen te meten, die potentieel representatief is voor de seizoenale temperatuurvariatie. Het bereik van temperatuur gebaseerd op de $\delta^{18}O$ en Mg/Ca van individueel gemeten foraminiferen valt samen met het seizonale temperatuurcontrast van het zeewater oppervlak (0-50 m) in de Middellandse Zee en Atlantische Oceaan. Dit betekent dat het mogelijk is om het seizoenale temperatuurcontrast (seizoenaliteit) te

reconstrueren, wanneer gebruik gemaakt wordt van het individueel meten van $\delta^{18}O$ en Mg/Ca aan het calciet van foraminiferen.

Het bepalen van de variabiliteit in Mg/Ca tussen individuen van dezelfde soort en populatie is van groot belang voor de nauwkeurigheid van de Mg/Ca-thermometer. Deze variabiliteit word grotendeels bepaald door biologische imperfecties in het calcificatie proces van het door foraminiferen gemaakte calciet. Kweekexperimenten onder gecontroleerde omstandigheden zorgen er voor dat de onzekerheid in temperatuur als een resultaat van de variabiliteit gekwantificeerd kan worden. De mate van onnauwkeurigheid wordt grotendeels bepaald door de gevoeligheid van de gebruikte soort-specifieke Mg/Ca-temperatuur kalibratie en de hoeveelheid gemeten foraminiferen.

De grote verschillen tussen de gevoeligheid van soort specifieke Mg/Ca-temperatuur kalibraties kunnen gebruikt worden om onderscheid te maken tussen de invloeden van temperatuur en zeewater Mg/Ca op de Mg/Ca waarden van foraminiferen. Magnesium concentraties in zeewater zijn relatief constant over een korte tijdschaal. Concentraties over langere tijdschalen fluctueren echter sterk, waardoor temperatuurreconstructies beïnvloed worden. Zeewater Mg/Ca waarden kunnen worden gereconstrueerd door gebruik te maken van het door temperatuur bepaalde verschil in magnesium inbouw (gevoeligheid) tussen porseleinen (hoog Mg) *Pyrgo* spp. en hyaliene (laag Mg) *Cibicidoides* spp. Het toepassen van deze methode op sedimentmonsters laat zien dat temperaturen, gebaseerd op Mg/Ca van foraminiferen, significant worden onderschat voor het Midden-Pleistoceen en eerder.

De twee belangrijkste parameters voor oceaancirculatie, en dus het klimaat op aarde, zijn temperatuur en het zoutgehalte (saliniteit) van het zeewater. Voor het reconstrueren van de temperatuur zijn meerdere proxies ontwikkeld. Een proxy die de directe en nauwkeurige reconstructie van saliniteit mogelijk maakt, is echter een van de meest belangrijke uitdagingen in de paleo-oceanografie. De Na/Ca waarden van de benthische foraminifeer *Ammonia tepida*, gekweekt in zeewater met verschillende saliniteit, vormen een nieuwe en onafhankelijke methode voor het nauwkeurig reconstrueren van de saliniteit van zeewater. Het toepassen van deze kalibratie op monsters in een sapropel (S5) uit de oostelijke Middellandse Zee laat zien dat de saliniteit snel daalde met 5 eenheden tijdens deze periode. Dit vormt het eerste onafhankelijke bewijs voor een grote 'verzoeting' van oppervlakte water in de Middellandse Zee tijdens het ontstaan van sapropelen. De Na/Ca waarden van het calciet van foraminiferen vormt dus een nauwkeurige en nieuwe proxy om de saliniteit van

zeewater betrouwbaar te reconstrueren.

Het ontstaan van sapropelen in de oostelijke Middellandse Zee wordt altijd vergezeld door een 'verzoeting' aan het zeewater oppervlak. De precieze herkomst van de toename in zoetwater is echter onbekend door het ontbreken van onafhankelijke proxies en/of habitat-scheiding van de nu gebruikte proxies. Temperatuurreconstructies die afhankelijk zijn van Mg/Ca gemeten aan foraminiferen, zijn bijvoorbeeld niet onafhankelijk van veranderingen in saliniteit. De inbouw van magnesium neemt namelijk toe met saliniteit als gevolg van de toegenomen activiteit van vrije magnesiumionen in verhouding tot de calciumionen. Dit zorgt er dus voor dat de Mg/Ca-temperatuur reconstructies door saliniteitsveranderingen beïnvloed worden. Deze invloed kan echter gekwantificeerd en, belangrijker, gecorrigeerd worden, door gebruik te maken van de aan dezelfde foraminiferen gemeten Na/Ca waarden. De gecorrigeerde temperaturen kunnen vervolgens gecombineerd worden met gegevens over saliniteit en $\delta^{18}O$. Dit laat zien dat de Middellandse Zee tijdens de formatie van een sapropel veranderd van een door verdamping gedomineerde zee met een toenemende saliniteit in oostelijke richting, in een zee met minder verdamping en een meer "Atlantisch" karakter. Deze verandering in de hydrologie van het Middellandse Zee bekken is waarschijnlijk belangrijker voor het vormen van sapropelen dan de toename in het debiet van de Nijl.

Curriculum Vitea

Jos Wit was born on the 15th of March 1982 in Haarlem, the Netherlands. He graduated from secondary school (VWO) at the 'Katholieke Scholengemeenschap Hoofddorp' in 2000. After which he obtained a Propadeause (Earth Sciences), Bachelor (Earth Sciences) and a Master degree (Quaternary Geology and Geo-ecology) at the Vrije Universiteit Amsterdam. During his Masters he participated in a 6 weeks fieldwork in Portugal to reconstruct the Holocene history of the Tagus River, boarded for a scientific cruise aboard the MS Marion Dufresne and developed a new proxy for seasonality in the Mediterranean Sea. In 2007 he started as a PhD-student for the Darwin Centre for Biogeosciences at the Geochemistry department of Utrecht University. His PhD-thesis focuses on the calibration, validation and application of foraminiferal carbonate based proxies.

Publications

Wit, J.C., Reichart, G-J., Jung, S.J.A., Kroon, D., 2010, Approaches to unravel seasonality in sea surface temperatures using paired single-specimen foraminiferal $\delta^{18}O$ and Mg/Ca analyses, *Paleoceanography 25*, PA4220, doi: 10.1029/2009PA001857.

Wit, J.C., De Nooijer, L.J., Barras, C., Jorissen, F., Reichart, G.J., 2012, A reappraisal of the vital effect in benthic foraminifera on Mg/Ca ratios: species specific uncertainty relationships, *Biogeosciences* 9, 1-12, doi: 10.5194/bg-9-1-2012.

Wit, J.C., Haig, J., Jorissen, F., Thomas, E., Reichart, G.J., 2012, Reconstructing ancient seawater Mg/Ca: Implications for temperature reconstructions based on foraminiferal Mg/Ca values, *Geochmimica et Cosmochimica Acta*, under review.

Wit, J.C., De Nooijer, B. Metcalf, Reichart, G.J., Ganssen, G., 2012, Unmixing of stable isotope signals using single specimen $\delta^{18}O$ analyses, *Geochemistry, Geophysics, Geosystems*, under review.

Wit, J.C., De Nooijer, De Lange, G.J., Reichart, G.J., Development and Application of a Novel, Direct Proxy for Paleo-Salinity, in preperation.

Invited Talks

Wit, J.C., Haig, J., Jorissen, F., Thomas, E., Reichart, G.J., 2010, Reconstructing the Mg/Ca ratio of seawater: Implications for Mg/Ca based paleo-climate reconstructions, NSG conference 2010, Utrecht, the Netherlands.

Conference Abstracts

Wit, J.C., Vis, G-J., Kasse, C., Prick, A., Prins, M., Kroon, D., Jung, S.J.A., Alt-Epping, U., 2006, A Holocene Land-Sea Correlation For River Tagus, Portugal, *Geophysical Research Abstracts*, Vol. 8, 10603.

Wit, J.C., Reichart, G-J., Jung, S.J.A., Kroon, D., 2008, Seasonality in the Mediterranean Sea: A calibration study using paired single specimen $d^{18}O$ and Mg/Ca measurements of *G. ruber alba*, *Geophysical Research Abstracts,* Vol 10, 09200.

Wit, J.C., Reichart, G-J., Dueñas-Bohórquez, A., de Lange, G.J., 2009, Assessing the effect of salinity on foraminiferal Mg/Ca by culturing *Bulimina marginata*, Darwin Days 2009, Veldhoven, the Netherlands.

Wit, J.C., Reichart Haig, J., Jorissen, F., Thomas, E., Reichart, G.J., 2010, Improving the Mg/Ca thermometer: seawater Mg/Ca history unravelled, Darwin Days/NAC 2010, Veldhoven, the Netherlands.

Wit, J.C., Haig, J., Jorissen, F., Thomas, E., Reichart, G,-J., 2010, Reconstructing Mg/Ca ratios of seawater and implications for Mg/Ca based climate reconstructions, *Geophysical Research Abstracts,* Vol 12, 3050, 2010

Wit, J.C., Barras, C., Jorissen, F., Reichart, G.J., 2011, Mg in foraminiferal calcite: Temperature vs Biology, Darwin Days 2011, Lunteren, the Netherlands.

Wit, J.C., De Nooijer, L.J., De Lange, G.J., Reichart, G,-J., 2012, Foraminiferal Na/Ca as a tool to reconstruct salinity, *Geophysical Research Abstracts,* Vol 14, 5731, 2012.

Dankwoord

En dan nu misschien wel het lastigst te schrijven, maar tevens ook het meest gelezen stukje tekst van mijn proefschrift. Hoe geef je vorm aan een eindeloze stroom van bedankjes, zonder iemand te vergeten? En hoe voorkom je dat het een saaie opsomming van personen wordt? Deze twee moeilijke vragen probeer ik in dit dankwoord te beantwoorden. Daarom zou ik allereerst iedereen willen bedanken voor het lezen, van in ieder geval dit stuk, van mijn proefschrift, om vervolgens aan een nog nader te benoemen persoon mijn excuses aan te bieden voor het vergeten te noemen van zijn/haar naam.

Om te beginnen wil ik hier mijn dagelijkse begeleider en Co-promotor Gert-Jan bedanken voor het mogelijk maken van dit onderzoek. Je hebt er niet alleen voor gezorgd dat het een mooi stuk werk is geworden, maar hebt dit ook gedaan in een plezierige sfeer, iets wat het doen van promotie-onderzoek aanzienlijk veraangenaamd. Verder wil ik je nog bedanken voor het dragen van Elvis/Johnny Cash-achtige cowboy laarzen. Het geluid van deze laarzen gaven altijd een tijdige waarschuwing vlak voor een lastige vraag als: “Is het al af? Waarom niet?”. Uiteraard ben ik ook een woord van dank verschuldigd aan mijn Promotor Gert, die op de juiste momenten het juiste commentaar had. Als laatste van mijn begeleiders wil ik Lennart bedanken. Alhoewel je niet officieel als co-promotor bij dit project betrokken bent geweest, heb je toch altijd tijd vrijgemaakt voor discussie en samengewerkt aan manuscripten of dat dit wel het geval was.

Promoveren gaat niet zonder paranimfen (eigenlijk wel, maar het is niet gebruikelijk) en daarom verdienen Marie-Louise en Hans ook een bedankje. ML je was (bijna) altijd af te leiden voor een goed dan wel nutteloos gesprek, een leuk concert of gewoon een bakkie thee of blikkie. Zonder jou was promoveren een stuk minder gezellig geweest. Hans, of Superhans, zoals je recentelijk nog genoemd bent. Bedankt voor alle Excel en statistiek vragen die ik op je heb mogen afvuren en voor de snelle antwoorden die doorgaans terug kwamen. Het deed me deugd dat de vragen in de loop der jaren ook steeds lastiger voor jou werden. Verder ben je als goede vriend natuurlijk ook mede verantwoordelijk voor de nodige sociale afleiding zonder welke het leven een stuk saaier wordt.

Zonder collega’s is het maar eenzaam op de universiteit. Daarom wil ik eerst Julia en Eveline bedanken. Ik ben de laatste van Z214 die promoveert en dat wel precies

2 jaar na de eerste. Ik wil jullie bedanken voor het gezelligste kantoor wat je je maar kan wensen en mogelijk maken van het: 'Het-zou-wel-eens-de-eerste/laatste-mooie-zonnige-dag-van-het-jaar-kunnen zijn'-concept. "Terrasje dan maar….". Verder natuurlijk voor het uit het raam kijken ("want het sneeuwt!"), de pepernoten, koekjes, snoepjes en al het andere snaaiwerk en bovenal de supergezellige sfeer. Els en Marie-Louise, bedankt voor het drinken van menig kopje thee en ik hoop dat jullie gehoor niet te veel beschadigd is van alle slechte grappen die ik de afgelopen 5 jaar op jullie heb afgevuurd. Verder wil ik in willekeurige volgorde Jordahna, Shauna, Adriana, Elisabeth, Cornelia, Marieke, Angela, Laura, Johan, Klaas (Zaagmans), Mohammed, Iuliana, Anna, Rick, Karoliina, Tom, Martin en Michiel bedanken. En uiteraard zijn daar ook nog de mensen van de "derde verdieping", Sander, Peter, Emmy, Appy en Niels. Jongens bedankt dat jullie mij af en toe als notoire koffiehater tolereerde in jullie goddelijke koffiehoek.

Promoveren valt of staat met de data. Zonder data valt er immers niets te onderzoeken. Helen, Dineke, Arnold, Pieter en Gijs, zonder jullie had ik nooit alle data kunnen verzamelen en dit proefschrift had dan ook onmogelijk geweest zonder jullie. Onze secretaresse en vraagbaak Pien zorgt er verder stiekem voor dat een hoop dingen toch gebeuren zonder dat je dit merkt, waarvoor dank.

Promoveren is leuk en volgens Gert-Jan ook "topsport", maar ook topsporters hebben periodes van rust en ontspanning nodig. Daarom wil ik Hans, Douwe, Marloes, Sonja, Joos, Esther, Martin, Jeroen, Mark, Aniska, Yannick, Thomas, Bart, Gaby en Barry bedanken. Bedankt voor alle momenten van "rust en ontspanning". Of het nu een weekendje weg was, winterport, concert, bbq, biertje hier, biertje daar, spelletje zus of spelletje zo, het was altijd gezellig.

Dan ben ik uiteraard nog een woord van dank verschuldigd aan mijn ouders. Jullie hebben mij gevormd tot wie ik ben en altijd de steun en ruimte gegeven in alles wat ik deed. Daarvoor kan ik jullie nooit genoeg bedanken, maar ik kan er altijd een poging toe wagen. Ook wil ik mijn zusje, Yvonne, bedanken voor de steun en interesse die ze altijd heeft getoond in mijn promotie, maar bovenal voor het zijn van mijn zusje en de wonderlijke wereld van roze en Hello Kitty. Als laatste wil ik graag Inge bedanken, al weet ik niet precies hoe. In de korte tijd dat we nu samen zijn, heb je laten zien hoe het is als iemand je onvoorwaardelijk steunt. Dat gevoel hoop ik nog lange tijd samen met jou vast te houden.